REGULATION OF HOST CELL DNA REPLICATION PROTEIN SMARCAL1 BY ADENOVIRUS

By

Reshma Bhanu Nazeer

A thesis submitted to

The University of Birmingham

For the degree of

DOCTOR OF PHILOSOPHY

Institute of Cancer and Genomic Sciences

The Medical School

The University of Birmingham

October 2019

"In the name of Almighty, the most beneficent, the most merciful"

Dedicated to my Beloved

Parents, Nazeer Khan and Fairoz Banu

Husband, Dr. Abdul Aslam Syed

And my Children,

Sobia Syed and Abdul Afu Syed

Abstract

Adenoviruses have evolved to inactivate host cell responses to DNA damage through interaction with host cell proteins and by targeting some of these proteins for ubiquitin-mediated proteolysis. Indeed, previous studies have suggested that early region proteins dysregulate ATR signalling pathways during infection by sequestering the MRE11-RAD50-NBS1 complex and promoting the proteasomal degradation of TopBP1. Moreover, the cellular E1B-55K-interacting protein, E1B-AP5 modulates ATR kinase activity during infection. Work presented here has established that adenovirus targets the cellular replication, and DNA damage response protein, SMARCAL1 for degradation in an E1B-55K/E4orf6 and Cullin Ring ligase-dependent manner. As such, we determined that the phosphorylation of SMARCAL1 residues, S123, S129 and S173 by ATR and CDK kinases promoted SMARCAL1 degradation during infection. We also determined that SMARCAL1 recruitment to viral replication centres during infection was partially dependent upon SMARCAL1 phosphorylation but was mainly dependent upon its ability to interact with the RPA complex. We also determined that E1B-55K interacted directly with SMARCAL1 in adenovirus E1-transformed cells and could modulate cellular DNA replication. Indeed, E1B-55K expression initially enhanced DNA replication fork speed but ultimately, promoted replication fork stalling. We propose that SMARCAL1 is targeted for degradation by adenoviruses to inhibit host cell DNA replication.

Acknowledgements

First and foremost, I am extremely grateful to Almighty, for showering his utmost blessings throughout my research journey to complete it successfully and by providing me with an opportunity to do my PhD in Dr Andy Turnell's lab.

I would like to express my sincere gratitude and deep thanks to my Supervisor Dr Andy Turnell for considering me for PhD in his prestigious lab and for being a big inspiration for my development as a Scientist. I have tried to learn as much of his intelligence, kindness, helpful nature and being there for his team at times of need. I really admired the way he ran a laboratory by mentoring as well as working at the bench. I am very thankful to Dr. Andy Turnell for helping me with experiments and supporting me always especially when my daughter was hospitalised.

I would like to acknowledge my thanks to Dr. Phil Byrd for helping me with sequencing and Dr. Eva Petermann for helping me with the DNA Fibre analysis.

I would like to thank every member of the Turnell laboratory, past and present. I am delighted to say it is the best laboratory to work in because of its members. Thank you, Terry, for being my friend, supporting me and helping me through the ups and downs of my research journey. Thank you Abeer for generating the cell lines, thank you Ahmed and thank you Jess F for all the help you guys provided, making my time enjoyable in the lab and making my experience one that I will always cherish.

Finally, I would like to thank my family for their constant support throughout, my parents for their prayers and encouragement, A big THANKS to my husband Dr. Abdul Aslam Syed for believing in me and supporting me unconditionally both mentally and financially by sponsoring my studies and taking care of our kids when I was struggling with my research, thank you so much. I would like to thank my dearest brother Dr. Kabir Khan Nazeer for his caring and moral support and looking after my kids when I was busy with my research. I would also like to thank my sisters Humera, Rashida, Muneera and my brother Moghani Khan Nazeer and rest of my family members and my friends for their constant encouragement and prayers. Last but not the least I would like to thank my lovely kids Sobia Syed and Abdul Afu Syed for not troubling me so much, putting up with me and showing their love and support and moreover for being my stress relievers. I would like to thank Almighty Allah for blessing me with wonderful life and a wonderful family.

"My Lord! Enrich me with knowledge." (Quran, 20:114)

"*No two things have been combined better than knowledge and patience" (Prophet Muhammad (peace be upon him))*

"O Allah I ask you for knowledge that benefits, and I seek refuge in you from knowledge that does not benefit." (Ibn Hibban, 82)

"Science without religion is lame, religion without science is blind." — Albert Einstein

"Nothing in life is to be feared, it is only to be understood. Now is the time to understand more, so that we may fear less." — Marie Curie

"If I have seen further it is by standing on the shoulders of Giants." – Issac Newton

"Science is not only a disciple of reason but also one of romance and passion." – Stephen Hawking

Table of Contents

LIST OF FIGURES

LIST OF TABLES

List of Abbreviations.

Ad	Adenovirus
Ad5	Adenovirus serotype 5
Ad12	Adenovirus serotype 12
Adpol	DNA polymerase
AH2	annealing helicase 2
APS	Ammonium persulphate
A-T	Ataxia telangiectasia
ATLD	Ataxia telangiectasia-like disorder
ATM	Ataxia telangiectasia Mutated
ATP	adenosine tri-phosphate
ATR	ATM-Rad3-Realted
ATRIP	ATR-interacting protein
Brdu	bromodeoxyuridine
BSA	bovine serum albumin
C-terimal	Carboxy-terminal
CAR	Coxsackievirus-adenovirus receptor
CBP	CREB binding protein
CDC	Cell division cycle
CDK	Cyclin-dependent kinase
CHK1	checkpoint kinase 1
CHK2	checkpoint kinase 2
CldU	5-Chloro-2′-deoxyuridine
CMV	Cytomegalovirus

CR	Conserved region
CRL	Cullin ring ligase
CtBP	C-terminal binding protein
CtIP	CtBP-interacting protein
Cul	Cullin
DAPI	4’,6-diamidino-2-phenylindole
Daxx	Death domain-associated protein
dCMP	Deoxycytidine monophosphate
DBP	DNA binding protein
DDR	DNA damage response
DDRi	DDR kinase inhibitors
DMEM	Dulbecco’s modified Eagles medium
DMSO	Dimethyl-sulphoxide
DNA	deoxyribonucleic acid
DNA-PK	DNA-dependent protein kinase
dNTP	deoxyribonucleotide triphosphate
dsDNA	double stranded DNA
DSBs	double stranded breaks
DTT	Dithiothrietol
DUB	De-ubiquitylating
E1A	early region 1A
E1B	early region 1B
E2	early region 2
E3	early region 3
E1B-AP5	E1B-55K-interacting protein

E4orf3	Early region 4 open reading frame 3
E4orf6	Early region 4 open reading frame 6
EBV	Epstein-Barr virus
EDTA	Ethylenediaminetetraacetic acid
FCS	Foetal calf serum
G1/G2	Gap phase 1/gap phase 2
GFP	green fluorescent protein
GST	Glutathione S-transferase
H1/H2	HARP1/HARP2
H2A	Histone 2A family member
γH2AX	H2AX phospho-serine 139
HARP	Hep-A related protein
HBV	Hepatitis B virus
HCV	Hepatitis C virus
HEK	Human embryonic kidney cells
HER	Human embryonic retinoblast cells
HIV-1	Human immunodeficiency virus type 1
HNRPU	Heterogeneous nuclear ribonucleoprotein U-like
HPV	Human papillomavirus
HR	homologous recombination
HRP	Horseradish peroxidase
HTLV-1	Human T-cell lymphotrophic virus 1
HU	Hydroxyurea
IdU	5-Iodo-2′-deoxyuridine
IF	Immunofluorescence

IgG	Immunoglobulin G
IP	Immunoprecipitation
IPTG	Isopropyl β-D-1-thiogalactopyranoside
IR	Ionising radiation
ITR	Inverted terminal repeats
KAP1	KRAB domain-associated protein
Kb	Kilo base
KDa	Kilo Dalton
KSHV	Kaposi's sarcoma-associated herpesvirus
Ku70/80	Lupus Ku autoantigen protein p70/p80
LB	Luria broth
MCM	minichromosome maintenance
MDC1	Mediator of DNA damage checkpoint
MDM2	Murine double minute 2
MG132	N-(benzyloxycarbonyl)leucinylleucinylleucinal
MHC	Major histocompatibility complex
MLP	Major late promoter
Mre11	Meiotic recombination 11
MRN	MRE 11-RAD50-NBS1
mRNA	Messenger RNA
N-terminal	Amino-terminal
NBS	Nijmegen breakage syndrome
NEDD8	Neural precursor cell-expressed developmentally down-regulated 8
NER	nucleotide excision repair

NES	N-terminal nuclear export signal
NF1	Nuclear factor 1
NF2	Nuclear factor 2
NF-kB	Nuclear factor-kappa B
NHEJ	non-homologous end joining
NLS	nuclear localisation signal
Non-sil	Non-silencing
NRS	Nuclear retention signal
P	Phosphorylated
PAGE	polyacrylamide gel electrophoresis
PARP	Poly (ADP-ribose) polymerase
PBS	Phosphate buffer saline
PCR	Polymerase chain reaction
PCNA	proliferating cell nuclear antigen
p.f.u	Plaque forming unit
PIKK	PI-3 kinase-related kinase
PML	Promyelocytic leukemia
POD	PML oncogenic domains
PP2A	Protein phosphatase 2A
pTP	TP precursor
ORF	Open reading frame
Rb	Retinoblastoma
RBD	RPA binding domain
RBX1	Ring-box 1
RFC	Replication factor C

RNA	Ribonucleic acid
RNP	Ribonucleoprotein
RPA	Replication protein A
RSV	Rous sarcoma virus
RT-PCR	Reverse transcriptase PCR
SD	Standard deviation
SDS	sodium dodecyl sulphate
SDS-PAGE	SDS-polyacrylamide gel electrophoresis
SIOD	Schimke immune-osseous dysplasia
SMARCAL1	SWI/SNF matrix associated actin dependent regulator of chromatin A-like 1
SMC1	Structural maintenance of chromosomes 1
SNF2	sucrose non-fermenting 2
shRNA	short hairpin RNA
siRNA	small interfering RNA
ssDNA	single stranded DNA
SSBs	single stranded DNA breaks
S/TQ	serine/threonine glutamine
SUMO-1	Small ubiquitin-like modifier 1
SV40	Simian virus 40
TBS	Tris-buffered saline
TBST	TBS containing Tween 20
TEMED	N,N,N',N' -tetramethylethylenediamine-1,2-diamine
TFIID	Transcription factor IID

TIF1	Transcriptional intermediary factor 1
Tipin	Timeless-interacting protein
Tim	Timeless
TopBP1	Topoisomerase (DNA) II binding protein 1
TP	Terminal protein
TRIM	Tripartite motif
Ub	Ubiquitin
UV	Ultraviolet
WB	Western blotting
w.t	Wild type
VRC	viral replication centres

CHAPTER 1

Introduction

1.1. Viruses and Cancer.

The World Health Organisation (WHO) International Agency for Research on Cancer (IARC) reported recently that estimates suggested that the global cancer burden had risen to 9.6 million deaths and 18.1 million new cases in 2018 (WHO, 2018). In this regard, it is extremely interesting to note that an earlier report suggested that 15-20 % of all cancers worldwide in 2012 were due to infection (WHO, 2012). Indeed, it was suggested that 2.1 million cases of new cancers in 2012 were attributable to infection and that up to one-quarter of all cancers in low- and middle- income countries were due to infections with human papilloma virus, hepatitis B and C viruses and other infectious agents, such as Helicobacter pylori (Plummer, de Martel et al. 2016).

1.2. Tumour viruses.

Human tumour viruses can be categorised into two groups, human DNA tumour viruses and human RNA viruses as listed in Table 1.1. The oncogenic protein products for these viruses have mostly been identified (Zheng 2010).

Taxonomic Grouping	Examples	Oncogenes	Tumor Types
1. DNA viruses			
Adenoviridae	Adenovirus types 12, 18, 31	E1A, E1B	Various solid tumors only in rodents
Hepadnaviridae	HBV	HBx	Hepatocellular carcinoma
Herpesviridae	EBV	LMP-1, BARF-1	Burkitt's lymphoma, B-cell lymphoma, NPC
	KSHV	vGPCR	Kaposi sarcoma, primary effusion lymphoma
Papovaviridae	Merkel cell polyomavirus	T antigens	Merkel cell carcinoma
	BK virus, JC virus		Solid tumors in rodents and primates
Papillomaviridae	HPV 16, 18, 31, 45	E6, E7	Cervical and anal cancer, Oral cancer
2. RNA Viruses			
Flaviviridae			
Hepacivirus	Hepatitis C virus	?	Hepatocellular carcinoma
Retroviridae			
HTLV	Human T-cell leukemia virus type I	Tax	Adult T-cell leukemia/lymphoma

Table 1.1. List of viruses and oncogenes Taken from: (Zheng 2010).

1.2.1. Historical background

Although it is now known that viral infection plays a major role in tumourigenesis with approximately 15 to 20 % of all human cancers being caused by infection, the role of infectious agents as tumour-promoting factors has only been appreciated in the last 50-100 years. Indeed, early studies in animal models of cancer, then later cell and molecular biological studies identified the causative agents of cancer. It was in 1907 when, Guiseppe Ciuffo, an Italian physician determined the relationship between human warts and transmissible agents (i.e. viruses) such that this proliferative disease could be passed from an individual with the disease to a healthy individual through the small transmissible agent, now known as HPV (Bergonzini, Salata et al. 2010). Not long after this Francis Peyton Rous, working at the Rockefeller Institute, identified that a sarcoma from breast tissue of a chicken could be transplanted into other chickens to promote tumour growth and moreover, determined that a cell-free preparation from the tumour could similarly induce tumorigenesis in other chickens. As such, Rous suggested that 'a minute parasitic organism' was responsible for causing the disease (Rous 1910, Rous 1911). This transmissible agent was later renamed Rous sarcoma virus (RSV) which is an RNA virus. In 1933, Richard Edwin Shope, also working at the Rockefeller, discovered the first mammalian DNA tumour virus, cottontail rabbit papilloma virus, also known as the Shope virus which caused a 'wart-like disease' on the skin of infected rabbits; histology showed that this virus infected the cutaneous epithelium of rabbits (Shope and Hurst 1933). This discovery was closely followed by the identification of another RNA virus, mouse mammary tumour virus (MMTV) by John J Bitner who showed for the first time that the extrachromosomal factor that caused breast tumours in mice could be transmitted through breast feeding in experimental mice (Bitner 1936).

Interest in tumour viruses was enhanced in 1950s with the identification of murine polyoma virus that causes salivary gland tumours in mice (Gross 1953). In 1962, Eddy discovered that another polyoma virus, SV40 was oncogenic in rhesus monkey kidney cells (Eddy, Borman et al. 1962). As SV40 is found in both monkeys and humans there has been much controversy as to whether SV40 causes tumours in humans, but it is now generally accepted, based on numerous studies that SV40 is unlikely to be a causative agent of cancer in humans (Engels, Katki et al. 2003, Engels, Chen et al. 2005).

The first tumour viruses in humans were discovered in 1960s and 1970s and initiated great interest in human tumour virology. In 1962, John Trentin identified human adenovirus as the first human oncogenic virus, when he determined that intrapulmonary injection of adenovirus 12, but not other adenovirus types, had the ability to induce tumours (sarcomas) in baby hamsters particularly on the 'mediastinum, the internal chest wall, or on the diaphragm' (Trentin, Yabe et al. 1962). Quite soon after Epstein Barr virus (EBV), also known as human herpes virus 4, was identified in cultured lymphoblasts from Burkitt's lymphoma by electron microscopy (Epstein, Achong et al. 1964). Hepatitis B virus (HBV) surface antigen was isolated in 1967 by Blumberg from blood from an Australian Aboriginal, and was later, deemed to be found in the serum of Hepatitis B-infected individuals (Blumberg, Gerstley et al. 1967) (Prince 1968). The HBV particle, a causative agent of hepatocellular carcinoma, was then found in the serum of patients suffering from Hepatitis B (Dane, Cameron et al. 1970).

Although early studies identified a role for papilloma viruses in the aetiology of tumours in rabbits (Shope and Hurst 1933), it was not until the 1970 and '80s when Harald Zur Hausen and colleagues established that multiple human papilloma virus (HPV) strains,

such as HPV11, 16 and 18, and not HSV-1 as previously thought, were causative agents for cervical cancer (Zur Hausen 1976, Dürst, Gissmann et al. 1983, Gissmann, Wolnik et al. 1983, Boshart, Gissmann et al. 1984). The first known human retrovirus to cause human cancer, human T-cell leukemia virus type 1 (HTLV-1) was identified from cultured lymphocytes from a patient with a T-cell lymphoma by Robert Gallo's group (Poiesz, Ruscetti et al. 1980). Human herpes virus 8 (HHV-8) was found to be associated with the majority of Kaposi's sarcomas in AIDS patients and was considered to be a causative agent (Chang, Cesarman et al. 1994). In this regard, the retrovirus HIV-1, was shown to facilitate KSHV (human herpes virus 8 (HHV-8)) induction of Kaposi sarcomas in AIDS patients, through immunosuppression (Cesarman, Damania et al. 2019). More recently, Merkel cell polyoma virus (MCV) was shown to be clonally integrated in skin cancers known as Merkel Cell Carcinoma by Chang and Moore in 2008 suggesting that the virus might contribute towards the pathogenesis of the disease (Feng, Shuda et al. 2008).

1.2.2. Viral oncogenes and carcinogenesis.

The next step in tumour virology was to determine the molecular basis of virus-induced tumourigenesis. More recently it has been recognized that viruses, or any infectious agent causes cancer either directly through the expression of viral oncogenes, or indirectly by the induction of chronic inflammation, induction of immunosuppression, inhibition of cellular apoptosis, or the induction of chromosomal instability and translocation (Kuper, Weimin et al. 2001, zur Hausen 2009).

The study of retroviruses has taught us much about the molecular basis of cancer. The first viral oncogene to be identified was *v-src* from RSV, which was found to correspond to a cellular gene, *c-src* that had been acquired by the virus and incorporated into the RSV genome (Stehelin, Varmus et al. 1976). It was later established that *v-src* and *c-src* gene products were tyrosine kinases and that the *v-src* gene product was a constitutively activated version of *c-src* that lacked a regulatory C-terminal domain, such that *v-src* was oncogenic and *c-src* was not (Coussens, Cooper et al. 1985). It has been suggested that the enhanced mitogenic activities of *v-src* promote uncontrolled cellular proliferation and cancer. Other retroviral oncogenes have subsequently been identified that similarly have a cellular origin and are often de-regulated in human cancer. For instance the transcription factor, v-Myc is the transforming protein of Avian myelocytomatosis virus MC29 (Vennstrom, Sheiness et al. 1982) and *c-myc* is often overexpresed in human cancers, such as Burkitt's lymphoma and neuroblastoma (Meyer and Penn 2008). Other examples include the *v-ras* oncogenes of Harvey, and Kirsten Sarcoma viruses, whose cellular equivalents are often constitutively activated in human cancers such as colon carcinoma (Simanshu, Nissley et al. 2017). In this regard the Ras protein functions as a molecular switch in the mitogenic Ras-Raf-MAPK pathway which is constitutively activated in cancers (Simanshu, Nissley et al. 2017).

Transforming DNA viruses also express their own distinct gene products that induce cancer. Whilst this will be discussed in detail later for adenoviruses, most DNA virus oncogene products inactivate the p53 and pRB cellular tumour suppressor proteins and other proteins involved in genomic stability to induce tumourigenesis. Although adenovirus is the main model for cellular transformation by DNA viruses, other viruses such as HPV and SV40 also target these pathways specifically. Indeed it is well known

that HPV E6 proteins inactivate p53, whilst HPV E7 proteins inactivate pRB and SV40 large T antigen targets both p53 and pRB (Ali and DeCaprio 2001, Viarisio, Gissmann et al. 2017). As viruses typically target the key cellular proteins to promote its replication, it is perhaps no surprise that inactivation of p53 and/or pRB proteins occurs in most human cancers.

1.3. Adenoviruses.

Adenoviruses are small, linear, non-enveloped, double-stranded (ds) DNA viruses with icosahedral, nucleocapsid symmetry ranging in size from size 26 to 45 kilobases (kb), with human adenoviruses around 35 kb. It was originally discovered in 1953 by Rowe and his colleagues and, independently in 1954 by Hillman and Werner, whilst working with viruses of the common cold. Rowe isolated viral particles from the adenoids and, as such adenovirus was originally named 'adenoid degenerating agent' (Rowe, Huebner et al. 1953). Hillman and Werner were studying a flu-like virus in army recruits and, independently, successfully isolated adenovirus form tracheal cells (Hillman and Werner, 1954). Interest in the molecular biology of adenoviruses grew enormously when Trentin determined that human Ad12 induced tumours in hamsters (Trentin et al., 1962). Indeed, adenovirus was the model system in which messenger RNA splicing was first discovered by Sharp and Roberts (Berk and Sharp 1977, Chow, Roberts et al. 1977). More generally however, adenoviruses are the causative agents of upper respiratory tract infections, conjunctivitis and gastroenteritis with lasting duration of infections mainly in immunocompromised patients (Turnell 2008). As adenoviruses are characterised as 'low risk' viruses, which can induce tumours in experimental animals, they can be used as tools to study in detail the molecular and cellular biology of the normal cell, and

cancer cell. More recently, adenoviruses have been used as vectors for gene delivery and therapy, and have been modified substantially to generate conditionally-replicating adenoviruses that have selective growth properties in cancer cells (Shaw and Suzuki 2016).

1.3.1. Classification.

David Baltimore classified adenoviruses as group one double-stranded (ds) DNA viruses in his Baltimore system of virus classification. Later in the 1960's the ICTV (International committee on taxonomy of viruses) placed adenoviruses in the family *Adenoviridae* and divided them into five *genera* depending on its ancestral types: *Mastadenoviridae* (infecting Mammals), *Aviadenoviridae* (infecting birds), *Atadenoviridae* (infecting reptiles), *Siadenoviridae* (infecting frogs, turkeys and raptors) and *IchtaAdenoviridae* (infecting Fish) (Norrby, Bartha et al. 1976). The *Mastadenoviridae* (human Adenoviruses Ad) are further divided in to seven species (A, B1, B2, C, D, E, F and G) depending on their haem agglutination and neutralization properties, which also reflects their oncogenic properties (Madisch, Harste et al. 2005).

Group	Types	Oncogenicity in rodents	Transformation in vitro
A	12, 18, 31	High	Yes
A (new)	61	Unknown	Unknown
B(new)	66, 68, 76, 77, 78, 79	Unknown	Unknown
B1	3, 7, 16, 21, 50	Moderate	Yes
B2	11, 14, 34, 35, 55	Moderate	Yes
C	1, 2, 5, 6, 89	Low or none	Yes
D	8, 9, 10, 13, 15, 17, 19, 20, 22-30, 32, 33, 36-39, 42-49, 51, 53, 54	Low or none	Yes
D (new)	56, 58, 59, 60, 62, 63, 64, 65, 67, 69, 70, 71, 72, 73, 74, 75, 80, 81, 82, 83, 84, 85, 86, 87, 88, 90, 91, 92, 93, 94, 95, 96, 97, 98, 99, 100, 101, 102, 103	Unknown	Unknown
E	4	Low or none	Yes
F	40, 41	None reported	Yes
G	52	None reported	Unknown

Table 1.2. Classification of Adenoviruses. Taken Adapted from,(Turnell 2008), (Dhingra A 2019), (http://hadvwg.gmu.edu/).

Human adenovirus serotypes can cause a wide range of infections in humans being dependent on the host immune response (Echavarria 2008). Although in recent years adenovirologists have begun to study the biology of different adenovirus types in more detail, most experimental studies have focussed on the closely related group C viruses, Ad2 and Ad5. Although Ad5 is non-tumourigenic it can transform human embryonic kidney cells, such that Ad5E1-transformed HEK293 cells are a widely utilised cell line for studying cellular functions (Graham, Smiley et al. 1977). The tumour-promoting Ad12, from group A, is also widely studied and can similarly transform human

embryonic retinoblast (HER) cells in tissue culture (Byrd, Brown et al. 1982). Although Ad12 induces undifferentiated tumours in new born hamsters, Ad12 is known to undergo fully productive replication cycle in human cell cultures, the probable explanation for the potential of Ad12 in crossing the barrier from humans to hamsters in its oncogenesis is, Ad12 when infects human cells, it kills all the infected cells with the productive interaction resulting in cells not transformed in to tumour cells, hence Ad12 is not identified as oncogenic in humans, however with the hit and run mechanism, Ad12 could be involved in human tumorigenesis (Doerfler W. 2007)

1.3.2. Adenovirus Structure and Genome.

Adenoviruses are amongst the largest non-enveloped viruses studied by electron microscopy and X-ray diffraction at a resolution of 3.5 Å, with a size of 150 MDa. The capsid, approximately 70 to 100 nm in size, is comprised of 252 capsomeres of which 240 are homotrimeric hexons forming the faces of the capsid, and the other 12 are penton bases that form the vertices of the capsid; small fibres with terminal knobs protrude from each penton base (Brenner and Horne 1959, Valentine and Pereira 1965)(Figure 1.1). Proteins IIIa, VI, VIII and IX also associate with the capsid and are thought to provide extra structural integrity to the capsid (Saban, Silvestry et al. 2006). The linear adenovirus dsDNA genome is 26 to 45 kb in size which is surrounded by capsid. The highly characterised adenovirus serotype 5 genome size is 36 kb and it encodes 40 proteins (Saha, Wong et al. 2014) and the adenovirus serotype 12 genome size is 34125bp and it encodes 27 proteins (Mariana Hosel 2001). In the well characterised Ad5 genome, depending on their expression patterns relative to viral DNA replication, the major transcription coding regions of adenoviruses are named as early genes: E1,

E2, E3 and E4, which are expressed before viral DNA replication, and late genes (L1 to L5) which are expressed after viral DNA replication. The intermediate genes (IVa2 and IX) and small VA RNAs are expressed before the late genes (Figure 1.2) (Russell 2000). Ad genomes are characterized by inverted repeated sequences (ITRs) that are located at both ends of the genome, which are 100-140 bp in size. Terminal protein (TP) associates covalently with the 5' terminus of each ITR and serves as a primer for adenovirus replication (see section 1.3). The origin of viral replication from which adenovirus DNA replication is initiated is located at 36-46 bp from the terminal end of the genome sequence.

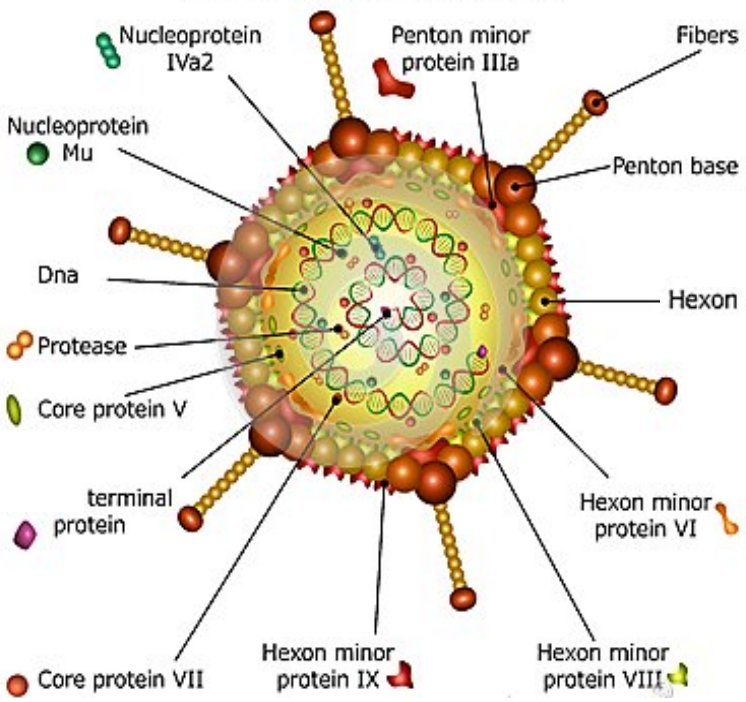

Figure 1.1. Schematic depiction of the Adenovirus virion. The image shows the arrangement of the proteins that comprise the viral capsid and also illustrates the linear dsDNA adenovirus genome and the viral proteins associated with the genome. Illustration taken from: (Gaurab Karki 2018).

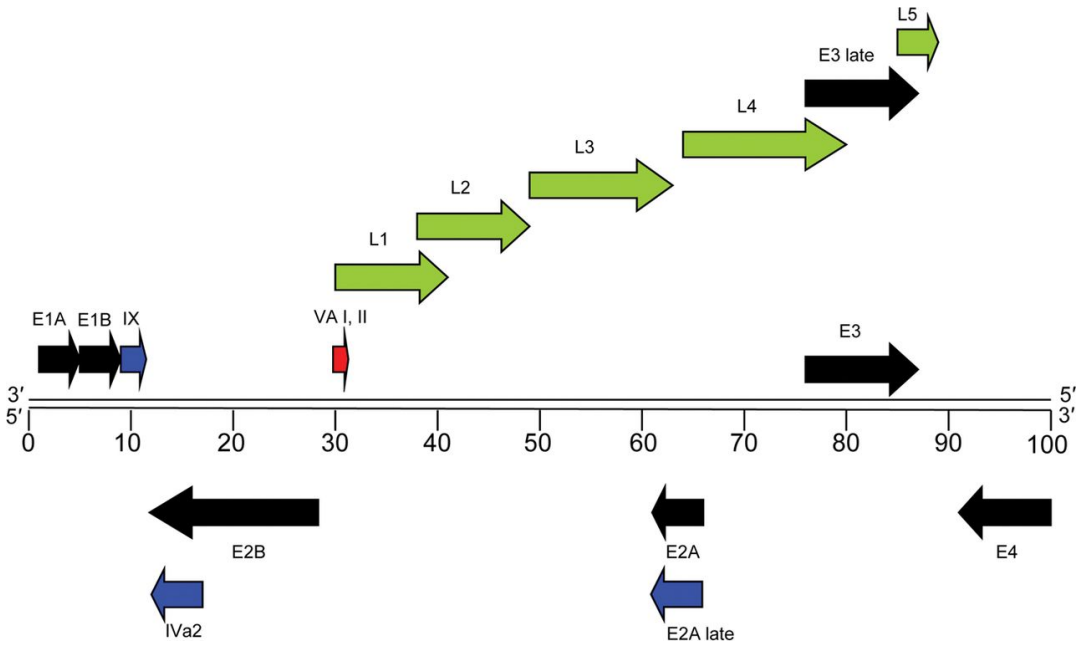

Figure 1.2. Schematic illustration showing Ad5 genomic transcription map. The panel outlines the gene expression profile form the Ad genome following viral infection. Black arrows represent E1A, E1B, E2A, E2B, E3 and E4 Ad early proteins, blue arrows indicate IX and IV2 intermediate proteins and green arrows highlights L1 – L5 late proteins. Taken from: (Hall, Blair Zajdel et al. 2010)

1.3.3. Adenovirus replication.

The successful propagation of adenovirus in the host cell depends on its ability to enter the host cell, replicate its genome and package itself into new virions for dissemination. Adenovirus DNA replication occurs approximately 6 to 8 hours post infection and within 40 hours of infection, Ad produces new virions in the infected cell. Different Ad proteins are involved in promoting viral DNA replication from virus entry into the cell to carry out successful viral DNA replication. Adenovirus cellular tropism is mainly defined by its fibre proteins which facilitate cell entry by attaching to the CAR receptor (Coxsackie virus and Adenovirus receptor)(Wu and Nemerow 2004). CAR is a 46 KDa Ig (immunoglobulin) super-family protein that act as a primary receptor for most of the

adenoviruses (Hartlerode, Morgan et al. 2015). The other important receptors are the membrane cofactor protein (MCP) also called as CD46, Desmoglein 2 (DSG2), Sialic acid and αvβ3/5 (Baker, Aguirre-Hernández et al. 2018). Some of the Ad proteins required to interact with distinct cellular receptors, and the residues implicated in binding are shown in the below Table 1.3 (Baker, Aguirre-Hernández et al. 2018).

Along with the CAR, adhesion of the penton base proteins to αvβ3/5 integrin receptors through clathrin-coated pits triggers the internalisation of the virus (Imelli, Meier et al. 2004). Endocytosis results in capsid dissociation and structural rearrangement of the viral particles. Viral particles utilise hexon association with cytoplasmic Dynein networks to transport to the nucleus whereupon they enter the host cell nucleus through nuclear pores to initiate viral DNA replication (Imelli, Meier et al. 2004, Wu and Nemerow 2004, Bremner, Scherer et al. 2009).

Receptor	Prototype Viral Receptor	Receptor Binding Residues	Previously Demonstrated Tropism Aablating Mutations
CAR	Ad5—Fiber Protein knob	A406; S408; P409; R412; Y477; R481; L485; Y491	KO1 (SP408-409EA); KO2 (ΔVK441-44s); KO3 (R460E); KO4 (ΔGK509-510); KO5 (ΔGT538-539); KO8 (N468T); KO9 (V466H); KO10 (P505A); KO11 (Δ404-581 Whole region)
			ΔTAYT (ΔTAYT489-492)
CD46	Ad35—Fiber Protein knob	F132; N133; T136; R169; M170; S172; N194; E192	F242; R279; S282
DSG2	Ad3—Fiber Protein Knob	N186; V189; S190; D261; F265; L292; L296; E299	N186D; V189G; S190P; D261N; F265L; L296R; E299V; ND186-261DN; ΔD261+L296R; NDL186-261-296DNR.
GD1a/Sialic acid	Ad37—Fiber Protein knob	Y308; Y312; P317; V322; K322	None reported
Blood Coagulation Factor X	Ad5—Hexon Protein HVR's	HVR regions 3; and 7 (Individual residues not clearly defined).	Ad5HVR48 (Ad5 with the HVR's of Ad48)
			HVR5-BAP (71aa BAP (Biofilm Associated Protein) peptide insert)
			HVR5* (TE268-269AT); HVR7* (ITEL420-422-423-425GNSY); E451Q
HSPG	Ad5—Fiber Protein shaft	KKTK91-94	S* (KKTK91-94GAGA); KKTK91-94RGDK
Integrin	Ad5—Penton Protein	R340, G341, D342	RGE (D342E)
			EGD (R340E)
MARCO	Ad5—Hexon Protein	HVR1; implied but not conclusively determined	None reported

Table 1.3. Host cell receptors targeted by adenovirus capsid proteins. Table taken from (Baker, Aguirre-Hernández et al. 2018).

There are three main replication proteins involved in adenovirus genome replication, the TP precursor protein (pTP), the Ad DNA polymerase protein (Ad pol) and the Ad DNA binding protein (Ad DBP) which are all transcribed from the E2 region (Holm,

Bergmann et al. 2002). pTP is an 80 kDa protein that acts as a primer for replication initiation and binds to both ssDNA and dsDNA, whilst Ad pol is a 140 kDa protein and belongs to the distant group of α-like DNA polymerases that utilises the pTP primer for replication initiation (Field, Gronostajski et al. 1984). Ad DBP is a multifunctional phospho-protein of approximately 55 kDa and is known to be involved in multiple activities during viral replication and is located in the nucleus of infected cell (Chang and Shenk 1990). For the initiation of Ad DNA replication, Ad Pol covalently links the β-OH group of a Ser residue in pTP to the α-phosphoryl group of dCMP (deoxycytidine monophosphate) to form the pTP/dCMP complex that functions as a primer for DNA synthesis (Liu, Naismith et al. 2003). Ad DBP binds to both ssDNA and dsDNA and stimulates the Ad pol by promoting the binding of cellular protein NFI to Ad pol (de Jong, van der Vliet et al. 2003, Hoeben and Uil 2013) (Rob C Hoeben 2013), and the cellular Oct-1 protein to pTP. Both cellular NFI and Oct-1 form the replication preinitiation complex with Ad pTP, pol and DBP, which in concert bind viral DNA and stimulate replication (Hoeben and Uil 2013). DBP also promotes DNA elongation in an ATP-dependent manner because of its helix destabilising activity and its ability to unwind DNA. The ability of the major replication proteins pTP, Ad pol and Ad DBP to form stable complexes with NFI and Oct-1 increases viral DNA replication up to 200 fold (de Jong, van der Vliet et al. 2003).

1.3.4. Ad early region gene E1A.

Adenoviral E1A gene products are the first to be transcribed, within an hour of viral infection (Yousef, Brandl et al. 2009). The mRNAs transcribed from E1A transcriptional units are 13S, 12S, 11S, 10S and 9S that produce, respectively, proteins

of 289, 243, 217, 171 and 55 amino acids in size. The 13S and 12S gene products are produced during early stages of infection, whilst the 9S, 10S and 11S gene products are produced during the late stages of infection, although their function is poorly understood. The 13S and 12S gene products differ in size by 46 amino acids (Conserved Region 3- CR3) in Ad5 and are produced by differential splicing of mRNA. 12S and 13S E1A gene products are highly modular with functional conserved regions CR1, CR2 and CR4 that are conserved between different Ad types and a less well conserved N-terminal region (NTR; Figure 2) that bind cellular protein targets (Boulanger and Blair 1991). The molecular weight of E1A 12S and 13S gene products is highly variable when analysed by SDS-PAGE, ranging from 35 to 48.0 and 40 -52 kDa respectively, due to the highly phosphorylated nature of E1A. The adenovirus E1A proteins are not DNA binding proteins (Yousef, Brandl et al. 2009), but they interact with cellular proteins that do interact directly with chromatin to regulate transcription (Figure 1.3) (Gallimore and Turnell 2001, Berk 2005).

Adenovirus E1A proteins play a major role in transcriptional activation and repression and function as cooperating oncoproteins in cellular transformation. This ability of E1A resides in its capacity to initiate DNA synthesis and cell cycle entry in quiescent cells through interaction with cellular proteins that regulate cell cycle progression, mitosis and apoptosis (Gallimore and Turnell 2001). E1A promotes transformation through its association with host cellular proteins like the Retinoblastoma family (pRB, p107 and p130) of transcriptional repressors, the CBP/p300 transcriptional co-activators, the transcriptional co-repressor CtBP proteins, TRAPP/p400 chromatin modifiers, and DYRK1 and DCAF7 cell growth regulators (Fuchs, Gerber et al. 2001, Gallimore and Turnell 2001, Cohen, Yousef et al. 2013). E1A can however, can also act as a

transformation suppressor and function as anti-oncogene in the absence of cooperating oncogenes (Frisch and Mymryk 2002).

1.3.5. Ad E1A 13S and 12S proteins.

The adenovirus CR3 domain in the 13S E1A gene product plays a vital role in gene regulation by acting as transcriptional activator for all early region promoters during infection and has served as a vital tool to study basic transcriptional processes (Pelka, Ablack et al. 2009). The CR3 region is composed of two regions: a zinc-finger region (amino-acids 147-177; Ad5) and a carboxyl-terminal region (amino acids 183-188; Ad5). The zinc finger region is responsible for binding to the general transcriptional machinery such as TBP. It has been established that the transactivation capacity of zinc-finger region of CR3 resides in its ability to bind to TBP, Mediator subunit, MED23/Sur2, and 19S, 20S and 26S proteasomes (Lee, Kao et al. 1991, Stevens, Cantin et al. 2002, Rasti, Grand et al. 2006). The carboxyl-terminal region of CR3 possesses a promoter-targeting region, which facilitates E1A interaction with several specific transcription factors like ATF1-3, SP1, USF and CBF/NF-Y and TBP-associated factors (TAFs). Co-activator proteins, like CBP/p300, also bind to the CR3 domain to regulate transcription. In oncogenic Ad serotypes of adenoviruses, there is a alanine-rich region in between the CR2 and CR3 domain, which plays a significant role in tumour induction (Figure 1.3) (Gallimore and Turnell 2001).

Unlike the 13S CR3 domain, which mainly functions as transcriptional activator, the smaller 12S E1A species, lacking CR3, has the capacity to function as both a transcriptional repressor and a transcriptional activator, in order to promote cell growth,

or apoptosis, and suppress differentiation (Gallimore and Turnell 2001). Specific binding regions present in CR1 and CR2 (LxCxE motif; Figure 1.3) are capable of binding the pocket domains of the cellular tumour suppressor proteins pRB, p107 and p130. The same pocket domains in the pRB family of proteins are required for binding E2F transcription factors and as a result, E1A expression blocks the E2F-interaction with pRB resulting in dissociation of E2F from the pRB complex resulting in E2F-driven S-phase induction, cell cycle progression and cellular transformation (Raychaudhuri, Bagchi et al. 1991, Berk 2005). The adenovirus E1A N-terminal region and CR1 domain binds to several other cellular protein complexes involved in chromatin remodelling, like histone-directed acetyltransferase (HATs), histone–directed deacetylases (HDACs) proteins, nucleosomal remodelling factors like SWI/SNF and nucleosomal associated proteins (Gallimore and Turnell 2001, Berk 2005). The HAT protein p300 was the first identified through its interaction with the NTR and CR1 regions of E1A; the closely related CREB-binding protein (CBP) was also found to associate with E1A through these regions. The p300/CBP HATs are approximately 300 kDa in size and activate transcription by acetylating core histone proteins (Berk 2005). E1A has the capacity to associate with functional CBP/p300 HAT activity and can also redistribute CBP/p300 to specific genomic loci during infection (Ferrari, Pellegrini et al. 2008, Horwitz, Zhang et al. 2008, Ferrari, Gou et al. 2014). Mutational studies have shown that the interaction of CR1 and CR2 with either pRB proteins or CBP/p300 proteins is required for E1A's ability to induce S-phase in quiescent cells, whereas CR1 domain interactions with both pRB and CBP/p300 proteins is required for cells to undergo mitosis and promote cellular transformation (Jelsma, Howe et al. 1989).

The C-terminal domain known as CR4 is encoded by Exon 2 of E1A (Figure 1.3). CR4 extends from amino acid residues 240 to 288 of E1A (Yousef, Brandl et al. 2009). CR4 interacts with cellular proteins CtBP-1, 2 and 3 (C-terminal binding proteins), which are named such as they were first identified through their interaction with the C-terminal region of E1A, in particular the PxDLS motif located in this region. CtBP are also known to interact with HDACs to repress transcription. Interestingly E1A acetylation by p300/CBP at amino acid K-239 adjacent to the CtBP-binding site inhibits CtBP association with E1A (Zhang, Yao et al. 2000). Apart from CtBP, CR4 also binds to the dual specific Tyrosine-regulated kinase proteins (DYRK 1A AND DYRK 1B) and DYRK 1A–co factor HAN 11 and these interactions aid virus infection and oncogenic transformation (Yousef, Brandl et al. 2009).

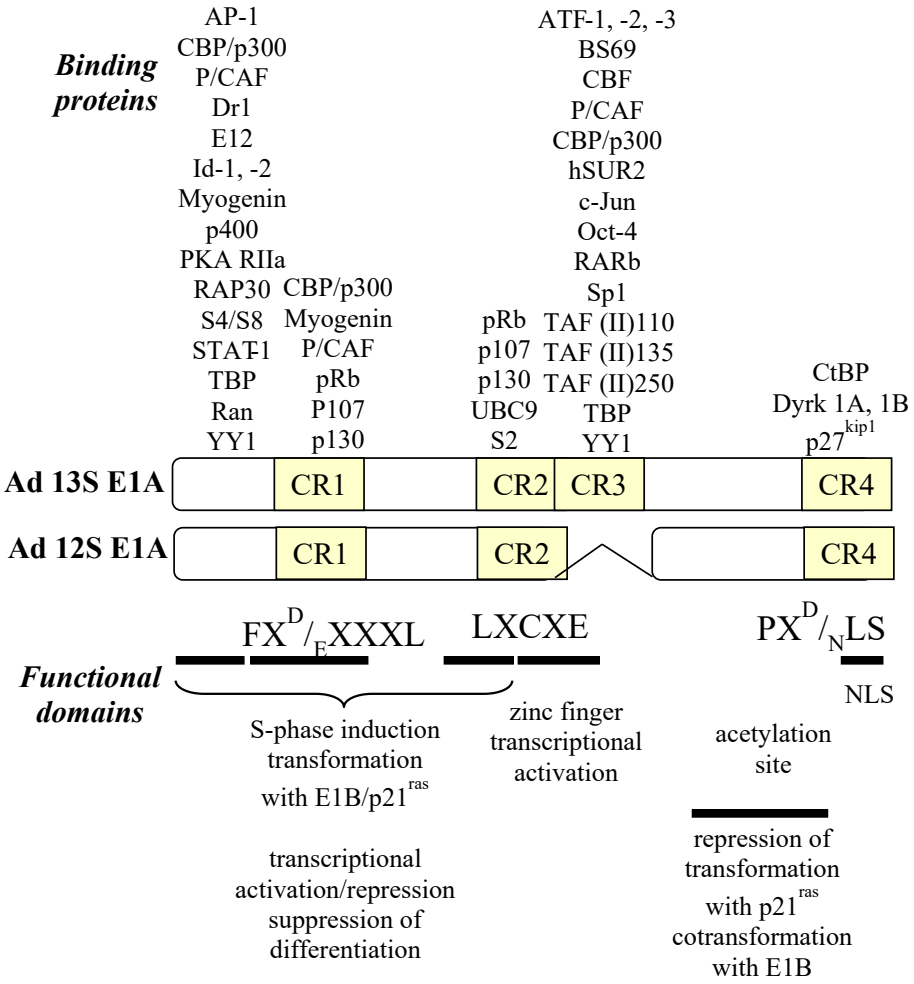

Figure 1.3. Schematic illustration showing the conserved regions of E1A, E1A-binding proteins and functional domains: The figure illustrates the conserved regions of Ad E1A species, and the key cellular proteins known to bind to the N-terminal region, CR1, CR2, CR3 and CR4 domains. The role of each E1A region in biological processes is also below each region. Taken from (Gallimore and Turnell 2001).

1.3.6. Ad early region gene E1B.

Adenovirus early region E1B gene products are involved in promoting viral DNA replication during infection and promoting cellular transformation. There are five different gene products encoded through alternative splicing of E1B mRNAs, of which E1B-55K (496R) and E1B-19K (156R) gene products are the best characterised in both

infection and transformation, where they co-operate with E1A in the transformation of rodent cells although they lack the ability to transform the cells individually. Research shows that both E1B-55K and E1B-19K together function to inhibit growth arrest and apoptosis (Sieber and Dobner 2007, Blackford and Grand 2009). Ad E1B-19K is a functional homologue of the BCL2 anti-apoptosis factor and binds to pro-apoptotic BAX, activated by tBID, and prevents the formation of BAK/BAX oligomers at mitochondrial membranes and thus inhibits apoptosis (Sundararajan, Cuconati et al. 2001, White 2001). A major role of the E1B-55K protein is to inhibit p53-dependnet apoptosis. Ad5 E1B-55K directly binds to p53 and protects cells from p53 dependent apoptosis through its ability to inhibit the activation of p53-dependent transcription programmes (Sarnow, Hearing et al. 1984, Yew and Berk 1992). E1B-55K and p53 have been shown to associate in cytoplasmic compartments known as aggresomes (Zantema, Schrier et al. 1985, Yew and Berk 1992). Ad5 E1B-55K is post-translationally modified by phosphorylation and SUMOylation whereas Ad12 E1B-55K is not known to be post-translationally modified by either phosphorylation or SUMOylation (Blackford and Grand 2009). Indeed, Ad5 E1B-55K is a SUMO-ligase and can self-SUMOylate as well as SUMOylate p53, which also serves to inhibit of p53 activity (Muller and Dobner 2008). Ad E1B-55K does not function in isolation and is known to cooperate with E4orf3 and E4orf6 during infection particularly to regulate host-cell shut-off of protein synthesis, and cooperate with these proteins and E1A in cellular transformation (Nevels, Rubenwolf et al. 1997, Nevels, Täuber et al. 1999, Nevels, Täuber et al. 2001).

Apart from E1B-55K and E1B-19K, the other three E1B proteins are E1B-84R, E1B-156R and E1B-93R named depending on their number of amino acids; their functional

role is not known however (Sieber and Dobner 2007). A Schematic representation of E1B region is shown Figure 1.4 (Zheng 2010).

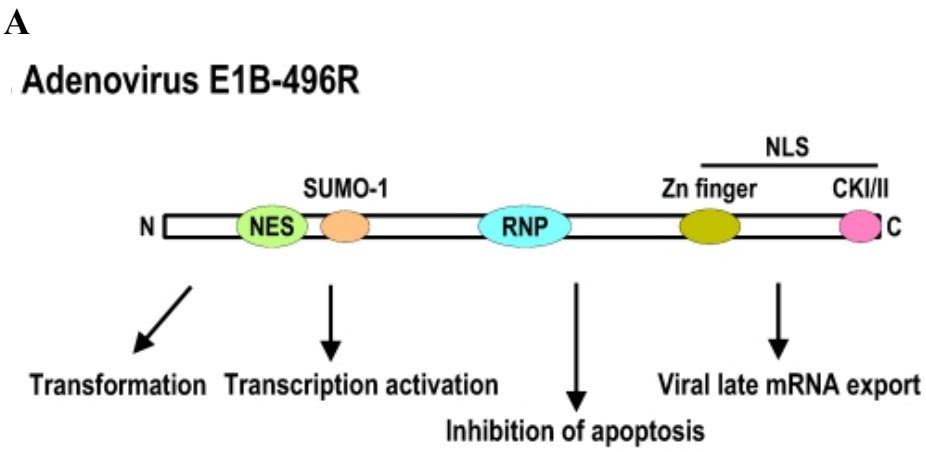

Figure 1.4.A. linear representation of E1B-55K and depiction of its functional roles. Full length (289R) E1A protein structure, conserved regions (CR1 to CR4), mapped domains and its biological functions are indicated (Zheng 2010).

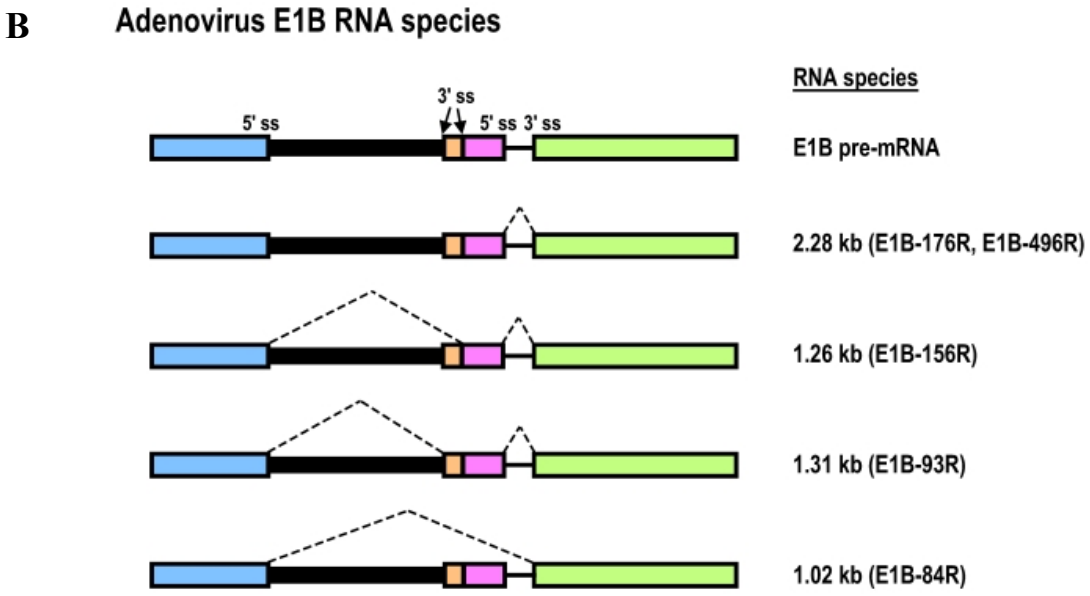

Figure 1.4.B. linear representation of E1B mRNA species. Alternative spliced species of E1B mRNA showing bidirectional splicing enhancer in green as exon 2 and the arrows indicating splicing factors and regulators that control splice site selection and dotted lines indicating splice direction. Figure taken from (Zheng 2010).

1.3.7. Adenovirus E3 region.

The E3 transcription region of adenoviruses is mainly involved in encoding different immunomodulatory proteins and serves to promote immune evasion. E3 is conserved in different Ad serotypes and also plays vital roles in releasing progeny virus during infection, through expression of the ADP (Adenovirus death protein) gene product that is expressed late during infection. The E3 region is known to encode nine different mRNA splice variants from two RNA precursors, E3A and E3B. E3 promoters involved in generating E3 transcripts are activated by transcription factors such as ATF, NF-1, AP-1 and NFkB and a TATA box (Brady and Wold 1988, Wold, Tollefson et al. 1995, Zhao, Chen et al. 2014). Among the proteins encoded by the E3 region, gp-19K is an abundantly synthesised viral early protein and integral transmembrane glycoprotein which serves to down-regulate major histocompatibility complex class I antigens during infection (Brady and Wold 1988, Wold, Tollefson et al. 1995). Additionally, E3 14.7K and 10.4K proteins are involved in inhibiting TNF (tumour necrosis factor)-dependent cytolysis, which is known to be an anti-viral factor (Krajcsi, Dimitrov et al. 1996).

1.3.8. Ad early region gene E4.

The transcription unit of the E4 region is located at the right-hand side of the Ad genome and is transcribed from the bottom strand, generating a primary transcript of 2800 nucleotides in length (Täuber and Dobner 2001). Alternative splicing of this transcript generates at least 18 E4 mRNAs that encode at least 7 different open reading frames (orf) orf1, orf2, orf3, orf3/4, orf4, orf6 AND orf6/7. Among these E4orf's, orf3, orf4 and orf6 have all been studied in detail (Halbert, Cutt et al. 1985, Thomas, Schaack et

al. 2001, Zhao, Chen et al. 2014). E4 proteins interact with multiple other cellular proteins involved in cell cycle survival and genome stability and play vital roles in viral DNA replication, virus assembly, transcription, translation and host cell shut off, as well as cooperating in Ad-mediated transformation (Nevels, Täuber et al. 2001, Täuber and Dobner 2001, Weitzman and Ornelles 2005, Ou, Kwiatkowski et al. 2012). Very little is known about the function of E4orf1 and E4orf2 during infection, although Ad9 E4orf1 is highly oncogenic and can induce mammary tumours in rodents (Thomas, Schaack et al. 2001). E4orf4 is known to associate with the regulatory B subunits of protein phosphatase 2A to induce p53-independent apoptosis and, as such, is a potential cancer therapeutic agent (Kleinberger and Shenk 1993, Shtrichman, Sharf et al. 2000). E4orf4 is also known to inhibit the E1A-dependent transactivation of viral promoters E2 and E4 (Kleinberger 2015). E4orf6/7 are involved in regulating E2F-dependent transcription in a similar way to E1A and induces apoptosis (Helin and Harlow 1994).

E4orf3 and E4orf6 are known to have overlapping, and significant roles, in both viral infection and cellular transformation and have been the source of intensive study (Täuber and Dobner 2001). Mutational analysis has shown that viral mutants lacking either E4orf3 or E4orf6 has little or no effect on the viral lytic life-cycle but mutants lacking both E4orf3 and E4orf6 have severe defects in viral replication, the accumulation of viral mRNA transcripts in the cytoplasm and host cell shut-off of protein synthesis (Halbert, Cutt et al. 1985). Furthermore, E4orf3 and E4orf6 associate with each other, and can similarly bind to E1B-55K and target E1B-55K to viral replication centres in the nucleus and prevent viral DNA concatemer formation (Halbert, Cutt et al. 1985, Huang and Hearing 1989, Weiden and Ginsberg 1994, Täuber and Dobner 2001, Stracker, Carson et al. 2002).

E4orf3 encodes a 11 kDa protein, which is highly conserved amongst different Ad types is and the first gene product of E4 region known to be found in infected cells. E4orf3 associates with the nuclear matrix to reorganise components of PML (promyelocytic leukemia)-containing bodies to nuclear tracks surrounding viral replication centres (Sarnow, Sullivan et al. 1982, Downey, Rowe et al. 1983, Carvalho, Seeler et al. 1995, König, Roth et al. 1999). Structural analyses revealed that E4orf3 exists in cells as a dimer subunit, which are able to assemble with other E3orf3 dimers through interactions in the C-terminal regions of the protein, to form linear and branched oligomer chains throughout the cell. The consequence of E4orf3 polymerisation is to create high affinity multivalent binding sites for cellular interacting proteins (Soria et al 2010). E4orf3 is known to inactivate the functions of known tumour suppressor proteins p53, TIF1α (TRIM24), TIF1β (TRIM28), TIF1γ (TRIM33) and PML through either direct interaction, or through modulation of epigenetic signalling pathways (Soria, Estermann et al. 2010, Forrester, Patel et al. 2012, Ou, Kwiatkowski et al. 2012). As such, E4orf3 inhibits the transcription activity of p53 through the epigenetic silencing of transcription activated by p53-responsive promoters by acting as scaffolds to direct heterochromatin assembly to silence transcription activated by p53 by targeting p53 target promoters (Soria, Estermann et al. 2010). A schematic representation of E4 region is shown in Figure 1.5 (Zhao, Chen et al. 2014). Interestingly, E4orf3, akin to E1B-55K, has been shown to be a SUMO E3 ligase and targets TIF1γ and TFII-I for SUMO-Targeted ubiquitin ligase-mediated degradation (Forrester, Patel et al. 2012, Bridges, Sohn et al. 2016, Sohn and Hearing 2016).

The E4orf6 mRNA encodes a highly conserved 34 kDa protein which contains an N-terminal NES (nuclear export sequence) and C-terminal NLS (nuclear localization

signal) along with an α-helical, arginine-rich, NRS (nuclear retention signal) that helps recruit the E1B-55K and E4orf6 complex to the nucleus (Orlando and Ornelles 1999). In isolation, E4orf6 binds directly to p53 through its C-terminal regulatory domain and inhibits the interaction of the N-terminal transactivation domain of p53 with a component of transcription factor (TFIID), TAFII31, thus, serving to inactivate p53-mediated transcription (Dobner, Horikoshi et al. 1996). Although many studies have studied these proteins in isolation, most of the functions of the E4orf6 are in cooperation with the E1B-55K protein. A consideration of their joint functions will be considered in detail later when discussing the relationship between adenovirus and host cell DNA damage response and repair pathways (see section 1.6).

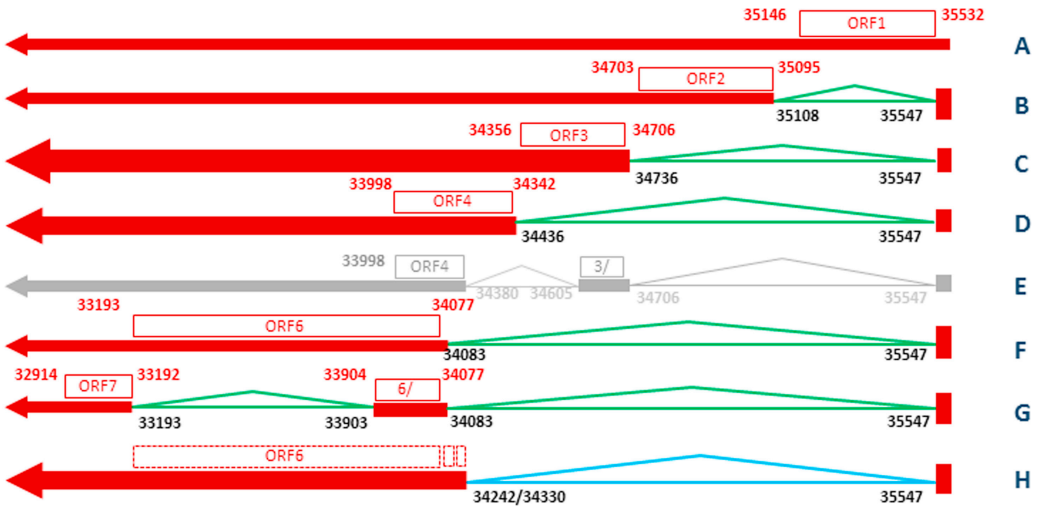

Figure 1.5. Linear representation of E4 gene products. Taken from (Zhao, Chen et al. 2014).

1.3.9. Biological importance of studying adenoviruses.

Since the discovery of adenovirus nearly 70 years ago by Rowe, Hillman and their colleagues and its discovery as a human oncogenic virus by John Trentin and colleagues, adenovirus has been widely used a model system in research to study the molecular and cellular biological processes of cellular transformation and tumourigenesis (Weitzman and Ornelles 2005). In this regard, a number of cellular proteins were first identified as interacting proteins for adenovirus proteins such as: p300, p400/TRRAP, CtBP, p107 and ATF, whilst although not originally identified using adenovirus, studies with adenovirus have taught us much about the function of the pRB and p53 tumour suppressors (Berk 2005). More recently E1 and E3 -deleted adenoviruses have been used as a gene-delivery vectors for gene therapy applications, and the development of conditionally-replicating/oncolytic adenoviruses have been used to selectively infect, and kill cancer cells (McCormick 2001, Lyle and McCormick 2010). Whilst adenovirus still has much to teach us about the individual functions of cellular proteins, and how viruses utilise, or inhibit, these proteins during viral infection or cellular transformation, developments in genomic and proteomic technologies have allowed us to study how viruses, or individual viral proteins function globally to modulate signalling pathways important in cell growth, death and survival pathways (Weitzman and Fradet-Turcotte 2018). Our laboratory, amongst many others, is particularly interested in utilising proteomic methods to understand how viruses and virus proteins regulate the cellular response to DNA damage in order to facilitate viral replication, such that we can also identify, and determine, the function of cellular proteins that participate in DNA damage response pathways.

1.4. The cellular response to DNA damage.

The DNA damage response (DDR) is a cellular surveillance pathway that detects DNA damage and initiates cellular signalling pathways to halt the cell cycle and repair the DNA damage faithfully, or if the damage is deemed too extensive, to induce senescence or cellular apoptosis (Jackson and Bartek 2009). As such, DNA is constantly exposed to genotoxic stress-causing agents like ultra-violet (UV) light, ionizing radiation (I.R.) and toxic chemicals that can cause ssDNA and dsDNA breaks that need to be detected and repaired (Ciccia and Elledge 2010). Similarly, the natural process of cellular DNA replication can lead to replication stalling can lead to DNA damage that also activates cellular DDR pathways (Cimprich and Cortez 2008). Heritable defects in the DDR pathway can cause autoimmune diseases, neurodegenerative disorders, growth retardation, and cardiovascular disorders and enhanced cancer susceptibility. Individuals with genetic mutations in DDR genes are commonly predisposed to tumour formation due to their sensitivity to DDR agents (Gorgoulis, Vassiliou et al. 2005). Examples of heritable syndromes that have defects in DDR genes include hereditary breast cancer caused by mutations in BRCA1 and BRCA2; Ataxia telangiectasia (A-T) caused by mutations in ATM; A-T mutated like disorder (ATLD) caused by mutations in MRE11; Li-Fraumeni syndrome (LFS) caused by mutations in p53; Fanconi Anaemia (FA) caused by mutations in FANC genes; Seckel syndrome caused by mutations in ATR; and Schimke immunoosseous dysplasia (SIOD) caused by mutations in SMARCAL1 (Jackson and Bartek 2009).

DDR signalling pathways are controlled principally by the three members of the phosphoinositide 3-kinase (PI3K)-related kinases – termed PIKKs which have kinase

domains located within their C-terminal regions and have a preference for phosphorylating serine or threonine residues followed by a glutamine (Abraham 2004). These dual serine/threonine protein kinases are known as AT mutated (ATM), ATM and Rad3-related (ATR) and DNA-dependant protein kinase (DNA-PK) which act as apical sensor protein kinases in regulating cell cycle checkpoint control, DDR, DNA replication and apoptosis in response to DNA damage (Abraham 2001, Turnell and Grand 2012).

1.4.1. DNA-dependent protein kinase (DNA-PK).

DNA-PK is the prototypic member of the PIKK family of kinases and is involved exclusively in the non-homologous end-joining pathway. It is comprised of a 450 kDa catalytic subunit (DNA-PKcs), and has two regulatory subunits, Ku70 and Ku86 (Sancar, Lindsey-Boltz et al. 2004). DNA-PK is activated when it is recruited to double-strand breaks (DSBs) through engagement of the Ku 70/86 subunits with broken DNA ends. Two DNA-PK molecules at broken DNA ends serve to secure the broken ends to be ligated and moreover, recruit DNA ligase IV – XRCC4 complexes which mend the broken ends of DNA in the absence of a DNA template (Turnell and Grand 2012).

1.4.2. ATM kinase.

Ataxia telangiectasia mutated (ATM) is a 350-kDa protein that participates in homologous recombination repair pathways. Germ cell mutation, and inactivation of ATM causes the autosomal recessive syndrome known as Ataxia-Telangiectesia (A-T),

which is characterised by immunodeficiency, cerebellar degeneration, radiosensitivity, genome instability and cancer predisposition (Sancar, Lindsey-Boltz et al. 2004). ATM normally exists as an inactive homodimer and its activity is stimulated *in vivo* by DSB's caused by agents such as ionizing radiation and activated, autophosphorylated, ATM binds to DSB's in monomeric form through its regulatory partner, the MRN (Mre11-Rad50-NBS1) complex. ATM subsequently phosphorylates a number of substrates including the Chk2 effector kinase, p53, H2AX, TIF1β/KAP1, BRCA1 and NBS1 which participate in the repair of damaged DNA (Sancar, Lindsey-Boltz et al. 2004, Turnell and Grand 2012). It also activates effector proteins through phosphorylation, such as p53 and CHK2, to regulate the signalling cascades that initiate cell cycle checkpoint control (Hirao, Kong et al. 2000).

1.4.3. ATR kinase.

The ATR gene encodes a protein of size 303 kDa. Heritable, hypomorphic mutations in the ATR gene gives rise to the human autosomal recessive disorder, Seckel syndrome, which is characterised by microcephaly and mental, and growth, retardation (Sancar, Lindsey-Boltz et al. 2004, Byun, Pacek et al. 2005). ATR is an essential gene in proliferating cells and recent data suggests that ATR participates in regulating fidelity of chromosome segregation during mitosis (Brown and Baltimore 2000, Kabeche, Nguyen et al. 2018). ATR in association with its regulator, ATRIP (ATR-interacting protein) forms an ATR-ATRIP complex that responds to genotoxic stress such as UV light and agents that inhibit cellular DNA replication (Cimprich and Cortez 2008). ATR senses ssDNA breaks generated either during the processing of DSBs or ssDNAs generated during DNA replication fork stalling. ATR serves as both a sensor and

transducer in the DDR and initiates G2/M checkpoint control through the phosphorylation and activation of the CHK1 kinase (Byun, Pacek et al. 2005, Matsuoka, Ballif et al. 2007). ssDNA breaks are initially sensed by the ssDNA binding protein RPA (Replication protein A) complex. RPA is a heterotrimeric protein complex composed of three subunits: RPA70, RPA32 and RPA14. RPA32 is hyperphosphorylated by PIKK family kinases in response to DNA damage and modulates the downstream regulation of DNA replication. RPA is also involved in recombination and repair pathways. The RPA-DNA complex plays a vital role in the DDR by recruiting ATR-ATRIP complex to RPA-coated ssDNA at DNA breaks (Binz, Sheehan et al. 2004, Chen and Wold 2014). Recruitment of ATR activator proteins such as TopBP1 is required for full activation of ATR (Kumagai, Lee et al. 2006), as is TopBP1's association with the RAD9-RAD1-HUS1 complex (Delacroix, Wagner et al. 2007). In response to genotoxic stress ATR, in addition to activating cell cycle checkpoints, also serves to prevent replication fork collapse and promote the repair of replication forks (Cortez 2015).

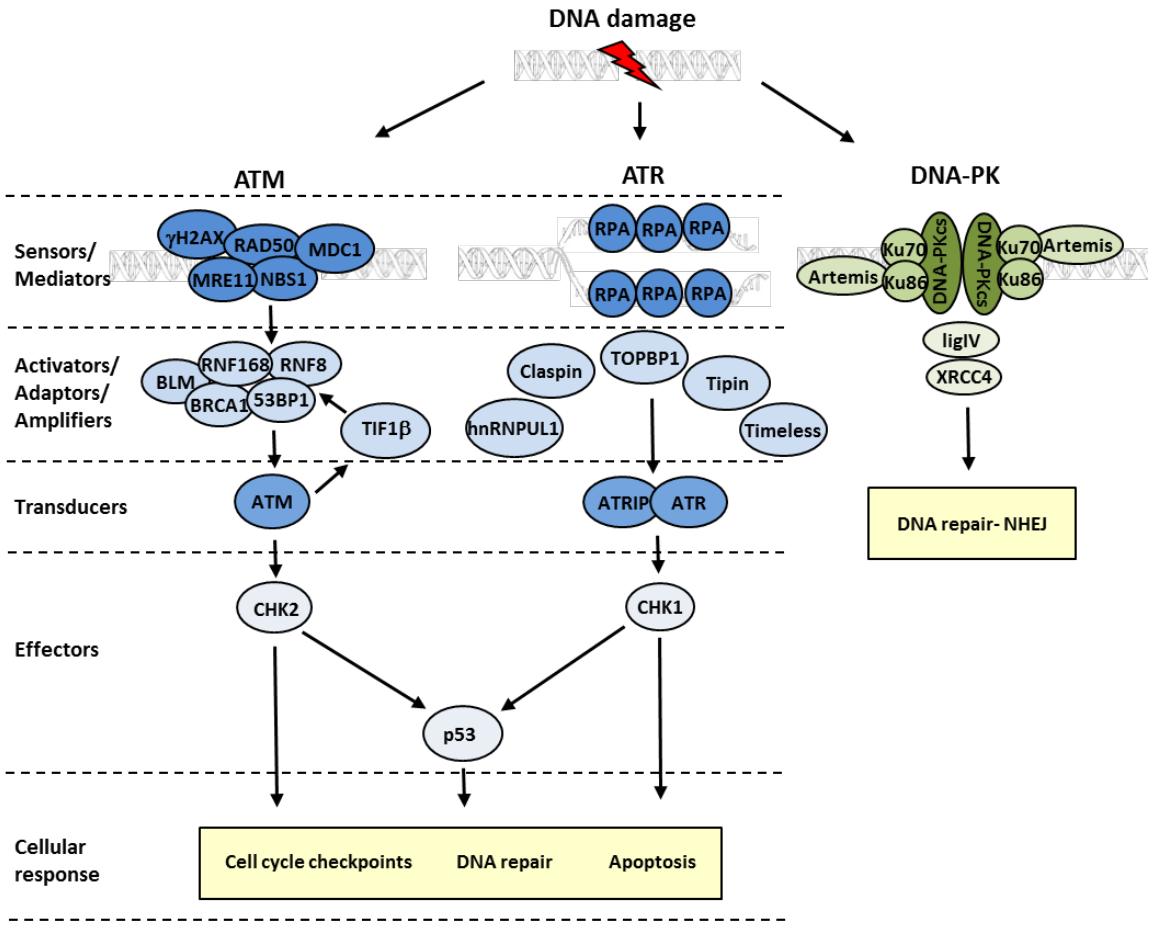

Figure 1.6. Role of ATM, ATR and DNA-PK in DDR signalling pathways. Image taken from (Turnell and Grand 2012).

1.5. The role of SMARCAL1 in cellular DNA replication and the DDR.

SMARCAL1 (SWI/SNF related matrix associated, actin-dependent, regulator of chromatin, sub family A like 1) is a distant subfamily member of the SNF2 chromatin-remodelling family of proteins (Figure 1.9A) (Flaus, Martin et al. 2006, Bansbach, Boerkoel et al. 2010). SMARCAL1 is mutated in SIOD (Schimke immunoosseous dysplasia), which is characterized by T-cell immunodeficiency, renal failure, skeletal

dysplasia, and, in approximately 50% of cases, microcephaly (Boerkoel, Takashima et al. 2002). SMARCAL1 is also known as HARP (Hep A-related protein) and functions as an ATP-dependent annealing helicase whose activity is stimulated by both ds and ss DNA, but is stimulated even more by DNA stem-loop and forked DNA structures (Muthuswami, Truman et al. 2000). It is a 954 residue protein and consists of an N-terminal RPA-binding domain, two tandem HARP domains, HARP1 and HARP2, which are essential for SMARCAL1 annealing activity, and two C-terminal SNF2/ATPase domains which couples ATP hydrolysis to DNA annealing of the complementary strands (Figure 1.9B; (Ghosal, Yuan et al. 2011). The ability of the N-terminal region of SMARCAL1 to bind RPA is important for SMARCAL1 recruitment to sites of DSBs and stalled or collapsed replication forks which serves to maintain genome integrity through its annealing helicase activity (Bansbach, Bétous et al. 2009, Ciccia, Bredemeyer et al. 2009, Postow, Woo et al. 2009).

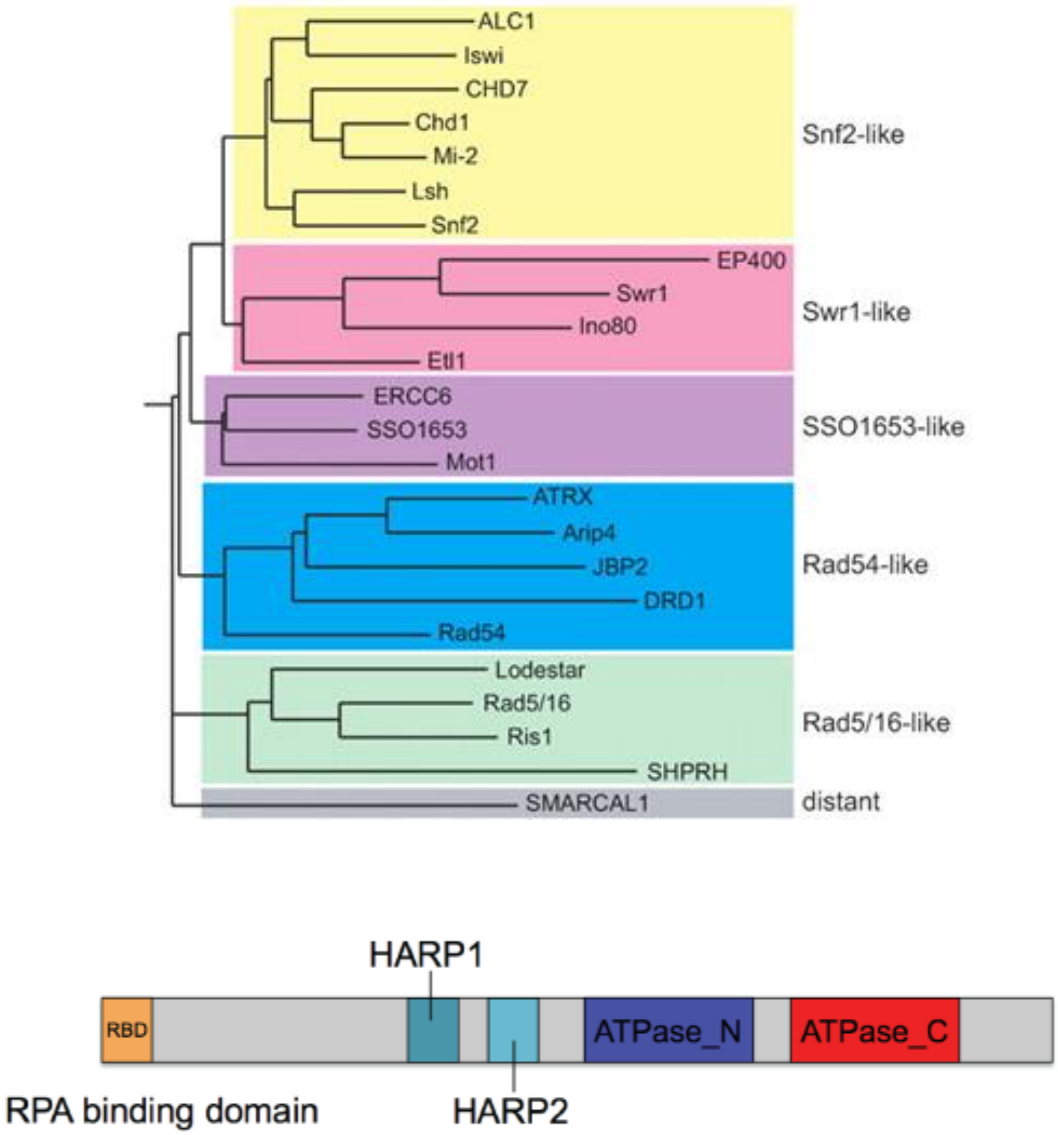

Figure 1.7. SWI/SNF2 family evolutionary relationship Figure taken from (Flaus, Martin et al. 2006) and SMARCAL1 protein domain structure taken from (Robbins 2012).

RNA interference studies determined that loss of the SMARCAL1 protein results in increased sensitivity to agents that cause DSBs or replication fork collapse leading to increased cell death (Bansbach, Bétous et al. 2009, Ciccia, Bredemeyer et al. 2009). Overexpression of SMARCAL1 similarly leads to replication-associated DNA damage (Bansbach, Bétous et al. 2009). Given that alterations in SMARCAL1 levels results in

the activation of the DDR and enhanced apoptosis SMARCAL1 could be a potential drug target for cancer therapy (Zhang, Fan et al. 2012).

1.5.1. Regulation of SMARCAL1 activities by the ATR kinase.

As SMARCAL1 is involved in cellular DNA replication and the cellular DDR it is not surprising that its activity is tightly regulated by the PIKK kinases, ATM, ATR and DNA-PK during unperturbed S-phase and in response to DNA damage and genotoxic stress (Bansbach, Bétous et al. 2009, Ciccia, Bredemeyer et al. 2009). As ATR is the principal PIKK kinase that monitors DNA replication through its ability to phosphorylate substrate proteins and prevent the accumulation of aberrant fork structures, limit fork collapse and promote fork stability, SMARCAL1 activity is tightly regulated by ATR (Ciccia, Bredemeyer et al. 2009, Bhat, Bétous et al. 2015). In response to stalled replication SMARCAL1 associates with stalled replication forks. In these circumstances ATR phosphorylates SMARCAL1 on S652 to limit its fork regression properties in order to prevent aberrant fork processing and fork collapse (Couch, Bansbach et al. 2013). Indeed, when ATR is inhibited specifically by small molecule inhibitors dysregulated SMARCAL1 activity can lead to fork collapse (Couch, Bansbach et al. 2013). In other circumstances, ATR can stimulate SMARCAL1 ATPase activity in order to promote SMARCAL1-catalysed fork regression activities through phosphorylation of SMARCAL1 on S889 (Carroll, Bansbach et al. 2013). S889 lies within a C-terminal auto-inhibitory domain of SMARCAL1 that phosphorylation by ATR relieves (Carroll, Bansbach et al. 2013). SMARCAL1 is known to be phosphorylated on multiple sites including S112, S123, S129, S172, S173, S198, S652 and S889 (Carroll, Bansbach et al. 2013). Despite the identification of these sites, the

biological role of most of these phosphorylation events is unknown. S112, S123, S129, S172, S173 and S198 lie close to the RPA-binding domain which are known to regulate cell cycle specific activities (Carroll, Bansbach et al. 2013). Of these sites S112, S123 and S129 are all SP motif, which could be targeted by CDKs, whereas S173 is a PIKK motif and S172 does not conform to any known motif. It will be interesting in the future to establish how phosphorylation at these sites modulates SMARCAL1 activity.

1.5.2. SMARCAL1 and telomere maintenance.

Telomeres, which protect chromosome ends and act as a cellular ageing monitor, are maintained by two independent pathways. The enzyme telomerase is a ribonucleoprotein that utilises an RNA template to add telomere sequence to the 3' end of telomeres, whilst the Alternative Lengthening of Telomere (ALT) pathway relies on homologous recombination. Telomerase is activated in approximately 90% of human cancers to maintain telomere length and the ALT pathways maintains telomere length in the remaining 10% of cancers (Shay and Wright 2019). SMARCAL1 has recently been shown to play an important regulatory role in the ALT pathway (Poole, Zhao et al. 2015, Cox, Maréchal et al. 2016). SMARCAL1 associates with telomeric DNA and localises at ALT telomeres in response to replication stress and promotes telomere stability by preventing replication fork collapse. Indeed, in the absence of SMARCAL1 stalled replication forks are processed to DSBs which promotes chromosome fusions (Figure 1.10) and the production of extrachromosomal telomere DNA, termed C-circles (Poole, Zhao et al. 2015, Cox, Maréchal et al. 2016). Interestingly, SMARCAL1 activity at telomeres is not dependent upon its interaction with the RPA complex and

SMARCAL1 does not increase the rate of telomere recombination through ALT (Poole, Zhao et al. 2015).

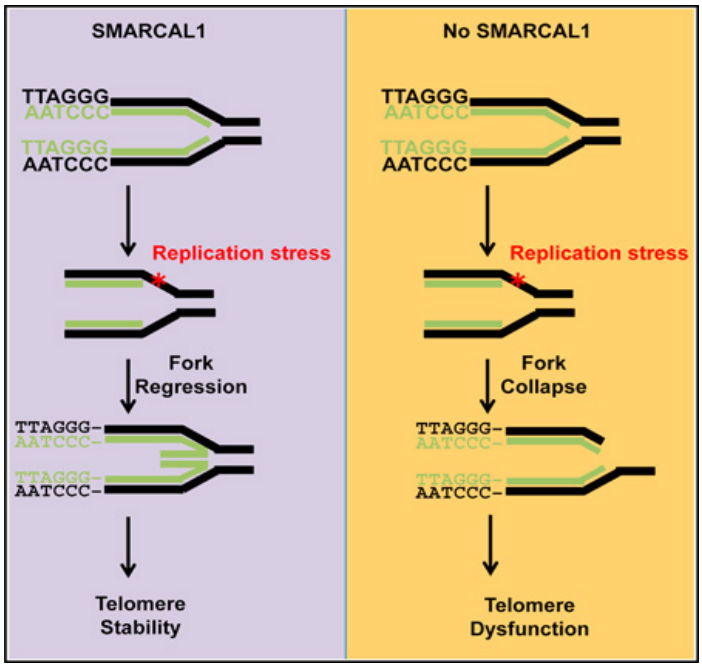

Figure 1.8. Role of SMARCAL1 in ALT telomere maintenance. Figure taken from (Cox, Maréchal et al. 2016).

1.6. Adenovirus and the DNA damage response.

Viruses are like other genotoxic agents that are known to initiate DDR repair pathways. Upon adenovirus infection, the linear Ad dsDNA genome mimics a host cell DSB, whilst DNA replication generates ssDNA intermediates. The host cell DDR machinery recognises these species as DNA breaks and initiates DDR signalling pathways that would ordinarily induce cell cycle arrest or apoptosis (Weitzman, Carson et al. 2004). Activation of DDR pathways following adenovirus infection would limit severely viral replication and are therefore considered anti-viral responses. Adenoviruses, like other viruses, have evolved antiviral defence strategies through the expression of their early

gene products to regulate host cell DDR pathways to support viral replication. It is perhaps, therefore no surprise that adenovirus has a greater ability to replicate to higher titres in cancer cells rather than primary cells, as key DDR proteins are often inactivated in cancer cells (e.g.(Turnell, Grand et al. 1999); (Bischoff, Kirn et al. 1996, Heise, Sampson-Johannes et al. 1997, Johnson, Shen et al. 2002, O'Shea, Johnson et al. 2004)). Given this relationship, and the fact that conditionally-replicating adenoviruses are potential agents for cancer therapy, understanding the relationship between adenovirus and cellular DDR pathways is important towards understanding the molecular basis of host cell-virus interactions and generating the most efficient oncolytic viruses (Weitzman and Ornelles 2005, Turnell and Grand 2012).

1.6.1. Regulation of p53 during infection.

Forty years ago David Lane, William Old, Arnold Levine and Michel Kress initially identified a 53 kDa cellular protein that associated with SV40 large T antigen and named it p53 (DeLeo, Jay et al. 1979, Kress, May et al. 1979, Lane and Crawford 1979, Linzer and Levine 1979). Initially, p53 was identified as oncogene as the species originally cloned was mutant, but later functional studies determined that the w.t. p53 protein acted as a tumour suppressor gene product (Vogelstein, Lane et al. 2000). As such, p53 has the ability to induce cell cycle arrest, senescence and apoptosis in response to cellular stresses such as ionizing radiation, U.V. light, changes in intracellular oxygen levels etc (Vogelstein, Lane et al. 2000, Surget, Khoury et al. 2014). To ensure that adenoviruses replicate in the presence of such a potent tumour suppressor, the virus has evolved numerous mechanisms to inactivate p53 during viral infection. In addition to the known roles of E1B-55K and E4orf6 to inhibit p53 transcriptional activity in isolation (see

sections 1.3.6. and 1.3.8.) it was later established by Johannes Bos's group that E1B-55K and E4orf6 cooperated to reduce p53 levels in the infected cell by reducing the half-life of the p53 protein (Steegenga, Riteco et al. 1998). In this regard they also demonstrated that E1B-55K and E4orf6 would similarly reduce the levels of mutant p53 in infected cells (Steegenga, Riteco et al. 1998). It was later established that E1B-55K and E4orf6 cooperate to target p53 for degradation through the ubiquitin-proteasome system (Querido, Blanchette et al. 2001). As such, E1B-55K was shown to serve as a receptor for the p53 substrate whereas E4orf6 through its ability to bind E1B-55K recruited a cellular ubiquitin ligase, CRL5 (Cullin-Ring Ligase 5), to E1B-55K-p53 complexes in order to promote the ubiquitin and 26S proteasome-mediated proteolysis of p53 (Figure 1.7; (Querido, Blanchette et al. 2001). Research from our laboratory later indicated that Ad12 E1B-55K and E4orf6 similarly targeted p53 for degradation by utilising CRL2, rather than CRL5 (Blackford, Patel et al. 2010).

1.6.2. Regulation of cellular protein degradation by E1B-55K and E4orf6.

Mass spectrometric identification of both cellular Ad5 E4orf6 and E1B-55K – interacting proteins identified CRLs as major targets for E1B-55K/E4orf6 complexes during infection (Querido, Blanchette et al. 2001, Harada, Shevchenko et al. 2002). Indeed, all components of CRLs were identified in these screens including the Cullin 5 and Elongin B and C proteins, and the Rbx1 ubiquitin ligase (Querido, Blanchette et al. 2001, Harada, Shevchenko et al. 2002). It was later established that whilst the zinc-finger binding region of E4orf6 was required for binding to E1B-55K, E4orf6 also possessed three BC boxes which promote E4orf6 association with Elongin B and C

components of CRLs to recruit the CRL to E1B-55K and associated cellular substrate for ubiquitin-mediated proteolysis (Blanchette, Cheng et al. 2004). It is known that the NEDD8-activating enzyme specifically enhances CRL activity through its ability to NEDDylate the associated Cullin subunit, which allows for a conformational change in the CRL complex and the dissociation of CAND1, a negative regulator of CRL activity (Duda, Borg et al. 2008). In this regard, our laboratory determined that during Ad5 infection Cullin 5 became NEDDylated, whilst during Ad12 infection Cullin 2 became NEDDylated, consistent with the roles of CRL5 in Ad5 infection and CRL2 in Ad12 infection (Blackford, Patel et al. 2010).

Adenovirus early region oncoproteins E1B-55K and E4orf6 are now known to target numerous host cellular proteins for degradation via the ubiquitin-proteasome system by utilising cellular CRLs. In this regard, adenovirus utilises the cellular ubiquitylation machinery, more often than not, to inhibit DDR signalling pathways and to negate the activation of the DDR during adenovirus infection that would prove detrimental to viral replication. These will be discussed in detail in the following sections. Other studies suggest that adenovirus does not just utilise cellular CRLs to inhibit the DDR. Indeed, the Branton laboratory determined that integrin α3 was degraded in an E1B-55K and E4orf6 dependent manner during infection (Dallaire, Blanchette et al. 2009). It was proposed that integrin α3 degradation during infection might affect cell-cell interactions which would promote the release and spread of progeny virus (Dallaire, Blanchette et al. 2009).

Other collaborative studies from our laboratory and David Matthews laboratory showed using quantitative mass spectrometric proteomics, and infection with adenovirus mutants, that ALCAM, EPHA2, PTPRF were major targets for E1B-55K/E4orf6 (and

E1B-55K/E4orf3) degradation in Ad5-infected cells (Fu, Turnell et al. 2017). As these proteins are, like integrin α3, critical regulators of cell signalling and cellular adhesion the degradation of these proteins might similarly facilitate virus release and spread. It has also been determined, through the expression of a dominant-negative Cullin 5 protein that CRL5 is important in the ability of E1B-55K/E4orf6 to promote the nuclear export of late viral mRNAs into the cytoplasm, though the cellular protein that is targeted for CRL5-mediated degradation is not known (Woo and Berk 2007). Other studies have suggested that E1B-55K can engage with CRL5, independently of E4orf6, to target the pro-apoptotic, Daxx (death-domain-associated protein), for degradation during Ad5 infection (Schreiner, Wimmer et al. 2010). How E1B-55K achieves this mechanistically however, is not known.

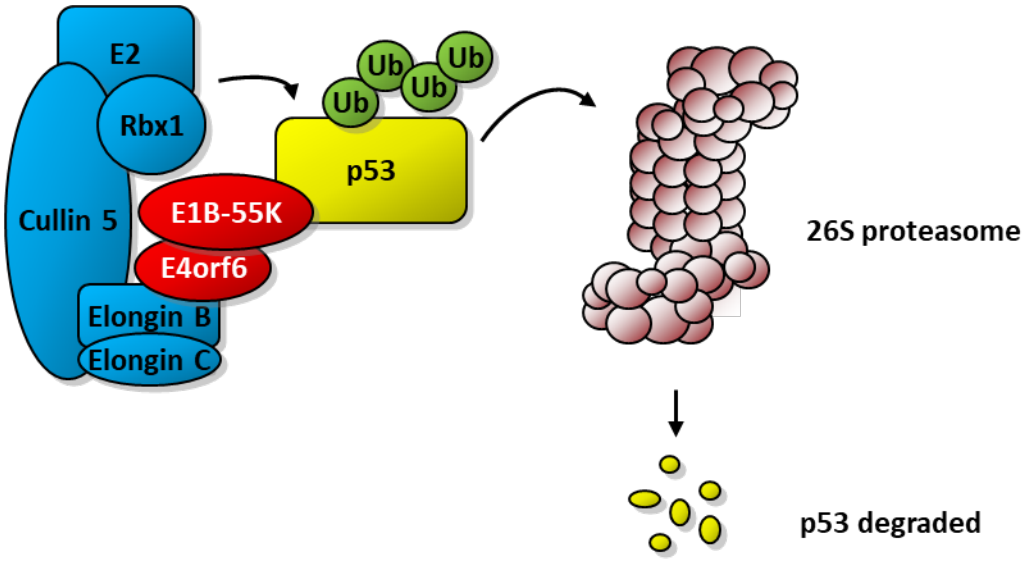

Figure 1.9. Ubiquitylation and degradation of p53 by 26S proteasome and Cullin Ring ligases.

1.6.3. Regulation of DNA-PK by adenovirus.

Early studies indicated that both E4orf3 and E4orf6 could inhibit DNA-PK-dependent V(D)J recombination through NHEJ by interacting directly with DNA-PKcs (Boyer, Rohleder et al. 1999). Moreover, E4orf3 and E4orf6 were also shown to inhibit adenovirus genome concatemerization (i.e. the ligation of multiple adenovirus genomes together) which would produce a viral genome that would not be able to be packaged inside the capsid, suggestive of the notion that these viral proteins inhibited the ability of DNA-PK to catalyse DSB repair (DSBR). Further work by the same group indicated that E1B-55K and E4orf6, but not E4orf3, could inhibit NHEJ directly during Ad5 infection by promoting the CRL5-dependent degradation of DNA ligase IV (Baker, Rohleder et al. 2007). It was determined that the α2 helix in the DNA ligase IV BRCT-1 domain was required for targeted degradation by adenovirus 5 during infection (Gilson, Greer et al. 2012), though it was not determined whether E1B-55K, or E4orf6 interacted with this BRCT-1 domain during infection, or whether it was a phospho-dependent interaction. It has recently been shown that the E4orf4 protein also interacts with DNA-PKcs during Ad5 infection where they co-localize at VRCs (Nebenzahl-Sharon, Shalata et al. 2019). It has been suggested that early during infection E4orf4 utilises DNA-PKcs to inhibit both the ATM and ATR pathways, through its ability to reduce ATM autophosphorylation and Chk1 activation whilst at later times post-infection E4orf4 inhibits DNA-PK activity to enhance virus replication (Nebenzahl-Sharon, Shalata et al. 2019).

1.6.4. Regulation of the ATM pathway by adenovirus.

As mentioned earlier and shown in Figure 1.6, DSBs are sensed by the MRN complex which then activates the ATM signalling pathway to promote cell cycle checkpoint control and DNA damage repair through HR, or induces apoptosis if the DNA damage is too great (Uziel, Lerenthal et al. 2003). The MRN complex and ATM are also components of the TRF2 telomere-binding complex and regulates telomere integrity (de Lange 2018). Adenoviruses are known to inactivate the ATM signalling pathway by targeting the MRN complex for degradation via the ubiquitin-proteasome system (Stracker, Carson et al. 2002). In studies similar to those of Boyer who looked at the role of DNA-PK in adenovirus genome concatemerization (Boyer, Rohleder et al. 1999), the studies by the Weitzman laboratory showed that the Ad5 E1B-55K-E4ORF6 mediated degradation of the MRN complex thorough the ubiquitin-proteasome system prevented adenovirus genome concatemerisation (Stracker, Carson et al. 2002). Further studies by the same group indicated that E4orf3 re-localized MRN components to PML-containing nuclear tracks and to cytoplasmic aggresomes to inhibit MRN function (Araujo, Stracker et al. 2005). Additionally, the Weitzman group also established that the RecQ helicase family member, BLM, which participates in the resection of DNA breaks is also targeted for proteasome-mediated degradation by E1B-55K and E4orf6 during Ad5 infection (Orazio, Naeger et al. 2011). It was also determined that E1B-55K could bind to BLM, independently of MRE11 and that BLM was detected close to sites of viral DNA synthesis in Ad5-infected cells, though whether BLM facilitated viral replication prior to its degradation was not determined (Orazio, Naeger et al. 2011).

1.6.5. Regulation of the ATR pathway by adenovirus.

ATR is an apical stress response kinase involved in regulating cellular DNA replication, DNA damage repair, cell cycle arrest and apoptosis (see section 1.4.3; (Cortez 2015)). Some of what we know about the relationship between adenoviruses and ATR comes from work performed in our laboratory, which has shown that Ad5 and Ad12 differentially regulate the ATR signalling pathway during infection (Blackford, Bruton et al. 2008). As such, it was established that the E1B-55K-interacting protein, E1B-AP5 participated in the ATR-mediated phosphorylation of RPA32 during both Ad5 and Ad12 infection and that E1B-AP5, ATRIP, RAD9 and RAD17 were all recruited to VRCs during infection with these viruses (Blackford, Bruton et al. 2008). Work from the Weitzman laboratory showed that Ad5 inhibited the ATR-dependent activation of Chk1 by promoting the E4orf3-dependent relocalization of MRN to PML-containing nuclear tracks, although they determined that many virus types, including Ad12 did not possess this ability as the key E4orf3 residue responsible in the Ad5 form was not conserved in Ad12 E4orf3 (Carson, Orazio et al. 2009). Our laboratory determined that Ad12 inhibits the ATR-dependent activation of Chk1, by promoting the ATR activator, TopBP1 for E4orf6-CRL2 dependent degradation (Blackford, Patel et al. 2010). As such, E4orf6 associated with both TopBP1 and CRL2 in order to promote TopBP1 degradation (Blackford, Bruton et al. 2008). It has also been demonstrated that a mutant adenovirus lacking E1B-19K, which sensitizes pancreatic cancer cells to cell death with the cytotoxic drugs gemcitabine and irinotecan, promotes the down-regulation of the cellular replication protein and ATR activator, Claspin during the infection, by both transcriptional and proteolysis in order to inhibit Chk1 activation which has the consequence of enhancing cell killing (Pantelidou, Cherubini et al. 2016). The down-

regulation of MRE11 also contributed to the attenuation of Chk1 activation (Pantelidou, Cherubini et al. 2016). Interestingly, it has been shown that Claspin and another replication protein and ATR activator, Timeless, are both excluded from newly replicated adenovirus dsDNA, suggesting both of these proteins attenuate adenovirus genome replication (Reyes, Kulej et al. 2017). Given these findings it is clear that adenovirus regulates ATR signalling pathways on multiple levels to promote viral replication.

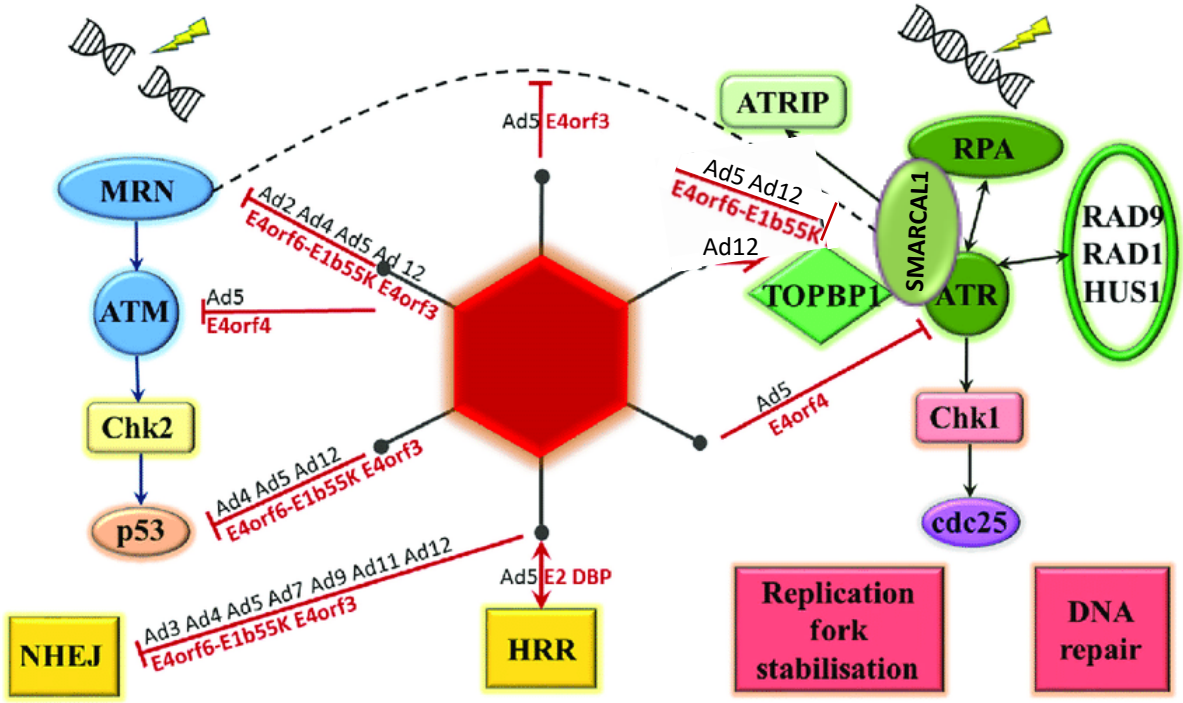

Figure 1.10. Regulation of ATM and ATR signalling pathways by different adenovirus serotypes. Schematic illustration of ATM and ATR pathways showing how different Ad early region proteins E1B-55k, E4orf3 and E4orf6 modulate the signalling pathways. Ad5 E4orf4 target ATM pathway, Ad5, Ad12 E4orf6-E1b-55K and E4orf3 target MRN complex, p53 and NHEJ pathway, whilst Ad5 E4orf3 and E4orf4 target ATR pathway, Ad12 E4orf6 target ATR activator TOPBP1 and Ad5 and Ad12 E4orf6-E1B-55K target RPA interacting protein and ATR substrate SMARCAL1 for degradation. Figure Adapted from (O'Cathail, Pokrovska et al. 2017).

1.7. Project aims.

The current literature indicates that adenoviruses have evolved specifically to engage with the host cell ubiquitin-proteasome system to evade DDR signalling pathways that would, otherwise be detrimental to adenovirus replication. Our laboratory has long been interested in how adenoviruses regulate the ATR signalling pathway, and have shown previously that adenoviruses target E1B-AP5 and TopBP1 in order to modulate ATR kinase function during infection. As adenovirus typically targets multiple components of the same pathway, we were interested to study the relationship between adenovirus and ATR in more detail. Indeed, previous work by a PhD student in our laboratory suggested that adenovirus targeted SMARCAL1 for degradation during infection in an E1B-55K/E4orf6- dependent manner. The main aim of this study was, therefore, to establish the molecular basis of SMARCAL1 degradation in Ad-infected cells, particularly the requirement for CRLs and other cellular proteins. As E1B-55K is known to affect p53 transcriptional activity we also wished to determine whether E1B-55K similarly, affected SMARCAL1 function in cellular DNA replication. The results of these studies are presented in this thesis.

CHAPTER 2

Materials and methods

2.1. CELL CULTURE TECHNIQUES:

2.1.1. Cell lines.

Cell line	Type	Origin	Source	Culture media
HEK293	epithelial	Ad5 E1-transformed embryonic kidney cells	human	DMEM
HER911	epithelial	Ad5 E1-transformed embryonic retinal cells	human	DMEM
GP2-293	epithelial	Ad5 E1-transformed embryonic kidney cells	human	DMEM
HER2	epithelial	Ad12 E1-transformed embryonic retinal cells	human	DMEM
HER3	epithelial	Ad12 E1-transformd embryonic retinal cells	human	DMEM
A549	epithelial	small cell lung carcinoma cells	human	DMEM
RPE-1	epithelial	Retinal pigment cells	human	DMEM

Table 2.1. List of cell lines used in this study

2.1.2. Maintenance of cell lines.

Adenovirus 5 E1-transfromed human embryo kidney cells (HEK293; (Graham, Smiley et al. 1977)), adenovirus 12 E1-transformed human embryonic retinal cells (HER2; (Byrd, Grand et al. 1988)), GP2-293 retroviral packaging cells (Clontech), A549 lung carcinoma cells (ATCC CCL-185), U2OS FRT cells (Thermofisher), and TERT-immortalized RPE-1 cells (ATCC CRL-4000) were all maintained and cultured in HEPES-buffered DMEM medium supplemented with 8% (v/v) foetal bovine serum

(FBS; Sigma-Aldrich) and L-glutamine (2 mM; Sigma-Aldrich). Cells were maintained at 37°C and kept at constant humidity and 5% (v/v) CO_2 in a Mars Safety class 2 safety cabinet (Scanlaf). Confluent cells were washed with warmed PBS and trypsinized with 1 ml of Trypsin (Gibco). Detached cells were resuspended in 9 ml of DMEM and seeded on to new dishes under sterile conditions in the laminar flow hood.

2.1.3. Cryopreservation of cells.

For long time storage of cells, cells were first trypsinised and then resuspended with DMEM containing 10% (v/v) DMSO (dimethyl sulphoxide), typically at a density of $5x10^6$ cells/ml, and placed in cryo-tubes (Thermo-Scientific). Cells were then cooled to -80˚C at a controlled rate of 1˚C/min with isopropanol using a Mr. Frosty™ freezing container. Frozen cells were transferred the following day to liquid nitrogen tanks at -180˚C for long time storage.

2.1.4. Recovery of cells from liquid nitrogen.

Cells were resurrected from liquid nitrogen by rapidly thawing in a water bath at 37˚C. Cells were immediately transferred in to centrifuge tube with 10 ml of DMEM and then pelleted at 1400 rpm for 5 min. Cells were then washed in fresh DMEM, subjected to re-centrifugation and resuspended in fresh DMEM, whereupon they were plated on to 10 cm dishes and incubated in humidified incubator at 37˚C.

2.2. CELL BIOLOGY TECHNIQUES:

2.2.1. Adenoviruses.

Wild type (w.t.) Ad5 and Ad12 (Huie) types were obtained from ATCC (American type culture collection), whilst Ad E1B-55K deletion viruses, Ad5 *dl1520* and Ad12 *dl620* were generated over 30 years ago and have been characterized and used extensively over this time (Barker and Berk 1987, Byrd, Grand et al. 1988, Turnell, Grand et al. 1999, Forrester, Patel et al. 2012). w.t. Ad5 and Ad5 *dl*1520 viruses were propagated on permissive Ad5E1 HEK293 cells, and w.t. Ad12 and Ad12 *dl*620 were propagated on HER3 cells. Titres of the viruses were determined by colony plaque assays on HER911 cells for Ad5 and HER3 cells for Ad12, respectively (Turnell, Grand et al. 1999).

2.2.2. Adenovirus infection.

Cells were infected with either w.t. Ad5 or w.t. Ad12 (Huie) in serum-free DMEM at an infectivity of 10 plaque forming units (p.f.u.) per cell for 2 h. Infected plates were incubated at 37˚C and cells were agitated every 10 min intervals to ensure an even spread of the virus. Following infection, excess virus was removed, and the medium was replaced with 10 ml of fresh DMEM + 8% (v/v) FBS and incubated at 37˚C in the incubator until required.

2.2.3. Transient DNA transfection.

Transfections were performed on retroviral packaging GP2-293 cells, which are HEK293 cells that express the essential viral packaging, *gag* (Group antigens polyprotein), and *pol* (reverse transcriptase) genes. GP2-293 cells were plated the day before transfection on 75 cm^2 flasks such that they were 70-80% confluent at the time

of transfection. For transfection, 10 µg of the appropriate pEGFP-C1-SMARCAL1 construct and 10 µg of pCMV-VSV-G was added to 200 µl of Opti-MEM (Invitrogen) in a sterile eppendorf tube and incubated for 5 min at room temperature. Similarly, 20 µl of Lipofectamine 2000 was added to a separate eppendorf tube containing 200 µl of Opti-MEM and incubated for 5 min. After this time, the DNA opti-MEM mixture and the transfection reagent mixture were combined, mixed gently and incubated at room temperature for 30 min to allow for the formation of DNA-liposome complexes. In the meantime, cells to be transfected were washed twice with Opti-MEM and then incubated in 4.6 ml of Opti-MEM. After 30 min incubation, the DNA-liposome complexes were added to the GP2-293 cells and incubated for 6 h at 37°C. After the incubation time, Opti-MEM was replaced with 10 ml of fresh DMEM-HEPES supplemented with 8% (v/v) FBS and 2 mM glutamine. Plasmid constructs used in this study are listed below.

Insert	**Vector**
w.t. SMARCAL1	pLEGFP-C1 (Clonetech)
SMARCAL1 S123A; SMARCAL1 S129A; SMARCAL1 S173A	pLEGFP-C1 (Clonetech)
SMARCAL1 S123A/S129A; SMARCAL1 S123A/S173A; SMARCAL1 S129A/S173A	pLEGFP-C1 (Clonetech)
SMARCAL1 S123A/S129A/S173A	pLEGFP-C1 (Clonetech)
G glycoprotein of the vesicular stomatitis virus	pCMV-VSV-G (Addgene)

Table 2.2. List of plasmids used in this study.

2.2.4. Retroviral transduction.

At 72 h post-transfection supernatant containing retrovirus particles was collected from the GP2-293 cell cultures and filtered using a 0.45 μM filter (Sartorious). As these cells produce high titre viruses and the A549 and RPE-1 cells transduce well, we typically did not need to concentrate the virus by centrifugation, or use cationic transfection agents such as Polybrene to facilitate transduction. Thus, RPE-1 and A549 cells seeded at very low density (10%) on 75 cm^2 flasks on the day of transduction and infected overnight with 5 ml of the appropriate retrovirus. Cells were then incubated in DMEM-HEPES for an additional 48 h, whereupon cells were trypsinized and seeded at 500 cells/10 cm dish. After a further 24 h incubation individual clones were 'picked' with a sterile 1ml pipette using a microscope placed in the tissue culture hood and positive clones were selected for using G418 (500 μg/ml; Gibco). Positive clones, identified using an EVOS fluorescent digital microscope were expanded on 24-well and then 6-well plates in order to generate enough cells for freezing and experimentation.

2.2.5. Drug treatments.

As and when required, cells were treated with drugs such as: caffeine (Sigma-Aldrich), the ATM inhibitor, KU-55933 (Sigma-Aldrich), the ATR inhibitor, AZD6738 (Cayman chemicals) and the CDK inhibitor, RO-3306 (Merk Millipore) to inhibit cellular kinases. Drugs that inhibit the ubiquitin-proteasome system such as: Nedd8-activating enzyme (NAE) inhibitor, MLN-4924 (Cayman chemicals), and proteasome inhibitors MG132 and salinosporamide A (SAL A; Sigma-Aldrich) were also used in this study. Ganciclovir (Sigma-Aldrich) was also used to inhibit adenoviral DNA replication. The concentrations of drugs used are detailed in the appropriate Figure legends.

2.3. PROTEIN BIOCHEMISTRY AND IMMUNOLOGICAL TECHNIQUES.

2.3.1. Cell lysis.

Cells were washed twice in ice-cold PBS and then lysed in either NETN lysis buffer (250 mM NaCl, 0.5 mM EDTA (pH 8.0), 50 mM (pH 7.5) Tris- HCL, 1% (v/v) NP-40), HiLo salt lysis buffer (50 mM Tris (pH 7.4). 0.825 M NaCl, 1% (v/v) NP-40), or UTB buffer (9 M urea, 50 mM Tris (pH7.4), 150 mM β-mercaptothanol). The cells lysed in UTB or HiLo salt buffer were sonicated for 15 sec at power setting, 5, using a Microson ultrasonic cell disruptor. Cells lysed in NETN buffer were Dounce-homogenized, on ice, using a tight pestle for 20 strokes with a 5 min break on ice after 10 strokes. The samples were then centrifuged at 13,000 rpm for 30 min at 4ºC and the clarified lysates collected for further analyses.

2.3.2. Bradford assay quantification of protein concentrations.

Bradford reagent (BIO-RAD) was diluted 1 in 5 with deionised H_20. 1 ml of the Bradford reagent was added, typically, to 4 µl of clarified cell lysates of unknown protein concentration. A standard curve of protein concentration was generated by adding 1ml of Bradford reagent to 0–30 µg of bovine serum albumin (BSA). Absorbance at 595 nm was then measured using a Cecil CE9200 spectrophotometer and the protein concentrations of the cell lysates were determined by reference to the standard curve.

2.3.3. SDS-polyacrylamide gel electrophoresis (SDS-PAGE).

Protein samples were mixed one-to-one with sample buffer (1 volume SDS (10% w/v): 2 volumes 9 M urea, 50 mM Tris (pH 7.4), 150 mM β-mercaptoethanol) and boiled at 95°C for 5 min prior to separation by SDS-PAGE. 50 µg of cell lysates and immunoprecipitated samples that had been prepared in sample buffer were separated according to molecular weight upon a 10% acrylamide (w/v) (acrylamide/bisacrylamide (37.5:1); Severn Biotech Ltd) gel containing 0.1 M Tris-Bicine (pH 8.3), 0.1% (w/v) SDS, 0.3% (v/v), TEMED and 0.06 % (w/v) ammonium persulphate. For the analysis of larger proteins 6 to 8 % acrylamide gels were used and for smaller proteins 12 to 14 % acrylamide gels were used. The vertical gel electrophoresis apparatus was assembled as per the manufacturer's guidelines (Hoefer). The gel mixture was then poured into the apparatus and a 15-well comb was inserted to create wells. Once the gel had polymerised the comb was removed, wells washed with deionized water and samples were loaded in to the wells that contained running buffer (100 mM Tris-bicine, 0.1% (w/v) SDS). Gels were run between 10 to 20 mA overnight in running buffer depending on the molecular weight of the proteins to be analysed.

2.3.4. Coomassie staining of gels.

Acrylamide gels were stained overnight in a colloidal coomassie solution that was comprised of coomassie brilliant blue G250 (0.1% (w/v); Fisher scientific), orthophosphoric acid (1.6% (v/v); Fisher scientific), ammonium sulphate (8% (w/v); Sigma-Aldrich) and methanol (20% (v/v)). Gels were washed extensively in distilled water and stored in the fridge prior to preparation for mass spectrometry.

2.3.5. Western blotting.

After separating proteins by SDS-PAGE, proteins were transferred on to nitrocellulose membrane in transfer buffer [(24 mM) Tris, (193 mM) Glycine, 20% (v/v) methanol] at 280 mA for 6h. The membrane was then blocked in 5% (w/v) Milk powder in TBST (Tris buffered saline-Tween 20) [20 mM Tris HCL (pH 7.5), 0.1% (v/v) Tween-20, 150 mM NaCl] for at least 1 h. The membrane was then cut according to the sizes of the proteins under investigation and washed once in TBST. Primary antibodies were diluted to the desired concentration in 5% (w/v) milk powder in TBST and incubated with the membrane overnight on a rocker at 4ºC. Blots were then washed three times in TBST (15 min each time) followed by incubation in the appropriate secondary conjugated HRP antibodies in 5% (w/v) milk powder in TBST for 3 h on a rocker at room temperature. The blots were then washed three times (15 min each time) in TBST and incubated in Immobilon chemiluminescent HRP reagent (Millipore) and exposed to blue X-ray film (Wolf laboratories) for the desired time. Protein bands were visualized after developing X-ray films in the dark room using an X-ograph developer.

2.3.6. Antibodies.

Antigen	Clone/code	Species	Usage	Supplier
SMARCAL1	sc-376377	mouse	WB, IP	Santa Cruz
Ad5 E1B-55K	2A6	mouse	WB, IP	In-house
Ad5 E1B-55K	pAb	rabbit	WB, IP	Eurogentec
Ad12 E1B-55K	XPH9	mouse	WB, IP	In-house
Ad5 E1B-55K	pAb	rabbit	WB, IP	Eurogentec
Ad12 E1A	M13	mouse	WB	In-house
Ad5 E4orf3	6A11	rat	WB	Thomas Dobner
Ad12 E4orf6	RSA3	mouse	WB	Thomas Dobner
p53	DO-1	mouse	WB, IP	David Lane
MRE11	12D7	mouse	WB	GeneTex
β-actin	AC-74	mouse	WB	Sigma-Aldrich
GFP	B-2	mouse	WB	Santa Cruz
Normal Mouse IgG	12-371	mouse	IP	Sigma-Aldrich
Normal Rabbit IgG	12-370	rabbit	IP	Millipore
bromodeoxyuridine	BU1/75	rat	IF	Abcam

bromodeoxyuridine	B44	mouse	IF	Becton Dickinson
Anti-mouse HRP	P044701-2	Goat	WB	Dako
Anti-rabbit HRP	PO39901-2	Swine	WB	Dako
Anti-mouse Alexa Fluoro 488	A32723	Goat	IF	Thermo Fisher
Anti-Rabbit Alexa Fluoro 594	A32731	Goat	IF	Thermo Fisher

Table 2.3. List of antibodies used in this study.
WB, Western blot; IF, immunofluorescence; IP, immunoprecipitation.

2.3.7. Immunoprecipitation.

Cells were lysed in NETN or HiLo buffers for immunoprecipitation. 10 µg of immunoprecipitating antibody, or normal IgG control antibody, was added to the lysates and incubated at 4°C overnight on a rotator. The next morning 20 µl of packed Protein G agarose beads (KPL) were added to the antibody-containing lysates and incubated at 4°C for 2 h on a rotator. The immunoprecipitates were then washed 3 times with the lysis buffer and repeated rounds of centrifugation at 13,000 rpm and 4°C. After sufficient washing, sample buffer was added to the beads and incubated at 95ºC for 5 min, and the samples prepared for SDS-PAGE.

2.3.8. Treatment of immunoprecipitates with λ-phosphatase.

λ-phosphatase is a broad-range Mn^{2+}-dependent protein phosphatase that cleaves phosphate groups from phospho-serine, phospho-threonine and phospho-tyrosine residues. To assess whether SMARCAL1 was phosphorylated following Ad5 and Ad12

infection, SMARCAL1 was immunoprecipitated from mock, and Ad5 and Ad12 -infected cell lysates using a SMARCAL1-specific antibody (see section 2.3.7). Immunoprecipitates were collected on protein G- sepharose beads and washed with 25 mM Tris (pH 7.4) prior to incubation in 1X λ-phosphatase buffer (NEBuffer), 1 mM $MnCl_2$ and 100 U of λ-phosphatase (NEB). Samples were then incubated for 1 hour in water bath at 30°C, after which they were resuspended in SDS-PAGE sample buffer and subjected to SDS-PAGE and Western blot analysis.

2.3.9. Mass Spectrometry.

To identify SMARCAL1 residues that were phosphorylated during Ad5 and Ad12 infection SMARCAL1 was immunoprecipitated from mock, and Ad -infected A549 cells (section 2.3.7). Immunoprecipitates were isolated on protein G Sepharose beads, re-suspended in SDS-PAGE sample buffer and separated on pre-cast Novex NuPage™ 4-12% bis- tris gels (Life technologies). The gel was then stained in coomassie Brilliant Blue as described in section 2.3.4. Multiple bands around the corresponding molecular weight of SMARCAL1 were excised with a sterile scalpel in a laminar flow cabinet and washed at room temperature, on a shaker, three times for a total time of 45 min, in a solution containing 50 mM Ammonium bicarbonate (ABC; Sigma-Aldrich) and 50% (v/v) Acetonitrile (ACN; Millipore). Note that all solutions were made using HPLC (High-Performance Liquid Chromatography)-grade H_2O (Chromanorm, VWR). Protein bands were then reduced with 50 mM dithiothreitol in a 10% (v/v) solution of ACN and 50 mM ABC at 56ºC for 1 h. The reducing solution was then removed and proteins were carboxymethylated, by incubation in the dark for 30 min, in a solution of 200 mM iodoacetamide in 10% (v/v) ACN and 50 mM ABC. The gel slices containing the protein bands were then washed three times for a total time of 45 min in 10% (v/v) ACN and

40mM ABC on a shaker at room temperature. The gel slices were then dehydrated by incubation with pure ACN for 1 h, on a shaker at room temperature. The dehydrated samples were then resuspended in sequence-grade modified trypsin (Promega) in a solution of 40mM ABC and 10% (v/v) ACN for rehydration and incubated overnight at 37ºC to generate tryptic peptides that could be analysed by mass spectrometry. The tryptic peptides were washed-out of the gel slices by washing with 3% (v/v) formic acid (Fisher scientific) and then dried in a DNA-mini-vacuum centrifuge for 3-4 h. The dried sample was then either stored at -20°C until required or resuspended in a solution of 1% (v/v) formic acid and 1% (v/v) ACN prior to analysis on a Q exactive HF hybrid quadrupole-Orbitrap mass spectrometer (ThermoFisher Scientific).

2.3.10. DNA fibre analysis.

Cells were labelled successively with 25µ M of CldU and 250 µM of IdU (both Sigma-Aldrich) for 20 min at 37°C. Cells were then washed twice with PBS, trypsinised and resuspended in PBS at 4°C and diluted to a density of $5x10^5$ cells/ml. Cell extracts containing DNA fibres were then prepared in spreading buffer (200 mM Tris-HCl (pH 7.4), 50 mM EDTA, 0.5% (v/v) SDS). For DNA spreading 2µl of cell extract was added to a microscope slide, dried for 5-7 min until fibres looked sticky but not dry, after which time 7 µl of spreading buffer was added and mixed gently with a pipette tip. Cell extracts were then incubated for approximately 2 min and the slides tilted slightly to let the drops containing the cell extracts run down the slides slowly (3-5 min). Microscope slides were then air dried the DNA fibres fixed in methanol/acetic acid (3:1) for 10 min. Slides could be stored at -20°C at this stage prior to immunostaining if required.

For immunostaining the slides were washed twice with distilled H_2O (5 min each time) and rinsed once with 2.5 M HCl; DNA was then denatured in 2.5 M HCl for 80 min. Slides were then rinsed twice with PBS, twice with blocking solution (PBS + 1% (w/v) BSA + 0.1% (v/v) Tween 20) and incubated in blocking solution for up to 1 h. DNA fibres were then co-stained with rat anti-bromodeoxyuridine (Abcam) and mouse anti-bromodeoxyuridine (Becton Dickinson) in blocking buffer for 1h. Fibres were then fixed with 4% (w/v) paraformaldehyde, washed twice with PBS and incubated further with anti-rat Alexa Fluor 555 and anti-mouse Alexa Fluor 488 for 1.5h. Finally, slides were mounted in mounting medium (vectashield antifade mounting medium, vector laboratories) and fibres analysed on a Nikon E600 microscope using a Nikon Plan Apo 60x (1.3-numeric-aperture) oil lens and Hamamatsu digital camera (C4742-95) and the Velocity acquisition software (Perkin Elmer). DNA fibre images were prepared using Image J software.

2.4. MOLECULAR BIOLOGY TECHNIQUES.

2.4.1. Media Preparation.

Luria Broth (LB) comprised of 1% (w/v) bactotryptone (Melford chemicals), 0.5% (w/v) yeast extract (Melford chemicals) and 1% (w/v) NaCl (Sigma-Aldrich). The pH was adjusted to 7.2 and the LB sterilized by autoclaving. To make 1.5% (w/v) LB-agar, 15 g of Agar was added to one litre of LB and sterilised by autoclaving. LB-agar was melted when needed and ampicillin (100µg/ml) was added. Plates were poured in a sterile laminar flow hood. Once the plates had cooled down, the plates were stacked and saved at 4°C for bacterial transformations.

2.4.2. Bacterial transformation.

Transformations were performed using one of the competent *E.coli* strains listed in Table 2.4. 100 ng of plasmid DNA was typically added to 20 µl of bacteria and incubated on ice for 30 min and then heat-shocked at 42ºC for 1 min to allow for plasmid entry. The bacteria were then rested on ice for 5 min, after which time 300 µl of Super Optimal broth with Catabolite repression (SOC) medium (2% (w/v) bactotryptone, 0.5% (w/v) yeast extract, 10 mM NaCl, 10 mM $MgCl_2$, 20 mM glucose; ThermoFisher Scientific) was added to the bacteria which were then incubated for 1 h in a shaker at 220 rpm. Cells were then plated on LB-agar plates in the presence of 100mg/ml ampicillin, air dried and incubated overnight at 37 ºC.

Bacterial Strain	**Provider**
Library efficiency DH5α	Invitrogen
Subcloning efficiency DH5α	Invitrogen
XL1-Blue supercompetent	Agilent technologies
XL1-Gold supercompetent	Agilent technologies
MAX Efficiency Stbl2 competent	Invitrogen

Table 2.4. List of bacterial strains used during this study.

2.4.3. Plasmid DNA Mini Preparation.

A single bacterial colony was picked from an agar plate and added to 5 ml of LB containing 100 µg/ml ampicillin, and incubated in a shaker overnight at 37 ºC. The next morning the tubes were centrifuged at 5,000 rpm for 5 min to pellet the bacteria. DNA was purified using a Sigma-Aldrich GenElute plasmid miniprep kit as outlined below. The pellet was resuspended in 250 µl of resuspension buffer containing RNase A and

transferred to a sterile eppendorf. 250 µl of lysis buffer was then added and the solution mixed by inversion. To precipitate cellular debris, 350 µl of neutralisation solution was added to the solution and inverted 4 to 6 times to mix. The tubes were then centrifuged at 13,000 rpm for 10 min to obtain the plasmid-containing supernatant. The plasmid-binding columns were prepared by washing with 500 µl of column preparation solution and centrifugation for 2 min. The waste eluate from the tubes was then discarded and supernatants containing plasmid DNA were added to the columns and centrifuged for 2 min at 13,000 rpm to allow for plasmid DNA association with the column matrix. The waste eluate from the columns was discarded and columns containing bound plasmid were washed sequentially with 500 µl of optional wash solution and 750 µl of wash solution by centrifugation. Waste eluates were discarded, and the empty columns were dried by centrifugation at 13,000 rpm for an additional 1 min. To elute the DNA, the columns were transferred to new sterile eppendorfs and 100 µl of nuclease-free distilled water (Ambion) was added. After 5 min incubation the columns were centrifuged for 2 min at 13,000 rpm to elute the plasmid DNA. The columns were discarded, and the eluted DNA was stored at -20ºC prior to use.

2.4.4. Plasmid DNA Maxi Preparation.

For larger scale plasmid DNA production, a single bacterial colony was picked from a an agar plate and inoculated in 5 ml of LB with 100 µg/ml ampicillin and incubated for 6 h in an orbital shaker at 37ºC. After the incubation period, the culture was transferred to 250 ml of LB containing 100 µg/ml ampicillin and grown overnight in an orbital-shaking incubator at 37ºC. The next morning the culture was centrifuged for 10 min at 5000 rpm at 4°C and plasmid DNA purified using the NucleoBond Xtra Maxi kit (Macherey-Nagel) as described below. The bacterial pellet was resuspended in 12 ml

resuspension buffer supplemented with RNase. Cells were then lysed by the addition of 12 ml of lysis buffer after which the plasmid-containing solution was mixed by inversion and incubated at room temperature for 5 min. Cellular debris was precipitated by the addition of 12 ml of neutralisation buffer which was then pelleted by centrifugation to generate a clarified supernatant that contained plasmid DNA. Plasmid purification columns were prepared by adding 25 ml of EQU solution, to the columns after which the supernatant containing plasmid DNA was gravity-fed onto the column to allow for binding of the plasmid DNA to the column. After binding the column was washed twice with 25 ml of Wash buffer, and once with 70% (v/v) ethanol. The DNA was then eluted into a clean tube by adding 15 ml of elution buffer. Following elution, plasmid DNA was precipitated upon the addition of 10.5 ml of isopropanol; plasmid-containing solutions were then centrifuged for 30 min at 15000 rpm and 4°C to pellet the DNA. In a sterile laminar flow cabinet, the pelleted DNA was washed twice with 70% (v/v) ethanol and then air-dried for 15 to 20 minutes until the DNA pellet became translucent. The DNA was then hydrated in an appropriate amount of nuclease free-water. The concentration and quality of the DNA was measured by a NanoDrop spectrophotpmeter ND-1000 (ThermoFisher Scientific) using ND-1000 spectrophotometer v3.2 software (ThermoFisher Scientific).

2.4.5. PCR-based site-directed mutagenesis.

Given the size of the SMARCAL1 cDNA and the corresponding p-CMV-EGFP-C1 vector, site-directed mutagenesis was performed using the QuikChange II XL site-directed mutagenesis kit (Agilent Technologies) by PCR using the oligonucleotides listed in Table 2.5. The PCR reaction was performed in a final volume of 50 µl and comprised (10X reaction buffer (5 µl), DNA template (10 ng), Forward and Reverse

mutagenic primers (500 nM), dNTPs (200 µM), Pfu Ultra DNA polymerase (2.5 U/µl) and nuclease-free distilled water to make up to the required volume. The PCR reaction was performed using a Thermal-cycler 2720 PCR machine (Applied Biosystems) with the following parameters: 95°C for 1 min followed by 18 cycles of 95°C for 50 sec, 60°C for 50 sec, 68°C at 1min/kb for 10 min. The PCR product was then subjected to digestion with the Dpn1 (10 U/µl) restriction enzyme at 37°C for 1 h in a water-bath. After digestion of the parental plasmid, 4 µl of DNA was added to 25 µl of supercompetent XL1-gold bacterial cells (Agilent Technologies) and the bacterial transformation performed as described in section 2.4.2. Individual colonies were then selected for mini-prep plasmid DNA preparation as discussed in the section 2.4.3. Sequencing was then performed using Sanger sequencing as outlined below to validate the incorporation of desired mutation into the SMARCAL open-reading frame.

Mutagenic Oligo name	**Sequence**
SMARCAL1 S123 F	GCTCTCACTGGAATCGCTCCTCCCTTGGC
SMARCAL1 S123 R	GCCAAGGGAGGAGCGATTCCAGTGAGAGC
SMARCAL1 S129 F	CCTCCCTTGGCACAAGCTCCTCCAGAGGTCCC
SMARCAL1 S129 R	GGGACCTCTGGAGGAGCTTGTGCCAAGGGAGG
SMARCAL1 S173 F	CCAAACCAAAGAGTGCCCAAGAGACACCAGC
SMARCAL1 S173 R	GCTGGTGTCTCTTGGGCACTCTTTGGTTTGG

Table 2.5. List of mutagenic primers used in this study.

2.4.6. Sanger sequencing.

Sequencing reactions were performed by PCR. In each 20 µl reaction there was 5 µl of mini-prep plasmid DNA (typically 100-200 ng), forward or reverse sequencing primers (10 ng/µl; listed in Table 2.6), 4 µl of 5X sequencing buffer, 1 µl of Big Dye (Applied Biosystems) and nuclease-free distilled water made up to 20 µl. The PCR reaction was carried out using the Thermal-cycler 2720 PCR machine using the following method: 25 cycles of 96°C for 10 sec, 55°C for 5 sec, 60°C for 4 min. After PCR, to each PCR reaction tube was added 62.5 µl of absolute ethanol, 3 µl of 3 M sodium acetate and 14.5 µl of nuclease-free distilled water. Samples were incubated at room temperature for 30 min to precipitate amplified DNA and then centrifuged at 13,000 rpm for 20 min to pellet the DNA. The supernatant was removed, and the pellet washed twice with 100 µl of 70% (v/v) ethanol followed by successive rounds of centrifugation at 13,000 rpm for 15 min. The supernatant was removed, and tubes were air dried, resuspended in 11 µl of Hi-Di, vortexed briefly and heated at 100ºC for 5 min before being cooled on ice for 5 min. Samples were then loaded into the wells of a plate for sequencing. Sequencing was carried out using a 3500xl Genetic Analyzer (Applied Biosystems) and analysed using Chromas Lite (Technelysium Pty Ltd.). Results were compared to the reference sequence using nucleotide NCBI BLAST (NIH).

Oligo name	Sequence
EGFP	5'-CATGGTCCTGCTGGAGTTCGTG-3'
pLNCX	5'-ACCTACAGGTGGGGTCTTTCATTCCC-3'
SMARCAL1 Seq1	5'- CACAGTCCACGTAGTCAAATGGCT-3'
SMARCAL1 Seq2	5'- TTGATTGGGTACAATGCGGAACTC-3'
SMARCAL1 Seq3	5'-CAAGTTCAGCTGGACCCTCTGCCC -3'
SMARCAL1 Seq4	5'- CTTCTTAGCAAGTTGGAAAAACAG-3'
SMARCAL1 Seq5	5'- ATAGTGGTGATTGCCCCAGGACGG-3'
SMARCAL1 Seq6	5'-CTGATCCAGGCTGAGGACCGCGTG -3'
SMARCAL1 Seq Rev1	5'-GCTGTGGGCATTTCTTCTGGCTTT -3'

Table 2.6. List of sequencing primers used in this study.

CHAPTER 3

Adenovirus targets SMARCAL1 for proteasome-mediated degradation during infection

Statement: Some of the Figures and Figure legends presented in this thesis have been published in J.Virol 2019 Jun 14;93(13); doi: 10.1128/JVI.00402-19 and will be highlighted as such. All of the Figures presented are my own work. The text from the J.Virol publication has not been used 'directly' in this thesis although there might be some overlap or similarity between the text in the thesis and the text in the publication.

3.1. Introduction

Accurate replication, and segregation, of the genome is essential for cell survival and genome maintenance; these cellular processes are controlled by the coordinated activities of cell cycle, DNA replication, and DNA response/repair and pro/anti-apoptotic proteins. Defects in the activities of any of these proteins can cause replication stress and DNA damage, which can lead ultimately to genome instability, cellular transformation and cancer (Kastan and Bartek 2004). The cellular response to DNA replication stress and DNA damage is controlled mainly by the phosphatidylinositol 3-kinase-related kinase (PIKK) family of kinases, comprising ATM, ATR and DNA-PK that function specifically as Ser/Thr-directed protein kinases (Abraham 2004). ATM functions specifically to regulate the cellular response to DNA double-strand (ds) breaks, whilst ATR functions to coordinate the response to single-stranded (ss)DNA that result during DNA replication and double-strand break repair (Blackford and Jackson 2017, Shibata and Jeggo 2018); DNA-PK functions to activate NHEJ repair and inhibit HR-mediated repair pathways (Blackford and Jackson 2017).

As adenovirus genome replication results in the production of large amounts of ssDNA and linear dsDNA that would otherwise activate the PIKK family of protein kinases, the virus has evolved to disable the anti-viral activities of the ATM, ATR and DNA-PK pathways in order to promote viral replication (Brestovitsky, Nebenzahl-Sharon et al. 2016). As such, adenoviruses have evolved to inhibit ATM, ATR and DNA-PK pathways through the targeted sequestration and/or degradation of number of cellular proteins such as the MRN complex, p53, TopBP1, DNA-PK$_{CS}$ and Ku70/Ku80 (Turnell and Grand 2012, Weitzman and Fradet-Turcotte 2018). Adenoviruses have also evolved

to utilize aspects of DNA response/repair pathways that possess inherent pro-viral activities. Indeed, previous work from our laboratory has revealed that the ATR kinase substrate and E1B-55K binding protein, E1B-AP5 participates in ATR-dependent phosphorylation events during infection (Blackford, Bruton et al. 2008).

As detailed above, the relationship between adenovirus and the ATR pathway is complex. ATR function is inhibited, to an extent, by the Ad-mediated degradation of MRN and TopBP1 (Carson, Orazio et al. 2009, Blackford, Patel et al. 2010), though ATR does retain the ability to phosphorylate RPA and H2AX during infection (Forrester, Sedgwick et al. 2011). Given this complexity, our laboratory has focused upon delineating the relationship between Ad infection and ATR kinase function in full. To these ends recent preliminary studies from our laboratory established that the protein levels of, the ATR substrate and DNA replication/damage response protein, SMARCAL1 are reduced following both Ad5 and Ad12 infection (F.S.I Qashqari, PhD thesis, The University of Birmingham, 2017). These studies determined that SMARCAL 1 is recruited to VRCs during infection and, suggested that the loss of SMARCAL1 was dependent upon E1B-55K and E4orf6 expression (F.S.I Qashqari, PhD thesis, The University of Birmingham, 2017). Despite these observations, a number of questions remain unanswered, particularly relating to the mechanism responsible for promoting SMARCAL1 loss. In particular, although a role for E1B-55K and E4orf6 in the regulation of SMARCAL1 expression has been determined, a role for Cullin-containing RING E3 ligases and the proteasome has yet to be investigated. Moreover, it has yet to be established whether SMARCAL1 is a substrate for ATM/ATR or DNA-PK kinases during infection, or whether these kinases contribute towards the loss of SMARCAL1 during infection. The principal aim of this chapter therefore was to

determine the mechanism that promoted the loss of SMARCAL1 protein during infection. The results of these studies are presented herein.

3.2. Results

3.2.1. SMARCAL1 protein levels are reduced following Ad5 and Ad12 infection.

As previous work in our laboratory has suggested that SMARCAL1 protein levels are reduced following Ad infection we first wished to confirm these findings. To do this we infected A549 cells with either w.t Ad5 or w.t. Ad12 and examined by Western blot (WB) the protein levels of SMARCAL1 at different time-points post infection [Figures 3.1A and 3.1B]. Consistent with earlier results, following the infection of A549 cells with w.t. Ad5 the levels of SMARCAL1 were reduced in a similar timeframe to p53, which has previously been shown to be targeted for degradation following Ad infection [cf lanes 7 and 8 with lanes 3 and 4, panels i and ii; Figure 3.1A]. Similarly, the levels of SMARCAL1 were also reduced following the infection of A549 cells with w.t. Ad12 [cf lanes 7 and 8 with lanes 3 and 4, panel I; Figure 3.1B]. Consistent with published observations the levels of p53 increased initially following Ad12 infection, before being degraded [Figure 3.1B, panel 2]. Interestingly, we also observed that the mobility of SMARCAL1 was retarded upon SDS-PAGE following the infection of A549 cells with either w.t. Ad5 or w.t. Ad12, which had not been acknowledged previously [cf lanes 5 and 6 with lanes 1 and 2, panel i; Figures 3.1A and 3.1B]. Taken together, these data indicate that SMARCAL1 protein levels are reduced following w.t. Ad5 and w.t. Ad12 infection.

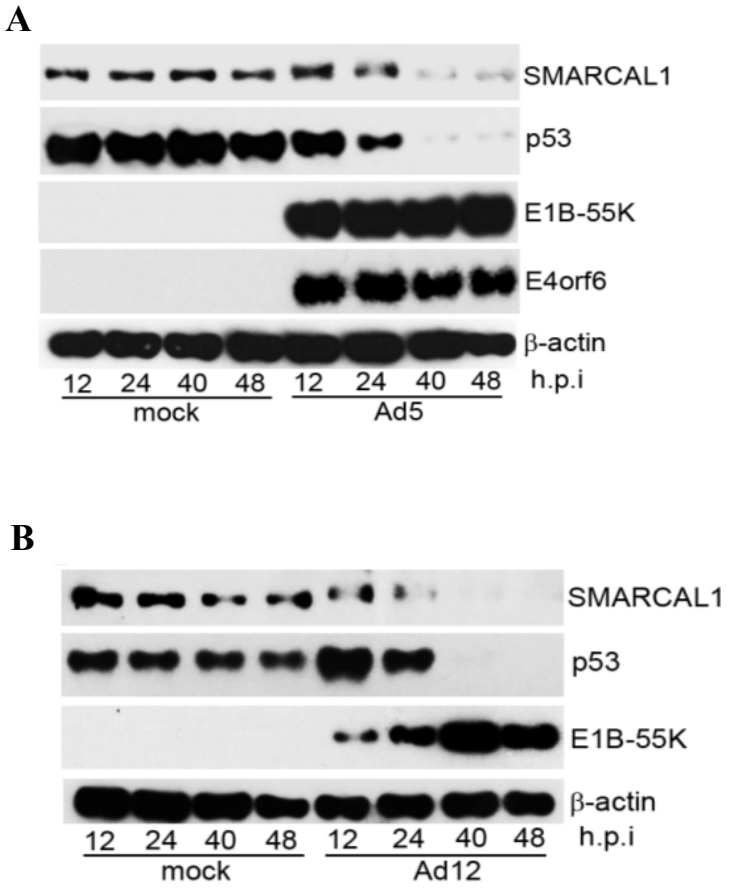

Figure 3.1: SMARCAL1 protein levels are reduced following Ad infection. A549 cells were mock treated (uninfected) or infected with w.t Ad5 (**A**) or w.t Ad12 (**B**) at 10 p.f.u./cell. Whole cell lysates were prepared at the appropriate times post-infection. 50μg protein samples were separated by SDS-PAGE and subjected to WB analysis using the appropriate antibodies. This figure is representative of three independent experiments. (Published in J.Virol 2019 by Nazeer et al).

3.2.2. SMARCAL1 is phosphorylated following both Ad5 and Ad12 infection.

In light of the observation that SMARCAL1 mobility was retarded upon SDS-PAGE during the early stages of Ad infection we hypothesised that SMARCAL1 might be phosphorylated following Ad infection, as protein phosphorylation often decreases protein mobility on SDS-PAGE (Hunter 1995, Cohen 2002). To test this hypothesis, we subjected SMARCAL1, isolated from mock and Ad -infected cells to an *in vitro* phosphatase assay. To do this we immunoprecipitated SMARCAL1 from mock-infected and Ad5- or Ad12- infected A549 cells, using an anti-SMARCAL1 antibody, and incubated the immunoprecipitates that had been collected on Protein G Sepharose beads, in the absence or presence of λ-phosphatase, and analysed the results following SDS-PAGE by WB for SMARCAL1. The results presented in Figure 3.2 show clearly that the mobility of SMARCAL1 isolated from Ad5 and Ad12 -infected A549 cells was retarded in the absence of λ-phosphatase relative to mock-infected cells [cf lanes 5 and 7 with lane 1; Figure 3.2]. These analyses also revealed that SMARCAL1 levels on SDS-PAGE was comparable to the protein levels observed for mock-infected cells, following λ-phosphatase treatment, suggesting that SMARCAL1 retardation on SDS-PAGE following Ad infection is due to phosphorylation [cf lanes 6 and 8 with lanes 1 and 2; Figure 3.2]. Treatment of mock-infected samples, and MLN4924-treated samples with λ-phosphatase increased modestly SMARCAL1 motility on SDS-PAGE suggesting that SMARCAL1 also exists as a phosphorylated species in non-infected A549 cells [cf lanes 2 and 4 with lanes 1 and 3; Figure 3.2]. Taken together, these data suggest that SMARCAL1 is subject to both Ad5 and Ad12 -induced phosphorylation during infection. These data also suggest that SMARCAL1 might be phosphorylated,

on different residues, in non-infected cells, albeit to a lesser extent.

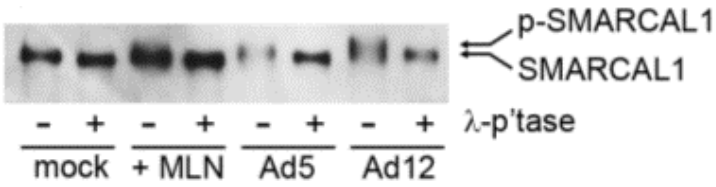

Figure 3.2: SMARCAL1 is phosphorylated following Ad5 and Ad12 infection. A549 cells were mock treated (uninfected) or infected with w.t. Ad5 or w.t. Ad12 at 10 p.f.u/cell, or treated with the NAE inhibitor, MLN4924. At 18h post-infection whole cell lysates were prepared in IP buffer and SMARCAL1 was immunoprecipitated using an anti-SMARCAL1 antibody on to protein G-Sepharose beads. IP's were then treated in the absence or presence of λ-phosphatase and subjected to SDS-PAGE and WB analysis. This figure is representative of three independent experiments. (Published in J.Virol 2019 by Nazeer et al).

3.2.3. SMARCAL1 is phosphorylated on S123, S129 and S173 following Ad5 and Ad12 infection.

As we established that SMARCAL1 was phosphorylated following both w.t. Ad5 and w.t. Ad12 infection we wished to identify the residues that were phosphorylated in response to Ad infection. To do this we harvested mock-, Ad5-, and Ad12- infected A549 cells at 18h post-infection, when we should observe significant phosphorylation [Figure 3.1] and subjected cell lysates to immunoprecipitation for SMARCAL1 with an anti-SMARCAL1 antibody. Following SDS-PAGE and the gel excision of SMARCAL1-containing bands, samples were processed accordingly for mass spectrometric analyses (see section 2.3.9, Materials and Methods), prior to analysis of tryptic peptides upon a Q Exactive HF hybrid quadrupole-Orbitrap mass spectrometer (ThermoFisher Scientific). Mass spectrometric analyses revealed that SMARCAL1 was phosphorylated on three residues following both Ad5 and Ad12 infection, S123, S129 and S173 [Figure 3.3A]; Table showing associated modifications is presented [Figure 3.3B]. We were, however unable to detect any SMARCAL1 phospho-residues in mock-infected cells despite the suggestive results from the λ-phosphatase experiment [data not shown]. S123 and S129 form part of SP motifs, which are known consensus sites for CDKs, and other cellular kinases such as MAPKs/ERKs. S173, forms part of an SQE motif, which is a known consensus site for ATM, ATR and DNA-PK. Sequence alignment revealed that all three residues were conserved amongst primates, whilst in other mammals these residues were less well conserved. For instance, S123 and S129 are conserved in dog, whilst S173 is not, and only S129 is conserved in mice [Figure 3.2C]. These data indicate that SMARCAL1 is phosphorylated during the early stages of both Ad5 and Ad12 infection.

A

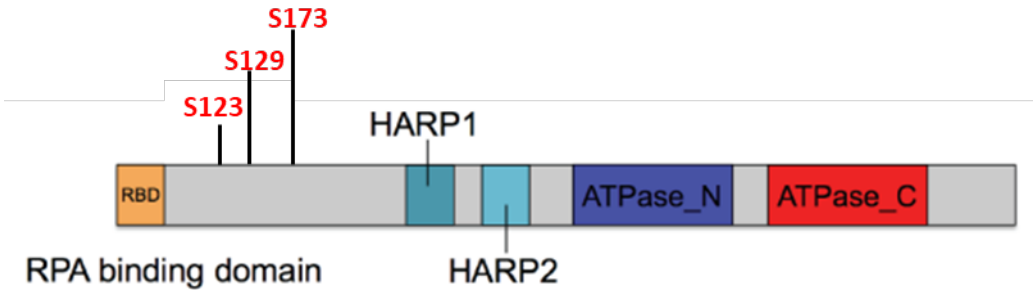

B

Ad Serotype	Phosphorylation Site	Peptides identified by MS
Ad5, Ad12	S123, S129	SQmALTGISPPLAQSPPEVPK
Ad5, Ad12	S173	KSSQETPAHS

C

Sequence	Modifications	Phosphoresidue
SQmALTGIsPPLAQsPPEVPK	M3(Oxidation); S9(Phospho) y+; S15(Phospho) y+	S123; S129
SQMALTGIsPPLAQsPPEVPK	S9(Phospho) y+; S15(Phospho) y+	S123; S129
SQMALTGISPPLAQsPPEVPK	S15(Phospho) y+, b+	S129
SsQETPAHSSGQPPR	S2(Phospho)	S173

D

```
HUMAN       LTGISPPLAQSPPEVPKQQLLSYELGQGHAQASPEIRFTPFANPTHKPLAKPKSSQETPAH   179
GORILLA     LTGISPPLAQSPPEVPKQQLLSYELGQGHAQASPEIRFTPFANPTHKPLAEAKSSQETPAH   179
CHIMPANZEE  LTGISPPLAQSPPEVPKQQLLSYELGQGHAQASPEIRFTPFANPTHKPLAKPKSSQETPAH   179
RH. MONKEY  LTGISPPLAQSPPEVPKQQLLSYELGQGHAEASPEIRFTPFAHPTHEPLAKAKNSQETPAR   179
ORANGUTAN   LTGISPPLAQSPPEVPKQQLLSYELGHGHAQASPEIRFTPFANPTHEPLAKAKSSQETPAH   179
DOG         LTGISPPLAQSPPEVPDQQLLGCALGQGHLQASHEARSTPFANPTPESLAKAKSFQKTPAS   185
MOUSE       ----------SPPGASNQPLLGYKSSEGQPQATW---------------------DTGAS   146
```

Figure 3.3: SMARCAL1 is phosphorylated following Ad5 and Ad12 infection. A549 cells were mock (uninfected) or infected with w.t Ad5 or w.t Ad12 (10 p.f.u/cell). At 18h post-infection whole cell lysates were prepared and SMARCAL1 was immunoprecipitated using an anti-SMARCAL1 antibody. IP's were subjected to SDS-PAGE whereupon SMARCAL1containing bands were isolated and subject to mass spectrometry. (**A**) phospho-residues identified following MS analyses; (**B**) other modifications identified on SMARCAL1 peptides identified by MS; (**D**) CLUSTAL Omega alignment of SMARCAL1 sequences from primates and other mammals. Shaded areas indicate phosphorylation motifs conserved between species. The MS studies are representative of two independent experiments. (Published in J.Virol 2019 by Nazeer et al).

3.2.4. Investigating a role for phosphorylation in the reduction of SMARCAL1 protein levels following Ad infection.

As we have determined that SMARCAL1 is phosphorylated during the early stages of Ad infection we wished to establish whether SMARCAL1 phosphorylation was an important pre-requisite for the Ad-induced reduction in SMARCAL1 protein levels. We therefore decide to use selective protein kinase inhibitors to determine whether they could attenuate the ability of Ad to target SMARCAL1 protein loss during infection.

3.2.4.1 The PIKK inhibitor, caffeine reduces the ability of Ad5 and Ad12 to promote the loss of SMARCAL1 protein.

As we determined that S173 of SMARCAL1 is phosphorylated during both Ad5 and Ad12 infection, and it forms part of an SQE motif- a known target for PIKK cellular kinases we decided to investigate whether caffeine, a broad-range PIKK family (Sarkaria, Busby et al. 1999, Block, Merkle et al. 2004), affected the ability of Ad to promote the reduction in SMARCAL1 protein levels. To do this we subjected A549 cells to mock infection, or infection with w.t Ad5 and w.t Ad12 and two hours post-infection we incubated cells in the absence or presence of caffeine (5 mM optimised dose) (Blackford, Bruton et al. 2008). At 24h and 48h post-infection we then harvested cell lysates and subjected them to SDS-PAGE and WB analysis [Figure 3.4]. WB analyses revealed that SMARCAL1 protein levels were stabilised to some extent in Ad5 infected A549 cells in the presence of caffeine, relative to Ad-infected cells that were not treated with caffeine [cf lanes 7 and 8 with lanes 5 and 6, panel I; Figure 3.4A]. WB analyses also revealed, however, that caffeine restricted significantly the ability of Ad12 to induce SMARCAL1 loss following infection [cf lanes 7 and 8 with lanes 5 and 6,

panel I; Figure 3.4B]. Caffeine did not, however, affect the ability of either w.t Ad5 or w.t Ad12 to promote the loss of the p53 protein [cf lanes 7 and 8 with lanes 5 and 6, panel ii; Figure 3.4A and and 3.4B]. Given that caffeine suppresses the Ad-induced loss of the SMARCAL1 protein these data suggest that the caffeine-sensitive PIKK family of kinases might be involved in the phosphorylation, and loss, of the SMARCAL1 protein during both Ad5 and Ad12 infection.

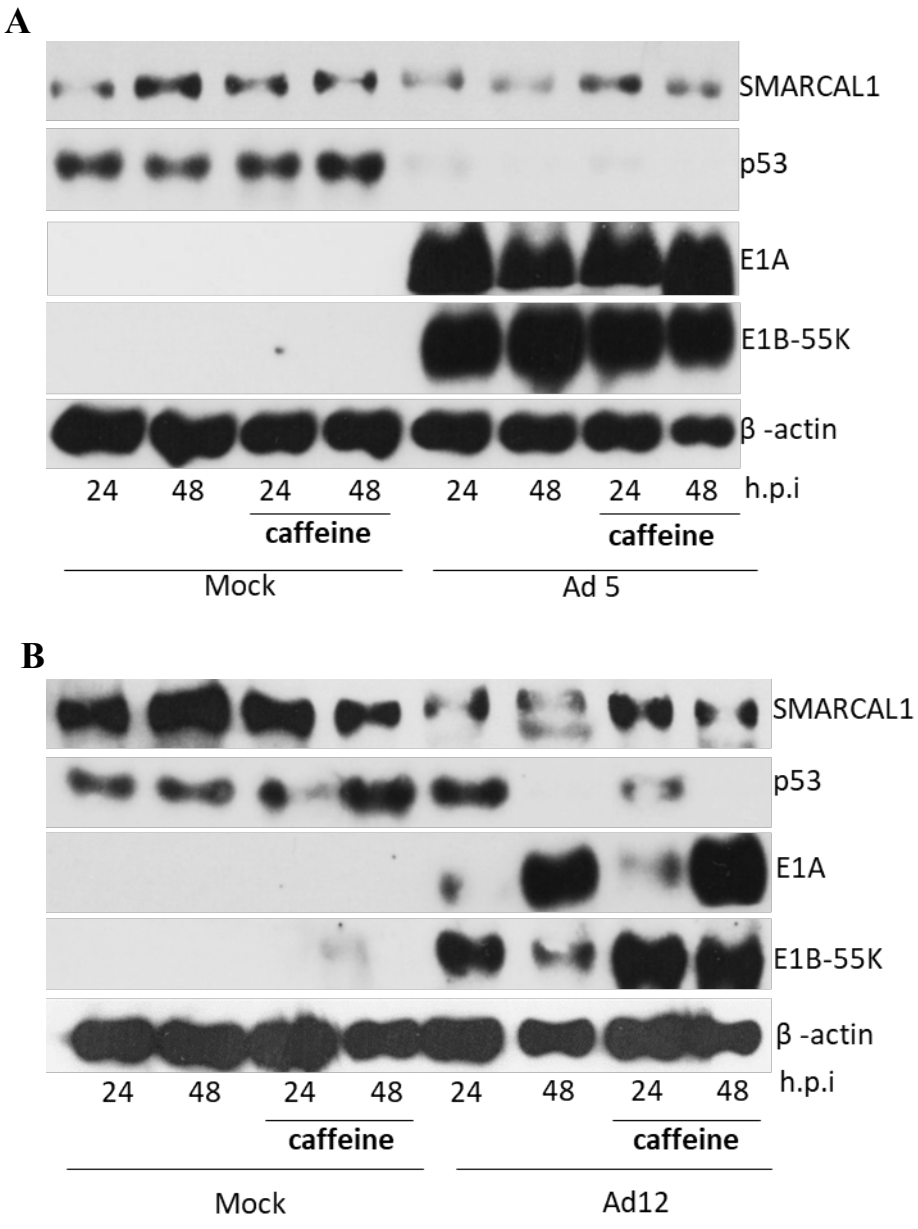

Figure 3.4: Effect of PIKK inhibitor, caffeine on SMARCAL1 and p53 levels during Ad12 infection: A549 cells were mock treated (uninfected) or infected with either w.t. Ad5 (**A**) or w.t. Ad12 (**B**) at 10 p.f.u./cell and treated with PIKK inhibitor Caffeine (5mM) following infection for the times indicated. Whole cell lysates were then prepared and 50μg protein samples were separated by SDS-PAGE and subjected to Western blot analysis using the appropriate antibodies. This figure is representative of three independent experiments.

3.2.4.2 The ATM inhibitor, KU-55933, does not affect the ability of Ad5 or Ad12 to promote the loss of the SMARCAL1 protein during infection.

Given that we have shown that caffeine-sensitive kinases are involved in the phosphorylation of SMARCAL1 following Ad infection, we next wanted to identify the caffeine-sensitive kinase responsible for SMARCAL1 phosphorylation. To do this we used more selective kinase inhibitors. First, we investigated the ability of the ATM kinase inhibitor, KU-55933 (Hickson, Zhao et al. 2004), to modulate the Ad-induced phosphorylation, and loss, of SMARCAL1 [Figure 3.5]. We therefore infected A549 cells with w.t. Ad5 or w.t. Ad12 then subsequently incubated infected cells in the absence or presence of the ATM kinase inhibitor prior to WB determination of SMARCAL1 protein levels [Figure 3.5]. WB analyses revealed that the ATM inhibitor did not affect the ability of w.t. Ad5 or w.t. Ad12 to promote the loss of the SMARCAL1 protein [cf lanes 7 and 8 with lanes 5 and 6, panel I; Figure 3.5A and 3.5B]. Similarly, WB analyses also revealed that the ATM inhibitor did not affect the ability of w.t. Ad5 or w.t. Ad12 to promote the loss of p53 [cf lanes 7 and 8 with lanes 5 and 6, panel ii; Figure 3.5A and 3.5B]. Taken together these data indicated that ATM does not induce the loss of the SMARCAL1 protein during infection, and by extension suggests that ATM does not phosphorylate SMARCAL1 during infection.

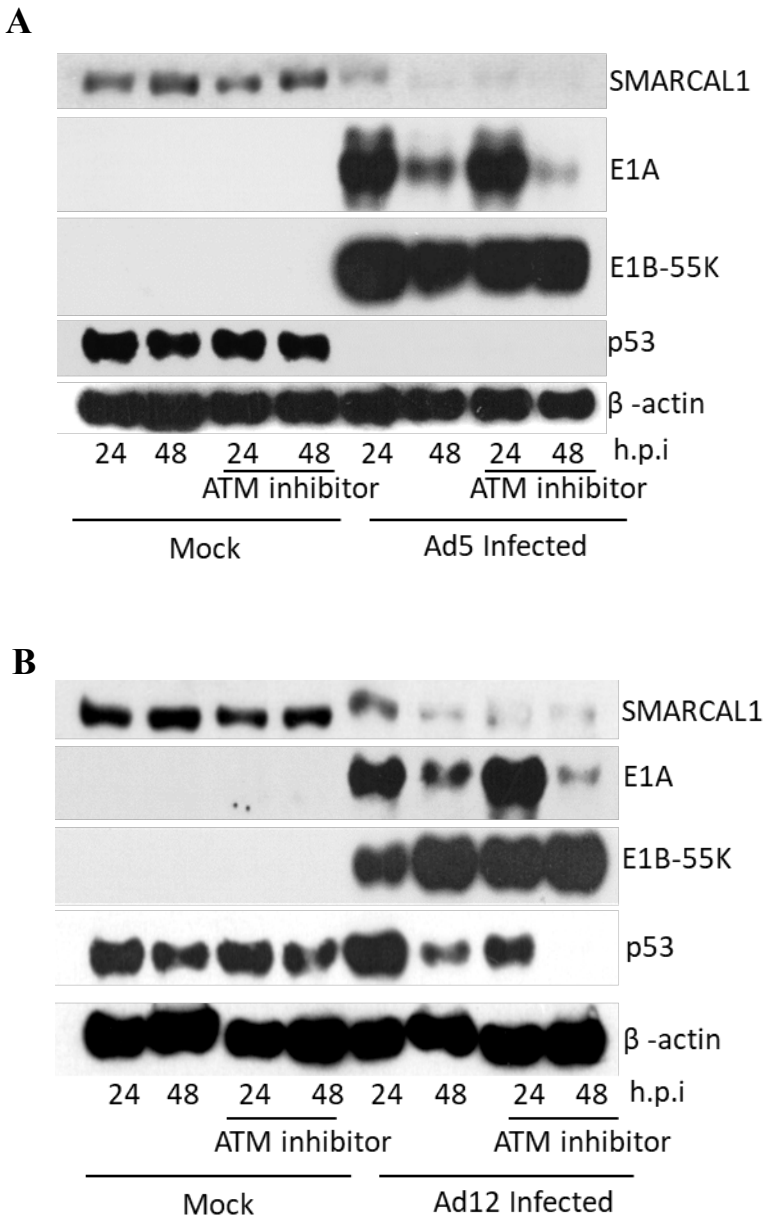

Figure 3.5: Effect of ATM kinase inhibition on SMARCAL1 degradation during Ad5 and Ad12 infection: A549 cells were either mock (uninfected) or infected with w.t Ad5 (**A**) or w.t. Ad12 (**B**) at 10 p.f.u./cell and treated with ATM kinase inhibitor (10μM) 2 hours post infection. Whole cell lysates were prepared at 24h and 48h post-infection. 50μg protein samples were separated by SDS-PAGE and subjected to Western blot analysis using the appropriate antibodies. This figure is representative of three independent experiments.

3.2.4.3. The ATR inhibitor, AZD-6738, reduces the ability of w.t. Ad5 and w.t. Ad12 to promote the loss of the SMARCAL1 protein during infection.

We next investigated whether ATR modulated the Ad-induced phosphorylation, and loss, of SMARCAL1 [Figure 3.6]. To do this we used the ATR-specific inhibitor, AZD-6738, which has been used previously to inhibit ATR function *in vivo* with IC_{50} value less than 1 μM (Vendetti, Lau et al. 2015, Min, Im et al. 2017) (Carrassa and Damia 2017). We therefore, infected A549 cells with w.t. Ad5 or w.t. Ad12 then subsequently incubated infected cells in the absence, or presence, of AZD-6738. Cell lysates were harvested at 24h and 48h post-infection, then subjected to SDS-PAGE and WB analysis to check the SMARCAL1 protein levels [Figure 3.6]. Interestingly, treatment of A549 cells with AZD-6738, limited, the loss of SMARCAL1 protein levels, albeit to a modest extent, in Ad5-infected A549 cells, relative to Ad5-infected cells not treated with the inhibitor [cf lanes 7 and 8 with lanes 5 and 6, panel I; Figure 3.6A]. More dramatically however, the treatment of A549 cells with AZD-6738 almost completely ablated the ability of w.t. Ad12 to promote the loss of the SMARCAL1 protein in Ad12-infected A549 cells, relative to Ad12-infected cells not treated with the inhibitor [cf lanes 7 and 8 with lanes 5 and 6, panel I; Figure 3.6B]. The ATR inhibitor did not however affect the ability of either w.t Ad5 or w.t Ad12 to promote the loss of the p53 protein [cf lanes 7 and 8 with lanes 5 and 6, panel ii; Figure 3.6A and 3.6B]. Taken together, these data suggest strongly that the ATR kinase phosphorylates SMARCAL1 during Ad infection, which ultimately contributes towards the Ad-induced loss of the SMARCAL1 protein during Ad infection.

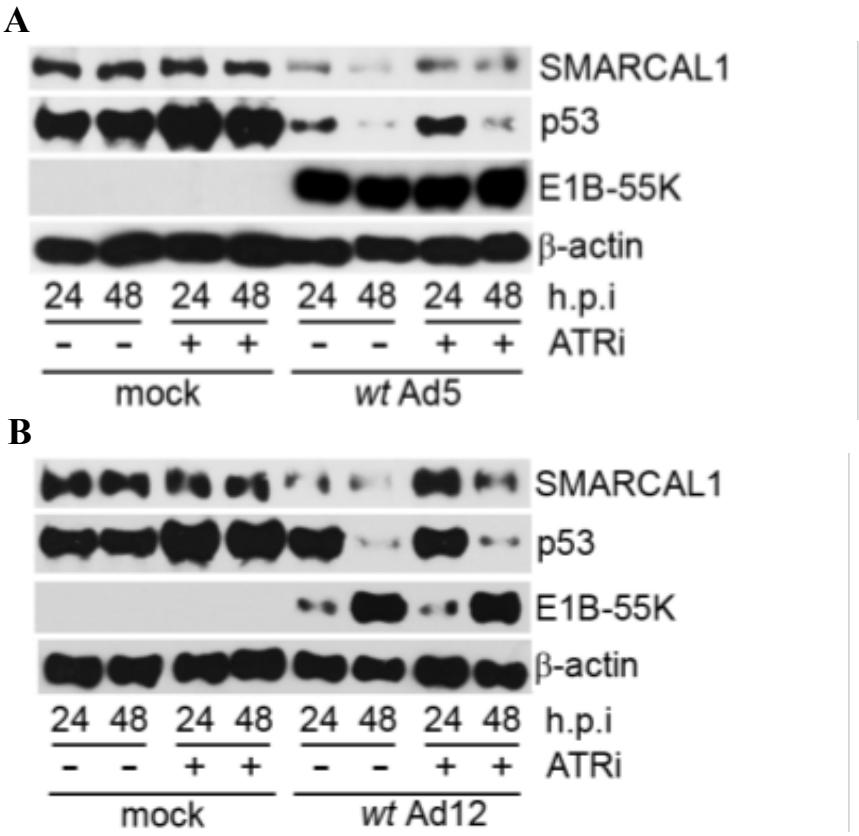

Figure 3.6: The ATR kinase inhibitor (AZD-6738) reduces the ability of Ad5 and Ad12 to promote SMARCAL1 degradation: A549 cells were mock (uninfected) or infected with w.t Ad5 (**A**) or w.t Ad12 (**B**) at 10 p.f.u/cell. Following infection cells were incubated in the absence or presence of the ATR inhibitor, AZD-6738 (1 μM). Samples were then harvested 24h and 48h post infection and 50μg protein samples subject to SDS-PAGE and WB analysis using the appropriate antibodies. (Published in J.Virol 2019 by Nazeer et al).

3.2.4.4. The CDK inhibitor, RO-3306, reduces the ability of w.t. Ad5 and w.t. Ad12 to promote the loss of the SMARCAL1 protein during infection.

As we determined by mass spectrometry that SMARCAL1 residues S123 and S129 were targeted for phosphorylation following both w.t. Ad5 and w.t. Ad12 infection we next sought to determine whether the kinase or kinases that target these residues, similarly promote the loss of SMARCAL1 protein in Ad-infected cells. As CDKs are known to be activated following Ad infection (Grand, Ibrahim et al. 1998) and S123 and S129 are part of SP motifs, known to be targeted by CDKs, we investigated whether the CDK inhibitor, RO-3306, affected the ability of Ad5 or Ad12 to promote the loss of SMARCAL1 in Ad-infected cells. RO-3306 is purportedly a CDK1-selective inhibitor but, at the concentrations used here will also inhibit CDK2, CDK4 and CDK6 (Vassilev, Tovar et al. 2006). We thus infected A549 cells with w.t Ad5 or w.t Ad12 then treated cells in the absence or presence of the CDK inhibitor, RO-3306 for the duration of the infectious life cycle [Figure 3.7]. We harvested the cells 24h and 48h post-infection and performed WB analyses for SMARCAL1. These analyses revealed that RO-3306, attenuated the ability of w.t. Ad5 to promote the loss of the SMARCAL1 protein, relative to Ad5-infected cells not treated with the CDK inhibitor [cf lanes 7 and 8 with lanes 5 and 6, panel i; Figure 3.7A]. In contrast, RO-3306, only modestly inhibited the ability of w.t. Ad12 to promote the loss of the SMARCAL1 protein, relative to Ad12-infected cells not treated with the CDK inhibitor [cf lanes 7 and 8 with lanes 5 and 6, panel i; Figure 3.7B]. Akin to the ATR inhibitor studies the CDK inhibitor did not affect the ability of either w.t Ad5 or w.t Ad12 to promote the loss of the p53 protein [cf lanes 7 and 8 with lanes 5 and 6, panel ii; Figure 3.7A and 3.7B]. These data suggest that a

CDK also phosphorylates SMARCAL1 during Ad infection and contributes towards the Ad-induced loss of the SMARCAL1 protein during infection.

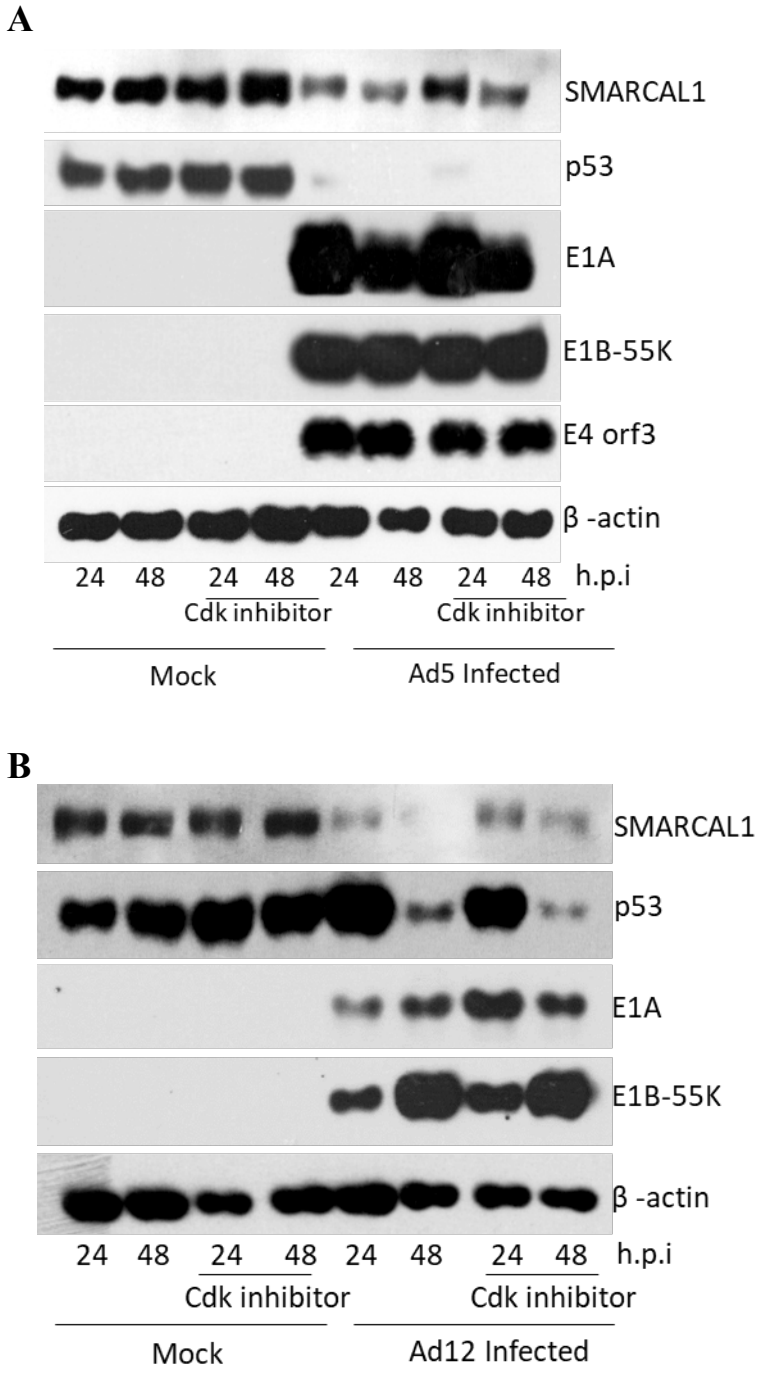

Figure 3.7: Effect of CDK inhibition on SMARCAL1 degradation during Ad5 and Ad12 infection: A549 cells were either mock infected (uninfected) or infected with w.t Ad5 (**A**) or w.t Ad12 (**B**) at 10 p.f.u/cell. Following infection cells were incubated in the absence, or presence, of the CDK kinase inhibitor, RO-3306 (9μM) for the duration of the experiment. Samples were then harvested 24h and 48h post infection and 50μg protein samples subject to SDS-PAGE and WB analysis using the appropriate antibodies. This figure is representative of three independent experiments.

3.2.4.5: ATR and CDK kinases cooperate to promote the loss of SMARCAL1 protein during w.t. Ad5 and w.t. Ad12 infection.

Given that ATR and CDK inhibitors, in isolation, do not ablate completely the ability of w.t. Ad5 or w.t. Ad12 to promote the loss of the SMARCAL1 protein during infection we next investigated whether dual inhibition of ATR and CDKs would prevent SMARCAL1 loss following Ad infection. To do this we infected A549 cells with w.t Ad5 or w.t Ad12 and immediately post-infection incubated cells in the absence, or presence of both the ATR kinase inhibitor, AZD-6738 and the CDK inhibitor RO-3306. We then harvested cells at 24h and 48h post-infection and subjected whole cell lysates to SDS-PAGE and WB analysis. In agreement with the notion that ATR and CDKs cooperate to modulate SMARCAL1 protein levels following infection treatment of w.t. Ad5-infected cells with both ATR and CDK inhibitors ablated completely the ability of w.t. Ad5 to promote the reduction in SMARCAL1 protein levels during infection [cf lanes 7 and 8 with lanes 5 and 6, panel I; Figure 3.8A]. Likewise, treatment of w.t. Ad12-infected cells with both ATR and CDK inhibitors ablated completely the ability of w.t. Ad12 to promote the reduction in SMARCAL1 protein levels during infection [cf lanes 7 and 8 with lanes 5 and 6, panel I; Figure 3.8B]. Interestingly however, treatment of both w.t. Ad5 and w.t. Ad12 -infected A549 cells with both ATR and CDK inhibitors did not affect the ability of these viruses to target the loss of the p53 protein during infection [cf lanes 7 and 8 with lanes 5 and 6, panel ii; Figure 3.8 A and B]. These data indicate that ATR and CDKs cooperate during Ad infection to regulate the levels of the SMARCAL1 protein.

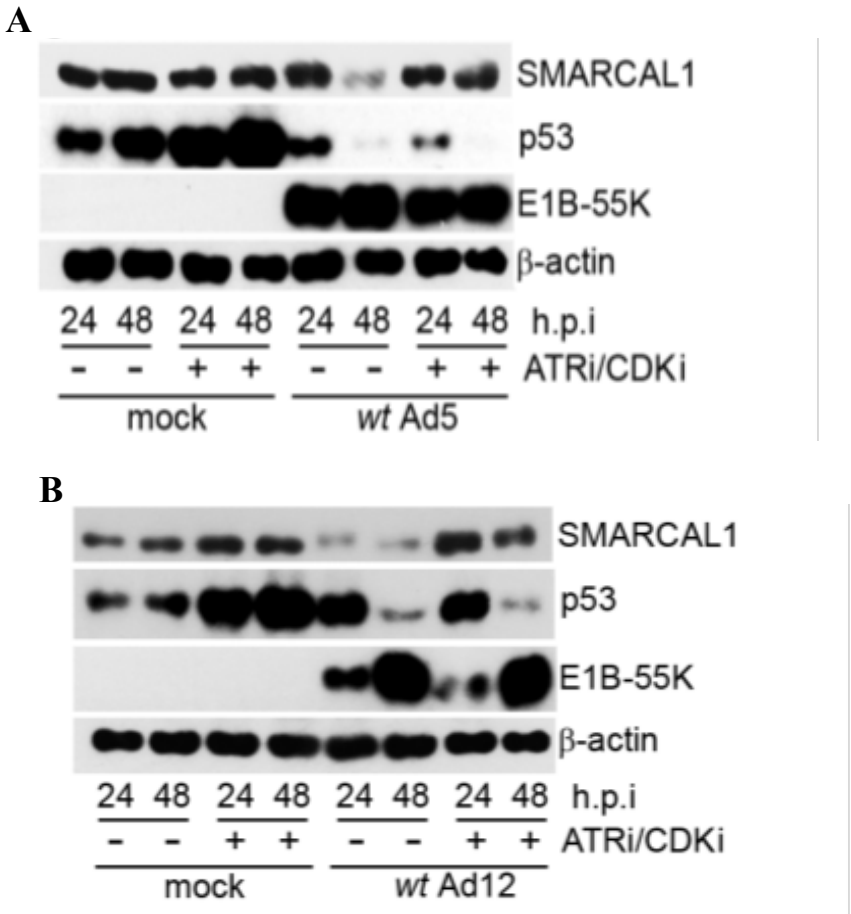

Figure 3.8: The degradation of SMARCAL1 following Ad5 and Ad12 infection is dependent on ATR and CDKs. A549 cells were either mock infected (uninfected), or infected with w.t Ad5 (**A**) or w.t Ad12 (**B**) at 10 p.f.u/cell. Following infection cells were incubated in the absence or presence of ATR and CDK inhibitors (AZD-6738 1μM and RO-3306 9μM). Samples were then harvested 24h and 48h post infection and 50μg protein samples subject to SDS-PAGE and WB analysis using the appropriate antibodies. This figure is representative of three independent experiments. (Published in J.Virol 2019 by Nazeer et al).

3.2.5. Investigating roles for Ad E1B-55K, the proteasome and Cullin Ring Ligases in the degradation of the SMARCAL1 protein following Ad infection.

Previous studies have determined that adenoviruses engage with cellular ubiquitin ligases to promote the ubiquitin-proteasome dependent degradation of host cell proteins such as p53, MRE11, DNA-ligase IV, TopBP1, BLM, Daxx and TIF1γ for proteolysis during infection in a manner that is dependent on early region protein expression (Querido, Blanchette et al. 2001, Harada, Shevchenko et al. 2002, Stracker, Carson et al. 2002, Blackford, Patel et al. 2010, Orazio, Naeger et al. 2011, Schreiner, Wimmer et al. 2011, Forrester, Patel et al. 2012). Given that SMARCAL1 protein levels mirror those of p53 during Ad infection, we next decided to establish whether SMARCAL1 was similarly, targeted by CRLs for proteasome-mediated degradation in an E1B-55K-dependent manner.

3.2.5.1. SMARCAL1 degradation during Ad infection is dependent upon E1B-55K expression.

Previous studies from our laboratory suggested that SMARCAL1 degradation was dependent upon E1B-55K and E4orf6 expression (F.S.I Qashqari, PhD thesis, The University of Birmingham, 2017). To confirm that the Ad-mediated degradation of SMARCAL1 was dependent upon E1B-55K expression we infected A549 cells with w.t. Ad5 and w.t. Ad12 and the corresponding E1B-55K deletion viruses, Ad5 *dl*1520 and Ad12 *dl*620 and analysed SMARCAL1 protein levels by WB analyses (Figure 3.9). Consistent with earlier observations our data suggested that, like p53, SMARCAL1 degradation during both Ad5 and Ad12 infection was dependent upon E1B-55K

expression (cf panels i and ii; Figures 3.9A and 3.9B). Moreover, our data also suggested that loss of E1B-55K did not limit the abilities of ATR and CDKs to target SMARCAL1 for phosphorylation during infection as there was an obvious retardation in SMARCAL1 mobility on SDS-PAGE following infection with either Ad5 *dl*1520, or Ad12 *dl*620 (cf lanes 5 and 6 with lanes 1, 2 and 3, panel i; Figures 3.9A and 3.9B).

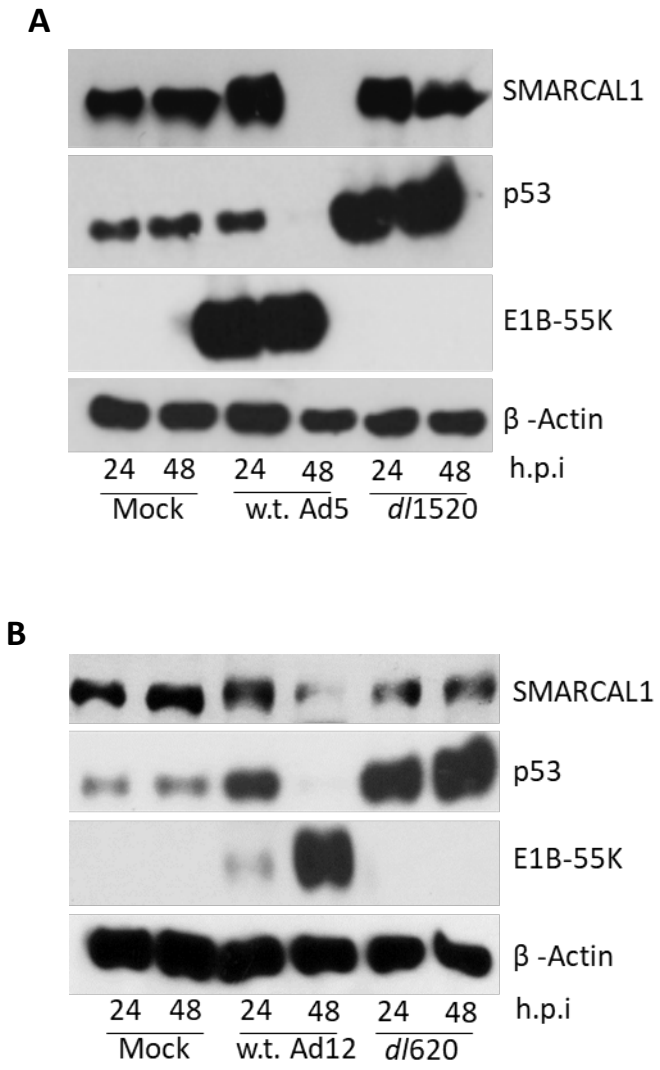

Figure 3.9: SMARCAL1 is degraded in an Ad E1B-55K-dependent manner following Ad5 and Ad12 infection: A549 cells were mock infected (uninfected) infected with either w.t. Ad5 and Ad5 *dl1520* **(A**) or w.t. Ad12 and Ad12 *dl*620 (**B**) at 10 p.f.u./cell. Whole cell lysates were prepared at appropriate times post-infection and 50µg protein samples were separated by SDS-PAGE and subjected to Western blot analysis using the appropriate antibodies. This figure is representative of three independent experiments.

3.2.5.2. The proteasome inhibitor, MG132 reduces the ability of w.t. Ad5 and w.t. Ad12 to degrade SMARCAL1 in Ad-infected cells.

To investigate whether the proteasome contributes towards the Ad-induced loss of the SMARCAL1 protein during infection we first investigated whether the peptide aldehyde and reversible proteasome inhibitor, MG132 (Lee and Goldberg 1996), could inhibit the ability of w.t. Ad5 and w.t. Ad12 to promote the loss of the SMARCAL1 protein. To do this, A549 cells were infected initially, with either w.t. Ad5 or w.t. Ad12, and immediately after infection incubated in the absence, or presence, of MG132. After the appropriate time post-infection cells were harvested and protein lysates subjected to SDS-PAGE and WB analyses [Figure 3.10 A and B]. Treatment of w.t. Ad5-infected A549 cells with MG132 appeared to reduce the rate of SMARCAL1 protein loss during infection relative to infected cells not treated with MG132, but did not prevent completely the loss of the SMARCAL1 protein [cf lanes 10-12 with lanes 7-9, panel I; Figure 3.10A]. Similarly, treatment of w.t. Ad12-infected A549 cells with MG132 also reduced the rate of SMARCAL1 protein loss during infection relative to infected cells not treated with MG132, but SMARCAL1 protein was still reduced significantly in the presence of MG132 [cf lanes 10-12 with lanes 7-9, panel I; Figure 3.10A]. MG132 did not affect the ability of w.t. Ad5 or w.t. Ad12 to promote the degradation of p53 [cf lanes 10-12 with lanes 7-9, panel ii; Figure 3.10 A and B]. Taken together, these data suggest that the proteasome might contribute towards the degradation of SMARCAL1 during infection, but indicate that the proteasome inhibitor, MG132 is possibly not that effective in inhibiting proteasome activity fully as it was unable to prevent the degradation of the known substrate, p53.

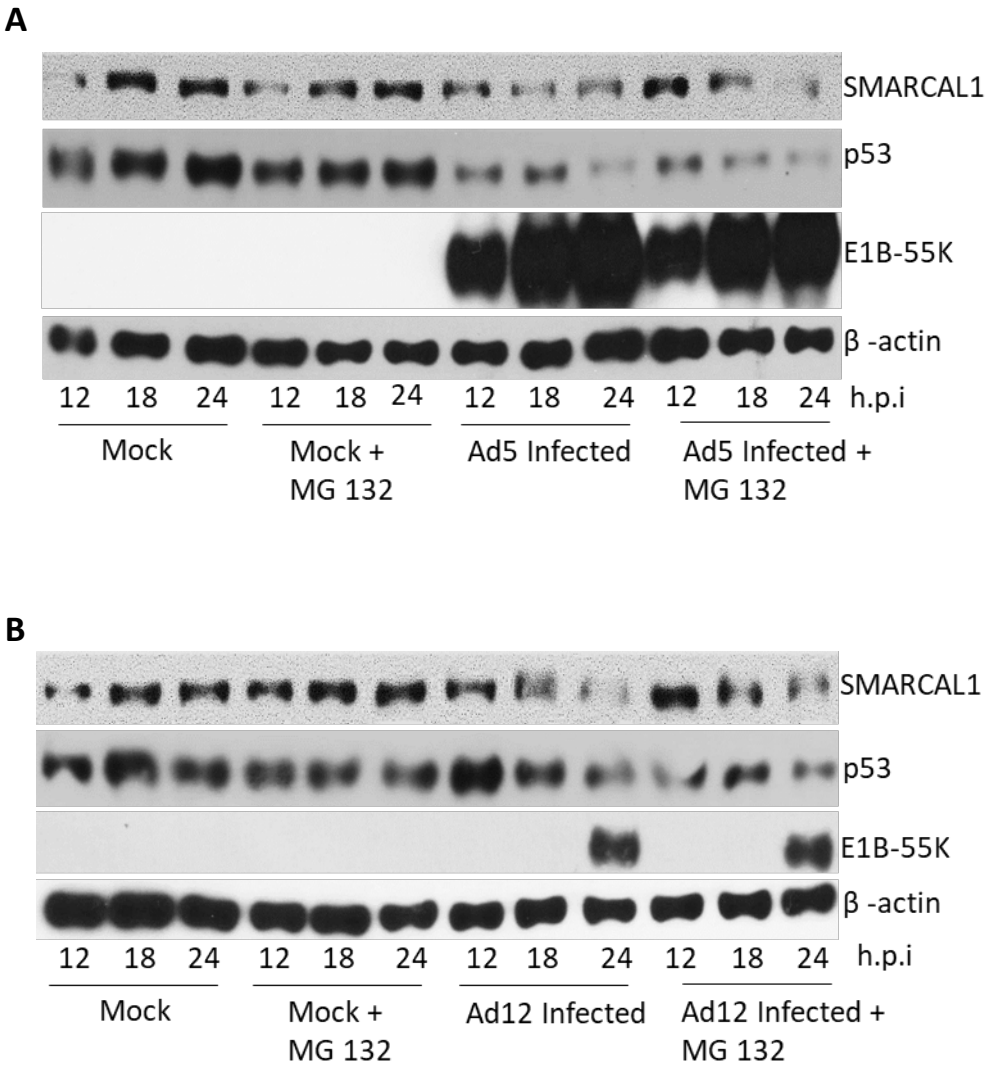

Figure 3.10: Investigating a role for the proteasome in the Ad-induced loss of SMARCAL1 during infection: A549 cells were either mock infected (uninfected) or infected with w.t Ad5 or w.t. Ad12 at 10 p.f.u./cell. Following infection cells were incubated in the absence, or presence of the proteasome inhibitor, MG132 (10 µM). Samples were then harvested 24h and 48h post infection and 50µg protein samples subject to SDS-PAGE and WB analysis using the appropriate antibodies. This figure is representative of two independent experiments.

3.2.5.3. The proteasome inhibitor Sal A has some effect on the ability of w.t. Ad5 and w.t. Ad12 to degrade SMARCAL1 in Ad-infected cells.

To establish further the role of the proteasome in the degradation of SMARCAL1 during infection, we decided to investigate the effects of the γ-lactam-β-lactone and irreversible proteasome inhibitor, Salinosporamide A (Sal A; also known as Marizomib) (Feling, Buchanan et al. 2003), upon the ability of w.t. Ad5 and w.t. Ad12 to promote SMARCAL1 loss during infection. As such, A549 cells were infected with either w.t. Ad5 or w.t. Ad12 then incubated in the absence or presence of Sal A, prior to harvesting cell lysates and subjecting them to SDS-PAGE and WB analyses. These analyses revealed that Sal A limited SMARCAL1 protein loss at 24h post-infection with w.t. Ad5, relative to infected cells not treated with Sal A, but clearly did not prevent the loss of the SMARCAL1 protein during infection [cf lanes 7 and 8 with lanes 5 and 6, panel I; Figure 3.11A]. Interestingly, however, Sal A had a more pronounced inhibitory effect on the ability of w.t. Ad12 to promote SMARCAL1 protein loss during infection relative to infected cells not treated with Sal A [cf lanes 7 and 8 with lanes 5 and 6, panel i; Figure 3.11B]. Sal A did not affect the ability of w.t. Ad12 to promote the degradation of p53 but appeared to limit p53 degradation following w.t. Ad5 infection [cf lanes 7 and 8 with lanes 5 and 6, panel ii; Figure 3.11 A and B]. The major caveat with these experiments, however, is that Sal A treatment alone appeared to stabilize SMARCAL1 and p53 protein levels in the absence of infection (e.g. cf lanes 3 and 4 with lanes 1 and 2, panels i and ii; Figure 3.11 A and B), which makes the interpretation of the results less clear. These results do suggest however that the proteasome does contribute towards SMARCAL1 degradation during infection. These data also suggest either that other

mechanisms contribute towards SMARCAL1 protein loss during infection, or that the proteasome retained some activity in those cells treated with proteasome inhibitors.

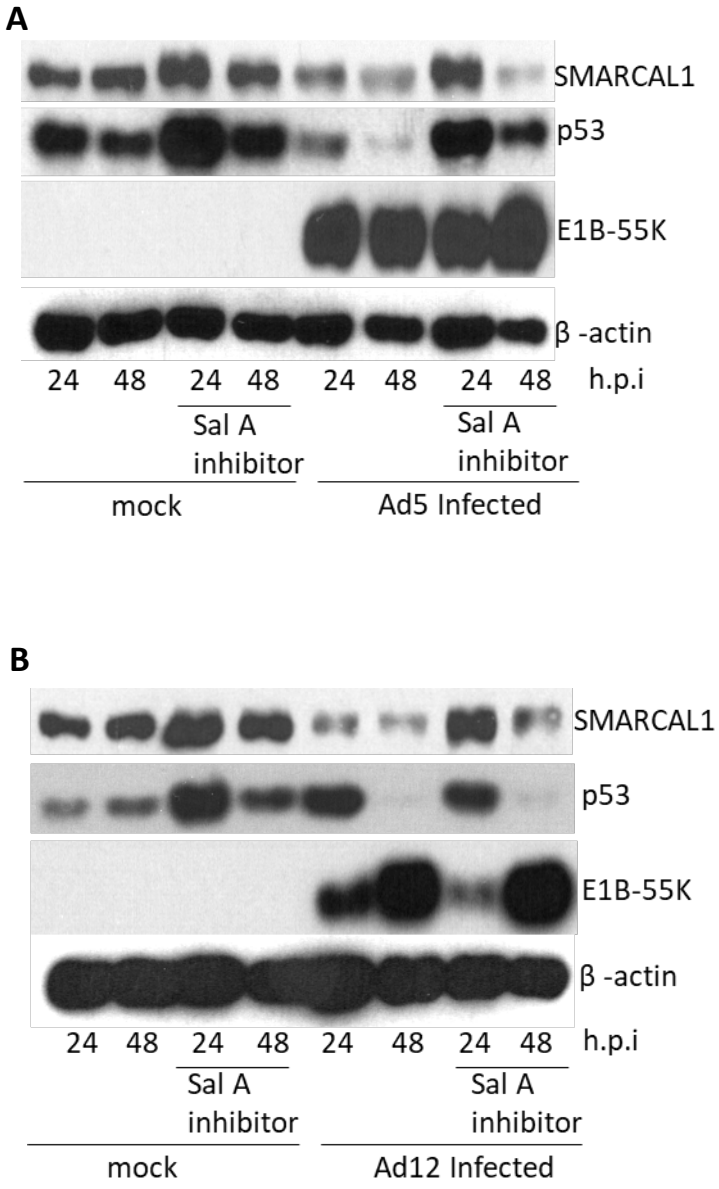

Figure 3.11: The proteasome inhibitor, Sal A, reduces SMARCAL1 degradation following Ad5 and Ad12 infection A549 cells were mock treated (uninfected) or infected with w.t Ad5 and w.t Ad12 at 10 p.f.u./cell and then treated with the proteasome inhibitor, Sal A (100nM). Samples were then harvested 24h and 48h post infection and 50μg protein samples subject to SDS-PAGE and WB analysis using the appropriate antibodies. This figure is representative of two independent experiments.

3.2.5.4: SMARCAL1 is targeted for degradation in a Cullin Ring Ligase-dependent manner during Ad infection.

Previous studies from our laboratory and data presented in this Chapter suggested that E1B-55K was required for the Ad5 and Ad12 -induced degradation of SMARCAL1 and that Ad5 E4orf6 was also required for the degradation of SMARCAL1 during Ad5 infection (Figure 3.9; F.S.I Qashqari, PhD thesis, The University of Birmingham, 2017). We reasoned therefore, that given the known role of these proteins that they would similarly engage with cellular CRLs to promote SMARCAL1 degradation during Ad infection. To investigate this possibility we took advantage of the observation that the NEDD8-activating enzyme (NAE) inhibitor, MLN4924, inhibits the NEDDylation, and activation of the Cullin component of CRLs (Soucy, Smith et al. 2009) (Nawrocki, Griffin et al. 2012).

We therefore infected A549 cells with either w.t Ad5 or w.t. Ad12 and subsequently treated the infected cells with NAE inhibitor, MLN4924 at different concentrations. We then harvested cell lysates at 24h and 48h post-infection and subjected them to SDS-PAGE and WB analyses. At 100nM MLN4924, the ability of w.t. Ad5 to promote the loss of SMARCAL1 was reduced slightly at 24h post-infection, relative to w.t. Ad5-infected cells not treated with MLN4924 [cf lane 7 with lane 3, panel i, Figure 3.12A]. At 500nM MLN4924, the ability of w.t. Ad5 to promote the loss of SMARCAL1 was ablated almost completely at 24h post-infection, relative to w.t. Ad5-infected cells not treated with MLN4924 [cf lane 10 with lane 3, panel i Figure 3.12A]. At 48h post-infection however, MLN4924 was unable to inhibit the ability of w.t. Ad5 to promote the loss of the SMARCAL1 protein, relative to w.t. Ad5-infected cells not treated with

MLN4924 [cf lanes 8 and 12 with lane 4, panel i; Figure 3.12A].

Similar results were seen following w.t. Ad12 infection. At 100nM MLN4924, the ability of w.t. Ad12 to promote SMARCAL1 loss was reduced slightly at both 24h and 48h post-infection, relative to w.t. Ad12-infected cells not treated with MLN4924 [cf lanes 7 and 8, with lanes 3 and 4, panel i, Figure 3.12B]. At 500nM MLN4924, the ability of w.t. Ad12 to promote SMARCAL1 loss was almost completely ablated at 24h post-infection, relative to w.t. Ad12-infected cells not treated with MLN4924 [cf lane 11 with lane 3, panel i, Figure 3.12A]. At 48h post-infection, MLN4924 still retained some capacity to inhibit the ability of w.t. Ad12 to promote the loss of SMARCAL1, relative to w.t. Ad12-infected cells not treated with MLN4924 [cf lane 12 with lane 4, panel i, Figure 3.12B]. 500nM MLN4924 appeared to have an inhibitory effect on the ability of both w.t. Ad5 and w.t. Ad12 to promote the degradation of p53 during infection [cf lanes 11 and 12 with lanes 3 and 4, panel ii, Figure 3.11 A and B] but these results were complicated by the observation that MLN-4924 treatment elevated p53 protein levels in non-infected cells [cf lanes 5 and 6, and lanes 9 and 10 with lanes 1 and 2, panel ii; Figure 3.11 A and B].

Taken together, these data suggest that E1B-55K and E4orf6 do utilise cellular CRLs to promote the degradation of SMARCAL1 during both w.t. Ad5 and w.t. Ad12 infection, but akin to the proteasome studies described earlier, suggest that adenovirus might also utilise other mechanisms to promote the degradation of SMARCAL1, and other substrates, such as p53, during infection.

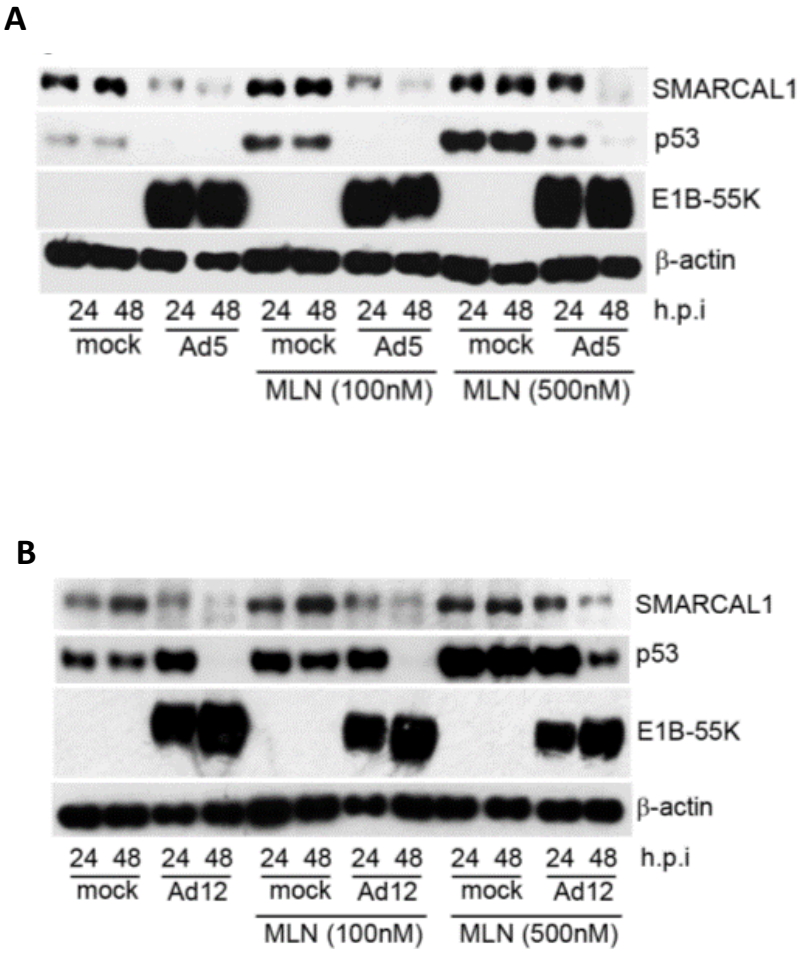

Figure 3.12: SMARCAL1 is degraded in a CRL-dependent manner following Ad5 and Ad12 infection: A549 cells were mock treated (uninfected) or infected with either w.t. Ad5 **(A**) or w.t. Ad12 (**B**) at 10 p.f.u./cell and then treated with NAE inhibitor, MLN4924 (at 100nM or 500nM) until harvested. Whole cell lysates were prepared at appropriate times post-infection and 50µg protein samples were separated by SDS-PAGE and subjected to Western blot analysis using the appropriate antibodies. This figure is representative of three independent experiments. (Published in J.Virol 2019 by Nazeer et al).

3.2.6. Ad genome replication is not required to initiate SMARCAL1 degradation.

As an important function of SMARCAL1 is to regulate cellular DNA replication, we were interested to investigate whether the loss of SMARCAL1 protein during infection was dependent upon the initiation of viral DNA replication. To investigate this possibility we took advantage of previous observations that established that Ganciclovir 200 to 500μM inhibited Ad genome replication (Faulds and Heel 1990, Ying, Tollefson et al. 2014). We therefore optimised the dose to 500 μM and infected A549 cells with either w.t Ad5 or w.t. Ad12 and then treated the infected cells with Ganciclovir. We subsequently harvested cell lysates at 24h and 48h post-infection and subjected them to SDS-PAGE and WB analyses and repeated the experiment thrice. These analyses revealed that treatment of both w.t. Ad5 and w.t. Ad12 -infected cells with Ganciclovir had no effect on the ability of these viruses, relative to cells not treated with Ganciclovir, to inhibit SMARCAL1 degradation during infection [cf lanes 7 and 8 with lanes 5 and 6, panel i, Figure 3.13 A and B]. Interestingly however, it appeared that treatment of Ad-infected cells with Ganciclovir did limit the ability of both w.t. Ad5 and w.t. Ad12 to target p53 for degradation [cf lanes 8 and 12 with lane 4, panel ii; Figure 3.13 A and B]. Taken together, these data suggest that adenoviral genome replication might not be required to induce SMARCAL1 degradation but does affect p53 degradation but might play a role in the degradation of p53.

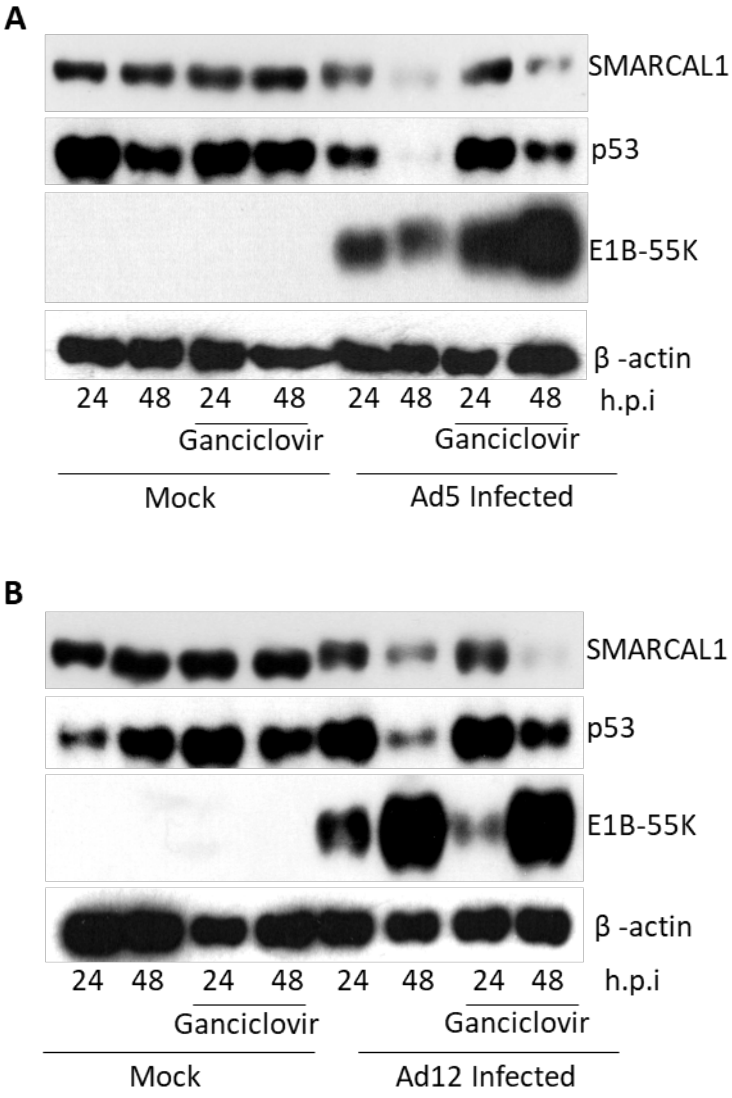

Figure 3.13: Ad replication inhibitor Ganciclovir does not affect the Ad-induced degradation of SMARCAL1: A549 cells were mock treated (uninfected) or infected with w.t. Ad5 (A) and w.t. Ad12 (B) at 10 p.f.u./cell and then treated with Ganciclovir (500μM) until harvested. Whole cell lysates were prepared at appropriate times post-infection and 50μg protein samples were separated by SDS-PAGE and subjected to Western blot analysis using the appropriate antibodies. This figure is representative of three independent experiments.

3.3. Discussion

As adenovirus genome replication results in the production of large amounts of ssDNA and linear dsDNA adenoviruses have developed numerous strategies to inhibit host cell DDR pathways and prevent cell cycle checkpoint activation and DNA repair; viral inhibition of DDR pathways prevents viral DNA concatenation and promotes viral DNA replication. One mechanism adenoviruses utilize to inhibit DDR pathways is to engage with the ubiquitin-proteasome system and target a number of host cell DDR proteins for ubiquitin-mediated degradation (Turnell and Grand 2012). In this regard, E1B-55K typically functions as an adaptor protein, binding to the cellular protein substrate to be degraded, and recruiting CRL2 or CRL5 to the substrate through its association with another viral protein, E4orf6 (Querido, Blanchette et al. 2001).

In this chapter we have shown that adenoviruses utilize the ubiquitin-proteasome system to target the cellular DNA replication protein, SMARCAL1 for degradation during Ad infection. As such, we first determined that the protein levels of SMARCAL1 were reduced significantly following infection of A549 cells with Ad5 and Ad12, in a manner similar to p53, a known target for the Ad ubiquitin ligase during infection (Figure 3.1). Interestingly, WB analyses also revealed that there was an obvious retardation of SMARCAL1 mobility on SDS-PAGE following Ad infection, suggesting that SMARCAL1 was post-translationally modified, prior to its degradation, in response to Ad infection (Figure 3.1). As mobility-shifts on SDS-PAGE are often due to changes in the phosphorylation status of the protein, and multiple cellular kinases are known to be activated in response to Ad infection (Turnell and Grand 2012) we next investigated whether SMARCAL1 was phosphorylated following Ad infection. To do this we treated

anti-SMARCAL1 immunoprecipitates from Ad5- and Ad12- infected cells with the broad range protein phosphatase, λ-phosphatase. Importantly, the λ-phosphatase assay revealed that SMARCAL1 was indeed, phosphorylated following both Ad5 and Ad12 infection (Figure 3.2). Mass spectrometric analyses then revealed that SMARCAL1 was phosphorylated on three specific residues during Ad infection: S123, S129 and S173 which are well conserved amongst higher mammals (Figure 3.3). S123 and S129 constitute part of a minimal CDK consensus site, SP, whilst S173 forms part of a PIKK family kinase consensus site, SQE (Figure 3.3).

As SMARCAL1 is subject to phosphorylation following Ad infection we next sought to investigate whether SMARCAL1 phosphorylation was required for SMARCAL1 degradation. Firstly, as S173 is likely to be phosphorylated by ATM, ATR or DNA-PK we investigated a generic role for these kinases in SMARCAL1 degradation by investigating the effects of the common PIKK family inhibitor, caffeine upon Ad-induced SMARCAL1 degradation. Consistent with a role for a caffeine-sensitive kinase in the Ad-mediated degradation of SMARCAL1, treatment of Ad-infected cells with caffeine reduced the ability of Ad5 and Ad12 to target SMARCAL1 for degradation (Figures 3.4). We next extended these studies to investigate specifically the role of ATM and ATR in SMARCAL1 phosphorylation following Ad infection. Studies with the ATM specific kinase inhibitor, KU-55933, established that ATM was not responsible for targeting SMARCAL1 for degradation during Ad5 and Ad12 infection (Figure 3.5). Given that the ATM activator, MRN, is targeted for degradation during Ad infection (Stracker, Carson et al. 2002) it is, perhaps, not surprising that ATM does not phosphorylate SMARCAL1 during infection. Interestingly however, previous studies from our laboratory suggested that H2AX phosphorylation during Ad infection was

dependent, to some extent, on ATM, whilst a more recent study suggested that the MRN complex was not absolutely required for ATM activation (Blackford, Bruton et al. 2008, Hartlerode, Morgan et al. 2015).

As we have previously shown that ATR was required for the Ad-mediated phosphorylation of RPA32, Smc1 and H2AX during Ad infection (Blackford, Bruton et al. 2008), we next investigated the effects of the ATR kinase inhibitor, AZD-6738, on the Ad-targeted degradation of SMARCAL1 (Figure 3.6). Interestingly, these studies indicated that inhibition of ATR kinase reduced significantly the ability of Ad12 to target SMARCAL1 for degradation and limited, to a modest extent, the ability of Ad5 to promote SMARCAL1 degradation (Figures 3.6). A possible explanation for these differences is that ATR is not activated to the same extent following Ad5 infection, as compared to an Ad12 infection and that Ad12 is more reliant on ATR during infection than Ad5 (Blackford, Bruton et al. 2008). In this regard the E1B-55K interacting protein, E1B-AP5 (hnRNPUL1) participates in the ATR-dependent phosphorylation of RPA32 in Ad12-infected cells (Blackford, Bruton et al. 2008). Given that Ad12 promotes the degradation of the ATR activator, TopBP1, in order to prevent Chk1 activation whilst Ad5 does not (Blackford, Patel et al. 2010), it would be interesting to re-evaluate whether ATR also participates in the degradation of TopBP1, or other known degradation targets, during Ad12 infection. In this regard, whilst early MS screens for ATM and ATR substrates by the Elledge group identified a number of SQ/TQ sites targeted for phosphorylation following treatment with ionizing radiation (Matsuoka, Ballif et al. 2007) there have been no reports since that ATR phosphorylates TopBP1 directly.

As SP motifs are substrates for CDKs which are known to be activated following Ad infection (Grand, Ibrahim et al. 1998), we next used a CDK inhibitor, RO-3306, to investigate whether CDKs were responsible for targeting SMARCAL1 for degradation following Ad infection (Figure 3.7). In contrast to the ATR inhibitor studies, we established that the CDK inhibitor, RO-3306, had a greater propensity to inhibit Ad5-mediated degradation of SMARCAL1, compared to Ad12, which was only limited modestly in its ability to target SMARCAL1 for degradation (Figure 3.7). These findings might suggest that Ad5 is more reliant on CDK activity during infection than Ad12. Given these differences in requirements for ATR or CDKs in different Ad types it would be extremely interesting to see, if first SMARCAL1 degradation is conserved between different Ad groups, and the differential contribution of ATR and CDKs in these processes. Indeed, our group have reported previously that different Ad types have evolved different strategies to combat the cellular DDR (Forrester, Sedgwick et al. 2011).

We did establish that ATR and CDK kinases co-operate during Ad infection to promote SMARCAL1 (Figure 3.8). At this stage, however, we cannot determine which CDK is involved in the phosphorylation of SMARCAL1, as RO-3306 inhibits CDK1, CDK2, CDK4 and CDK6 kinases at the concentrations used in these experiments. It will be important in the future to establish which CDK is responsible for SMARCAL1 phosphorylation during infection. To do this we should use more specific inhibitors of CDK1, CDK2 and CDK4 and CDK6, or use siRNA/CRISPR to deplete these kinases prior to Ad infection. Given that Ad infection promotes cell entry into S-phase it is likely that CDK2, or CDK1 are the most likely candidates that phosphorylate SMARCAL1 during infection.

It is well established that the adenovirus oncoproteins E1B-55K and E4orf6 work in concert to promote the CRL-mediated degradation of host cell proteins, such as p53 and MRE11 for degradation via the ubiquitin-proteasome system during infection (Querido, Blanchette et al. 2001). As studies presented in this Chapter (Figure 3.9) and from others in our laboratory, indicated that SMARCAL1 is degraded in an E1B-55K and E4orf6 - dependent manner (F.S.I Qashqari, PhD thesis, The University of Birmingham, 2017), we next sought to establish a requirement for the ubiquitin-proteasome system in SMARCAL1 degradation. The peptide aldehyde, reversible proteasome inhibitor, MG132 (Pehere, Nguyen et al. 2019) reduced the ability of Ad5 and Ad12 to promote SMARCAL1 degradation during infection, particularly at early time-points post-infection though it did not ultimately prevent SMARCAL1 degradation; MG132 did not affect the ability of Ad5 or Ad12 to target p53 for degradation (Figure 3.10). We also used the irreversible proteasomal inhibitor, Sal A (Gulder and Moore 2010), to establish the role of the proteasome in SMARCAL1 (and p53) degradation. Unfortunately, although treatment with Sal A limited SMARCAL1 and p53 degradation following infection, treatment of mock-infected cells with SalA clearly increased the basal levels of these proteins, which complicates the interpretation of the data (Figure 3.11). It is clear from published studies investigating the role of CRLs in adenovirus-mediated degradation of cellular proteins that the inhibitory effects of proteasome inhibitors upon the Ad-mediated degradation of cellular substrates are not fully restorative (e.g. MRE11 (Stracker, Carson et al. 2002)). Moreover, some studies have not performed experiments showing the effects of proteasome inhibitors on Ad-mediated degradation, or have performed these experiments, but lack the appropriate controls (e.g. p53, (Steegenga, Riteco et al. 1998, Querido, Blanchette et al. 2001). Explanations for these observations are not immediately apparent. It could be that the Ad-induced targeting of large amounts

of substrates for proteasome degradation, ultimately out-compete reversible inhibitors such that degradation is delayed, but not inhibited. It is also possible that combinations of proteasome inhibitors should be used to ensure complete inhibition of 20S β1, β2 and β5 proteolytic activities.

As CRLs are known to be utilized by adenovirus in the targeted degradation of host cell proteins we next investigated whether SMARCAL1 was similarly targeted for degradation via the action of cellular CRLs. As CRLs are activated by cullin NEDDylation we used an NEDD8 activating enzyme, inhibitor MLN 4924 to prevent CRL activation (Lan, Tang et al. 2016). Akin to the proteasome studies we determined that MLN 4924 reduced the rate of SMARCAL1 degradation in both Ad5 and Ad12 – infected cells but did not inhibit fully SMARCAL1 degradation (Figure 3.12). These data are entirely consistent with a role for CRLs in the Ad-mediated degradation of SMARCAL1, but suggest also, that Ad might overcome CRL inhibition, or alternatively, use different viral oncoproteins, cellular ubiquitin ligases, or cellular or viral proteases to promote the degradation of SMARCAL1 during infection. Indeed, our laboratory has shown previously that E4orf3 does not use CRLs in the targeted degradation of TIF1γ and HPV targets host cellular pRB protein for degradation utilising different cellular ubiquitin ligases (Bischof, Nacerddine et al. 2005, Forrester, Patel et al. 2012). Moreover, it would be interesting to determine the effects of cell permeable lysosomal/autophagic (e.g. chloroquinone) and apoptotic (Z-VAD-FMK) inhibitors on the ability of Ad to target SMARCAL1 (and other substrates) for degradation as the contribution of these proteases has yet to be explored.

The ability of Ad oncoproteins to usurp the control of host cell pathways through the proteasomal-mediated degradation of cellular proteins that possess anti-viral activity to promote viral replication is well established. Given that SMARCAL1 is known to regulate cellular DNA replication, we also investigated whether the Ad DNA replication inhibitor, Ganciclovir, affected the ability of Ad to target SMARCAL1 for degradation, but it did not, suggesting that SMARCAL1 degradation occurs prior to the onset of Ad DNA replication (Figure 3.13). Interestingly, though p53 degradation did seem to be dependent to some extent on the initiation of Ad replication as Ganciclovir did limit p53 degradation during infection (Figure 3.13).

In conclusion, we have shown here that ATR kinase and, an unidentified, CDK phosphorylate SMARCAL1 directly upon residues S123, S129 and S173 following Ad infection, which results in the E1B-55K/E4orf6, and CRL-targeted degradation of SMARCAL1. The specific requirement for SMARCAL1 phosphorylation during infection is considered in the next chapter.

CHAPTER 4

Role of the RPA complex and phosphorylation in the recruitment of SMARCAL1 to viral replication centres

4.1: Introduction.

Adenoviruses are known to neutralise host cell DDR pathways and inhibit anti-viral signalling pathways in order to promote viral DNA replication (Weitzman, Carson et al. 2004, Turnell and Grand 2012, Weitzman and Fradet-Turcotte 2018). In this regard, adenoviruses have been shown to inhibit ATM, ATR and DNA-PK pathways by targeting activators, or effectors, for CRL- and proteasome- dependent degradation (e.g. (Querido, Blanchette et al. 2001, Stracker, Carson et al. 2002, Baker, Rohleder et al. 2007, Blackford, Patel et al. 2010)). In chapter 3 of this thesis we determined that the DDR protein, and ATR substrate, SMARCAL1, was phosphorylated and targeted for degradation following both Ad5 and Ad12 infection. In this regard, we found that SMARCAL1 degradation was dependent upon the ATR- and CDK- dependent phosphorylation of SMARCAL1 (Chapter 3). As such, we showed by mass spectrometry that SMARCAL1 was phosphorylated at residues 123, 129 and 173 by ATR and CDK kinases during Ad infection (Chapter 3). All of these SMARCAL1 residues have previously been identified by David Cortez's group as targets for phosphorylation *in vivo* (Carroll, Bansbach et al. 2013). S173 lies within an ATM/ATR/DNA-PK SQE consensus site and is phosphorylated, in a DDR kinase-dependent manner, in response to cellular replication stress following hydroxyurea treatment (Carroll, Bansbach et al. 2013). These studies also demonstrated that phosphorylation of S173 did not affect the intrinsic ATPase activity of SMARCAL1. Indeed, the biological significance of phosphorylation at this site remains to be determined. S123 and S129 lie within an N-terminal cluster of SP residues in SMARCAL1 that have been shown to be phosphorylated by CDKs *in vivo* (Carroll, Bansbach et al. 2013). It is presumed that these sites might be involved in regulating SMARCAL1 cell cycle-specific activities such as replication fork processing, though

such activities have yet to be ascribed to these residues (Bansbach, Bétous et al. 2009). SMARCAL1 is known to be recruited to sites of DNA damage through its ability to interact with the ssDNA-binding protein complex, RPA (Ciccia 2009, LA Poole 2017). It has been suggested that high affinity binding sites on RPA allow SMARCAL1 to associate with RPA-bound ssDNA, and that RPA orientates itself relative to replication fork junctions to allow SMARCAL1 access to DNA for remodelling of replication forks whilst bound to RPA (Bhat, Bétous et al. 2015).

Given that SMARCAL1 is targeted for degradation in an ATR- and CDK- dependent manner during Ad infection (Chapter 3), and that SMARCAL1 residues S123, S129 and S173 are all phosphorylated during the early stages of Ad infection (Chapter 3) we wished to determine the functional significance of S123, S129 and S173 SMARCAL1 phosphorylation upon SMARCAL1 degradation during Ad infection. Moreover, as SMARCAL1 has been shown to be recruited to Ad VRCs (Chapter 3), we also wished to establish whether SMARCAL1 phosphorylation at one or more of these sites promotes SMARCAL1 recruitment to VRCs during infection. Additionally, as SMARCAL1 is a known RPA-binding protein (Bansbach, Bétous et al. 2009, Ciccia, Bredemeyer et al. 2009) and co-localizes with RPA at VRCs during Ad infection (Chapter 3), we also wished to establish whether the RPA complex regulates SMARCAL1 localization, or promotes SMARCAL1 degradation, during Ad infection. The results of these findings are presented in this chapter.

4.2: Results.

4.2.1. Generation of inhibitory phosphorylation-defective SMARCAL1 mutants

To begin to investigate the effects of SMARCAL1 phosphorylation on SMARCAL1 function during infection we utilised a retroviral plasmid that expressed w.t. SMARCAL1 as an N-terminally tagged GFP construct under the control of a CMV promoter (pLEGFP-SMARCAL1). In an attempt to ablate the responsiveness of SMARCAL1 to ATR- and CDK- dependent phosphorylation at residues S123, S129 and S173, we performed site-directed mutagenesis on the pLEGFP-SMARCAL1 construct to generate Serine to Alanine mutants for all three sites identified (S123A, S129A and S173A). We then employed Sanger sequencing, in the context of the entire open reading frame (2,865 base pairs), to verify the generation of the appropriate mutants [Figure 4.1A]. In the expectation that phosphorylation of S123, S129 and S173 might cooperate to regulate SMARCAL1 function, we also generated the corresponding double (S123A/S129A, S123A/S173A and S129A/S173A) and triple (S123A/S129A/S173A) phosphorylation-defective SMARCAL1 mutants and validated their integrity by Sanger sequencing [Figures 4.1B and 4.1C, respectively].

To generate clonal cell lines that express w.t., or mutant, GFP-SMARCAL1 fusion proteins we next transfected GP-293 cells with appropriate pLEGFP-SMARCAL1 and VSV-G constructs and, 96h post-transfection isolated replication-defective retroviral particles to transduce either A549, or RPE-1 cells that were seeded at low density (see materials and methods, section 2.2.4 for detailed description). Seventy-two hours following retroviral transduction of A549 and RPE-1 cells we seeded transduced cells

at 500/cells per 10cm dish and isolated clonal cell lines, under selection with G418 (500 μg/ml), approximately two weeks later with a 1ml pipette tip, using a low power light microscope under aseptic conditions. Using this technique, we were able to isolate both A549 (Figure 4.2), and RPE-1 (data not shown), clonal cell lines that expressed constitutively w.t. GFP-SMARCAL1 and GFP-SMARCAL1 mutants that possessed residues that could no longer be phosphorylated on particular SMARCAL1 residues (Figure 4.2). In this regard, clonal cell lines expressed almost identical levels of w.t. SMARCAL1 and phosphorylation-defective SMARCAL1 mutants, consistent with the ability of retroviruses to integrate their genomes at only one site in the infected cell (Figure 4.2).

A

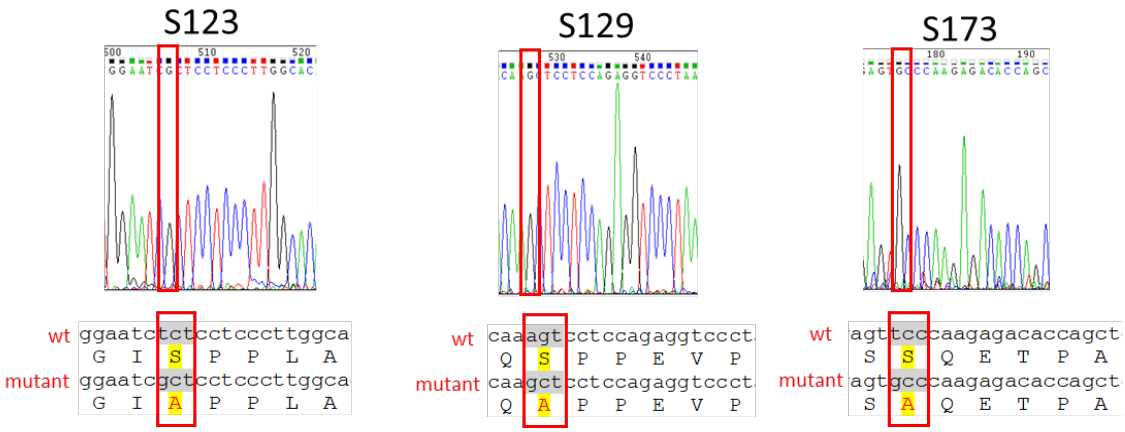

Figure 4.1A to 4.1C. Generation of SMARCAL1 phosphorylation-defective mutants: Using the QuikChange XL site-directed mutagenesis Kit (see material and methods, section..), we mutated the phospho-acceptor serine residues to alanine for all the three phosphorylation sites identified S123, S129 and S173 (**A**) and also generated, S123-S129, S123-S173 and S129-S173 double (**B**), and S123-S129-S173 triple (**C**) serine to alanine phosphorylation defective mutants. The images presented were generated with Chromas and are graphical representations of Sanger sequencing showing the mutated residues.

Bi]

S123/129

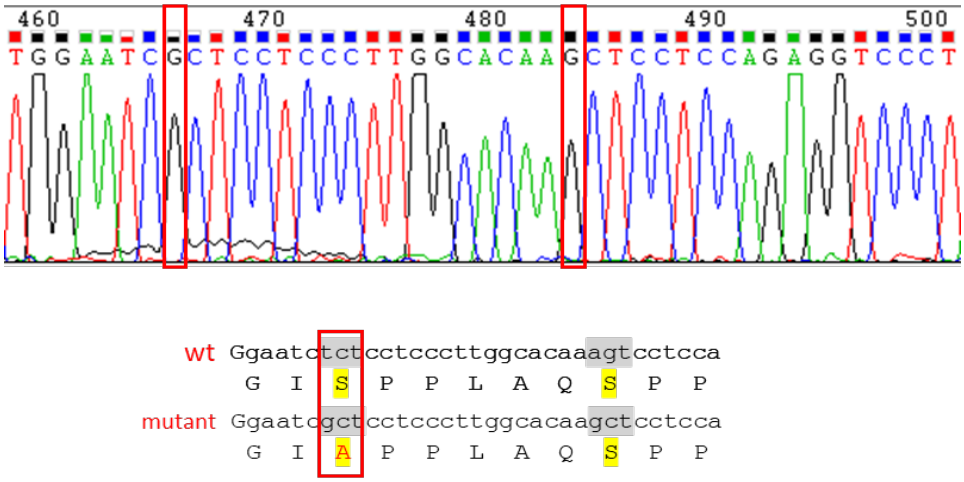
460
470
480
490
500
TGGAATCGCTCCTCCCTTGGCACAAGCTCCTCCAGAGGTCCCT
wt Ggaatctctcctcccttggcacaaagtcctcca
G I S P P L A Q S P P
mutant Ggaatcgctcctcccttggcacaagctcctcca
G I A P P L A Q S P P

Bii] S123/173

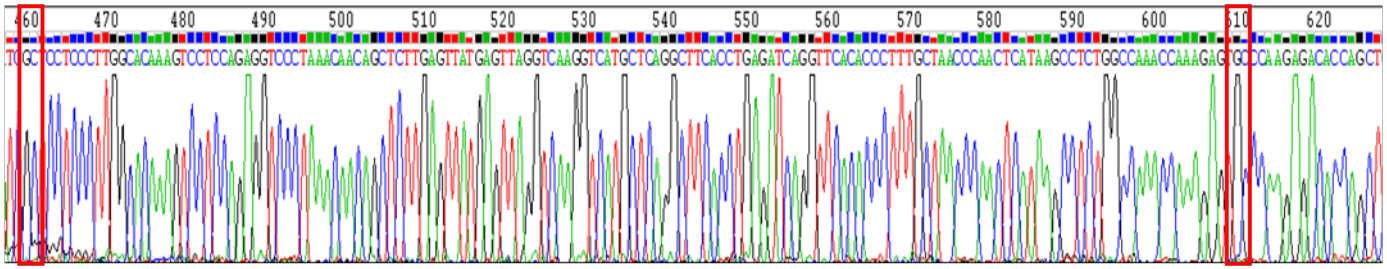
460 470 480 490 500 510 520 530 540 550 560 570 580 590 600 610 620

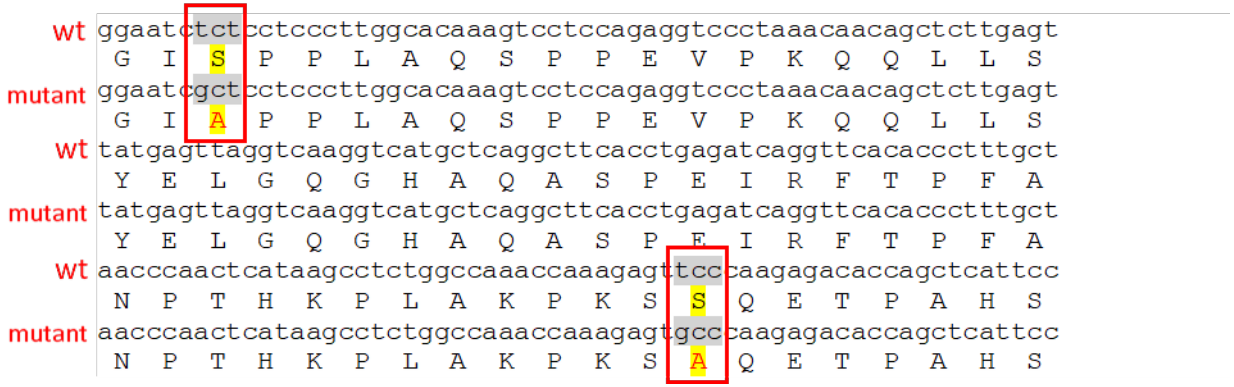
wt ggaatctctcctcccttggcacaaagtcctccagaggtccctaaacaacagctcttgagt
G I S P P L A Q S P P E V P K Q Q L L S
mutant ggaatcgctcctcccttggcacaaagtcctccagaggtccctaaacaacagctcttgagt
G I A P P L A Q S P P E V P K Q Q L L S
wt tatgagttaggtcaaggtcatgctcaggcttcacctgagatcaggttcacacccttgct
Y E L G Q G H A Q A S P E I R F T P F A
mutant tatgagttaggtcaaggtcatgctcaggcttcacctgagatcaggttcacacccttgct
Y E L G Q G H A Q A S P E I R F T P F A
wt aacccaactcataagcctctggccaaaccaaagagttcccaagagacaccagctcattcc
N P T H K P L A K P K S S Q E T P A H S
mutant aacccaactcataagcctctggccaaaccaaagagtgcccaagagacaccagctcattcc
N P T H K P L A K P K S A Q E T P A H S

Biii] S129/173

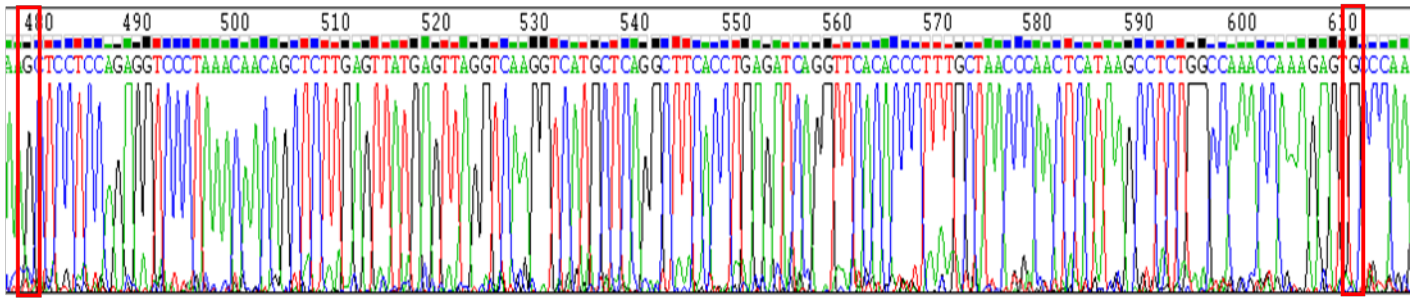

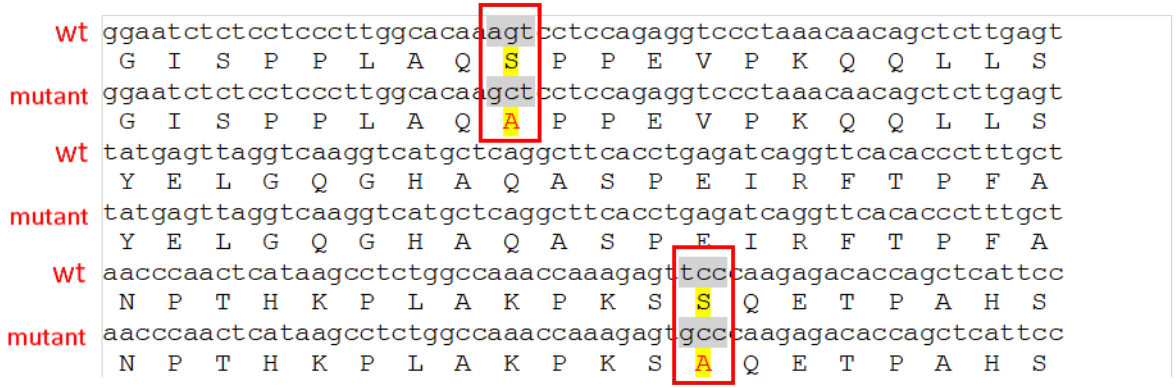

1C] S123/129/173

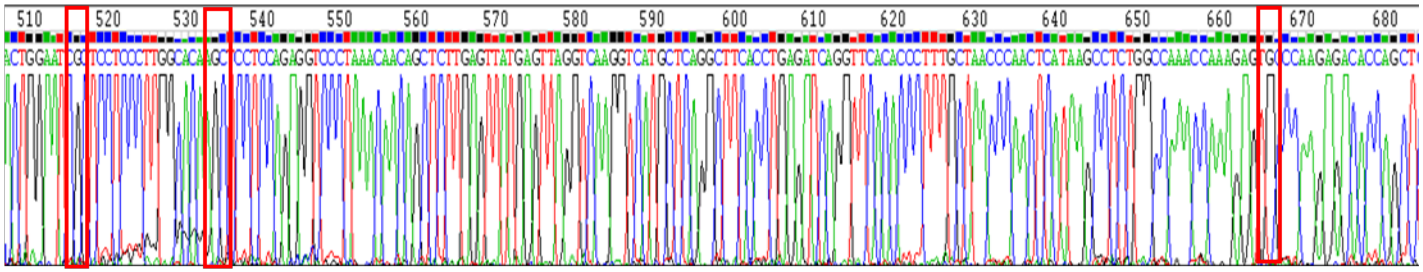

wt ggaatctctcctcccttggcacaaagtcctccagaggtccctaaacaacagctcttgagt
G I S P P L A Q S P P E V P K Q Q L L S
mutant ggaatcgctcctcccttggcacaagctcctccagaggtccctaaacaacagctcttgagt
G I A P P L A Q A P P E V P K Q Q L L S
wt tatgagttaggtcaaggtcatgctcaggcttcacctgagatcaggttcacacccttgct
Y E L G Q G H A Q A S P E I R F T P F A
mutant tatgagttaggtcaaggtcatgctcaggcttcacctgagatcaggttcacacccttgct
Y E L G Q G H A Q A S P E I R F T P F A
wt aacccaactcataagcctctggccaaaccaaagagttcccaagagacaccagctcattcc
N P T H K P L A K P K S S Q E T P A H S
mutant aacccaactcataagcctctggccaaaccaaagagtgcccaagagacaccagctcattcc
N P T H K P L A K P K S A Q E T P A H S

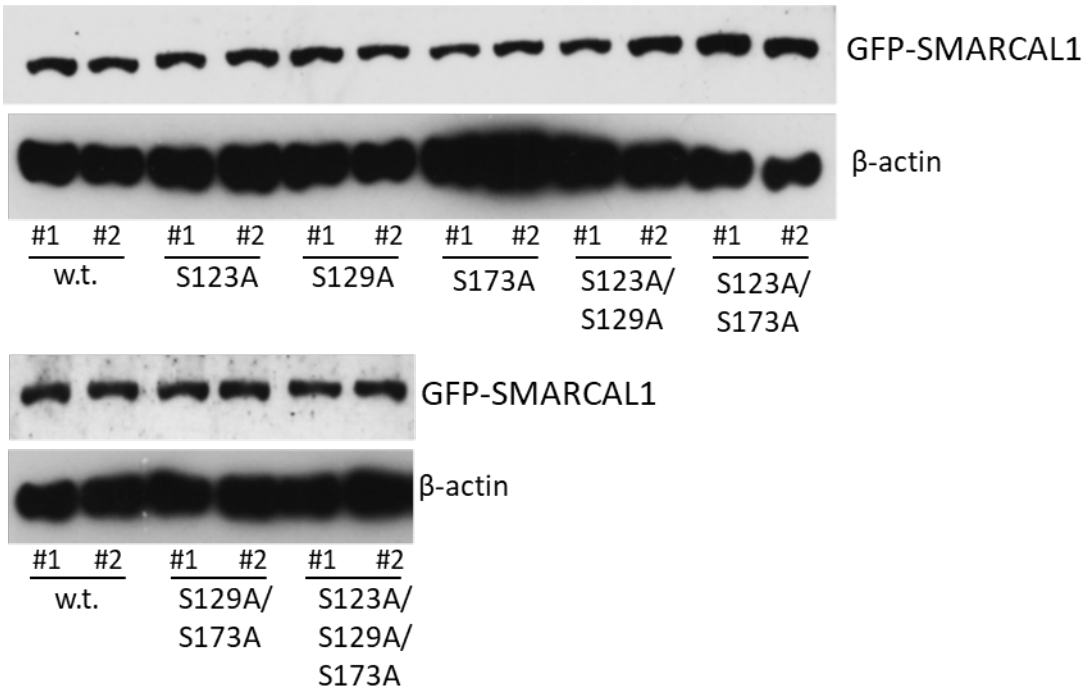

Figure 4.2. GFP-SMARCAL1 protein expression in A549 clonal cell lines. Individual w.t. GFP-SMARCAL1 and GFP-SMARCAL1 mutant clones were expanded and harvested; protein lysates were separated by SDS-PAGE, prior to Western blot analyses for GFP (SMARCAL1) and β-actin. These data are representative of two individual experiments.

4.2.2. Investigating the effects of phosphorylation upon SMARCAL1 degradation in A549 cells.

A primary objective of this study was to use the GFP-SMARCAL1 phosphorylation-defective mutants to investigate further, whether phosphorylation upon these residues was an essential prerequisite for Ad-induced SMARCAL1 degradation given that ATR and CDK inhibitors limited SMARCAL1 degradation during infection (Figures 3.6-3.8, Chapter 3). To begin to address this possibility we infected two A549 clonal cell-lines that constitutively expressed w.t. GFP-SMARCAL1 with either w.t. Ad5, or w.t. Ad12 and examined the levels of GFP-SMARCAL1 species by WB at appropriate times post-infection (Figure 4.3). Consistent with Ad infection, E1B-55K was expressed following infection of these A549 cell derivatives with either w.t. Ad5, or w.t. Ad12 (panels iii and iv, Figure 4.3). Moreover, and as expected, p53 was targeted for degradation early during Ad5 infection, and later following Ad12 infection (panel ii, Figure 4.3). Despite these observations however, GFP-SMARCAL1 was at very low levels in mock-infected cells, relative to Ad5 and Ad12 infected cells where it was vastly overexpressed (panel i, Figure 4.3). In this regard, the exposure time for the WB was a few seconds for the GFP blot following Ad infection, whereas previously we required 5 minutes to visualise GFP in uninfected cells (Figure 4.2). Whilst there was modest decrease in the levels w.t. GFP-SMARCAL1 at late times post Ad5 and Ad12 infection the levels of GFP-SMARCAL1 were elevated substantially following infection. These data indicate that, in contrast to endogenous SMARCAL1, the protein levels of GFP-SMARCAL1 are increased, not decreased, following Ad infection. To investigate this phenomenon further we infected constitutively expressing w.t. GFP-SMARCAL1 A549 cells with either w.t. Ad5, or w.t. Ad12 and determined GFP-SMARCAL1 protein levels in cells

by live-cell imaging of GFP fluorescence (panels i-iii, Figure 4.4). Consistent with the WB analyses, GFP-SMARCAL1 protein levels were low in mock-infected cells and high in both Ad5- and Ad12- infected A549 cells (cf panel i with panels ii and iii, Figure 4.4). GFP-SMARCAL1 was pan-nuclear in mock-infected cells (panel i, Figure 4.4) whilst GFP alone was distributed evenly throughout the cell (data not shown) indicating that SMARCAL1 dictates the cellular localization of the fusion protein. Moreover, in support of previous observations in our laboratory (F.S.I Qashqari, PhD thesis, The University of Birmingham, 2017) GFP-SMARCAL1 was redistributed to nuclear structures, that resembled VRCs, during infection (panels ii and iii, Figure 4.4). These data indicate that GFP-SMARCAL1 behaves differently to the endogenous SMARCAL1 protein. These results will be considered fully in the discussion at the end of this chapter. However, given these results, we reasoned that w.t. and mutant GFP-SMARCAL1 cell lines could not be used to investigate the role of site-specific phosphorylation events in SMARCAL1 degradation during Ad infection.

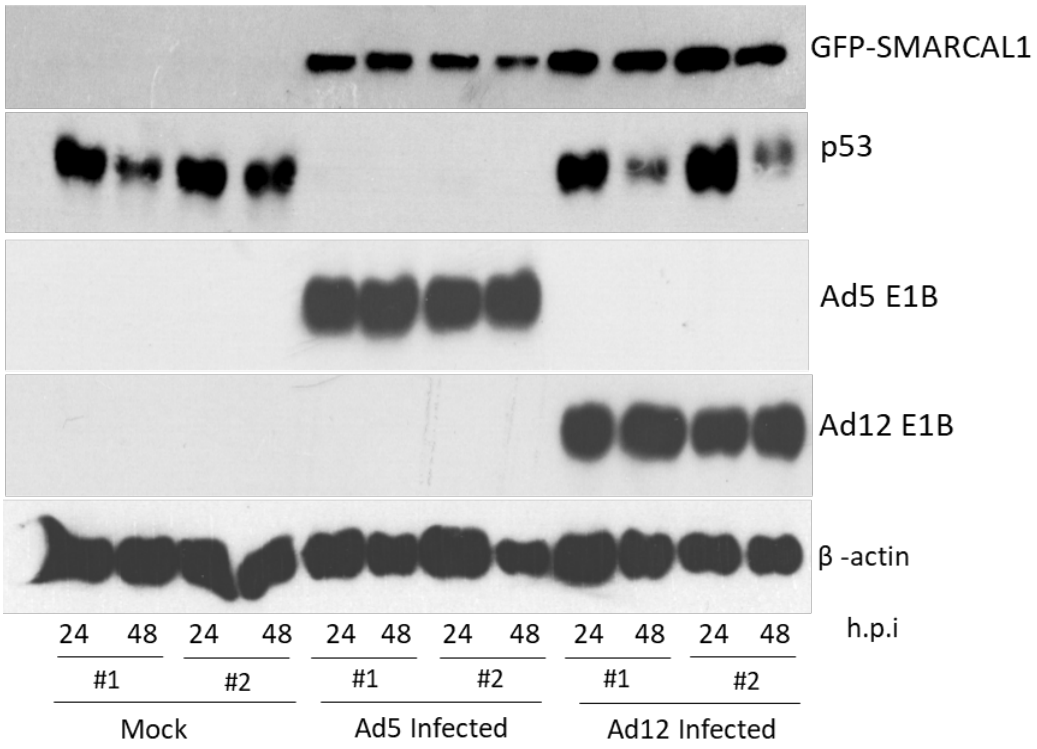

Figure 4.3. GFP-SMARCAL1 protein expression is increased following w.t. Ad5 and Ad12 infection. A549 clonal cell lines expressing WT GFP-SMARCAL1 were either mock infected or infected with WT Ad5 and WT Ad12 at 10 pfu/cell. Cells were harvested at the time indicated and protein lysates separated by SDS-PAGE, prior to Western blot analyses for GFP (SMARCAL1), Ad5 E1B-55K, Ad12 E1B-55K and β-actin. These data are representative of two individual experiments.

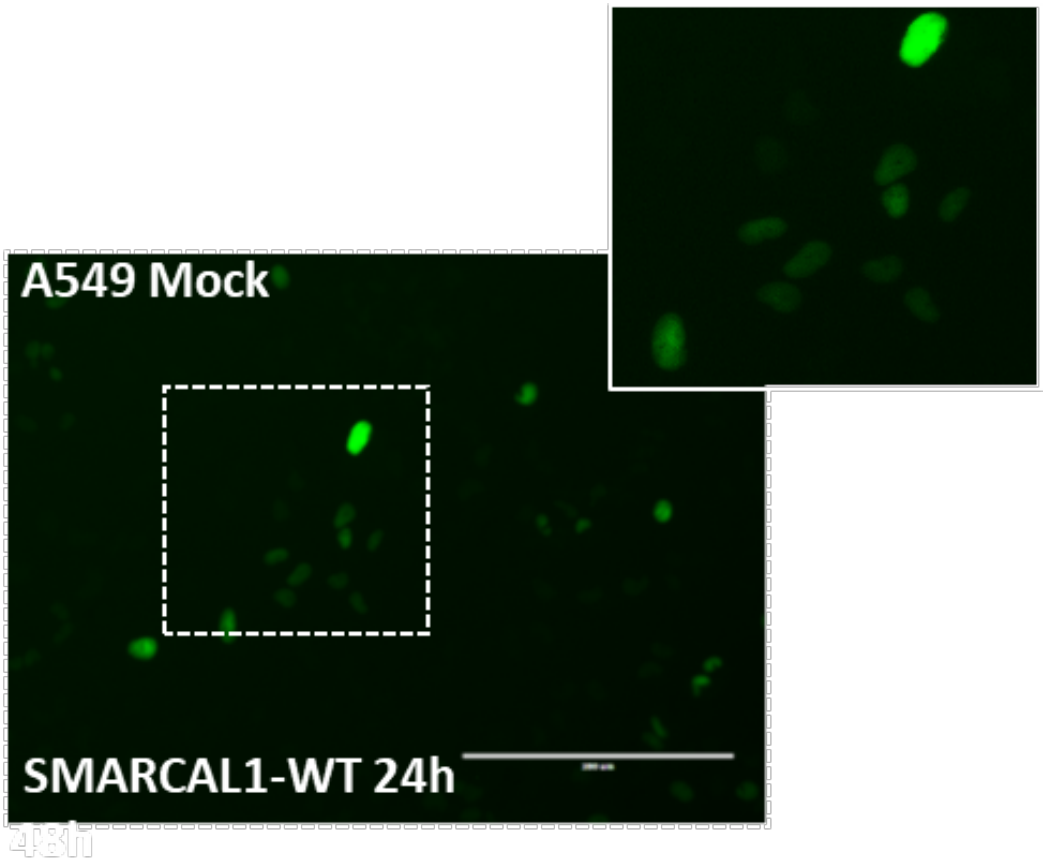
A549 Mock
SMARCAL1-WT 24h
48h
A549 Ad5
SMARCAL1-WT 24h
48h

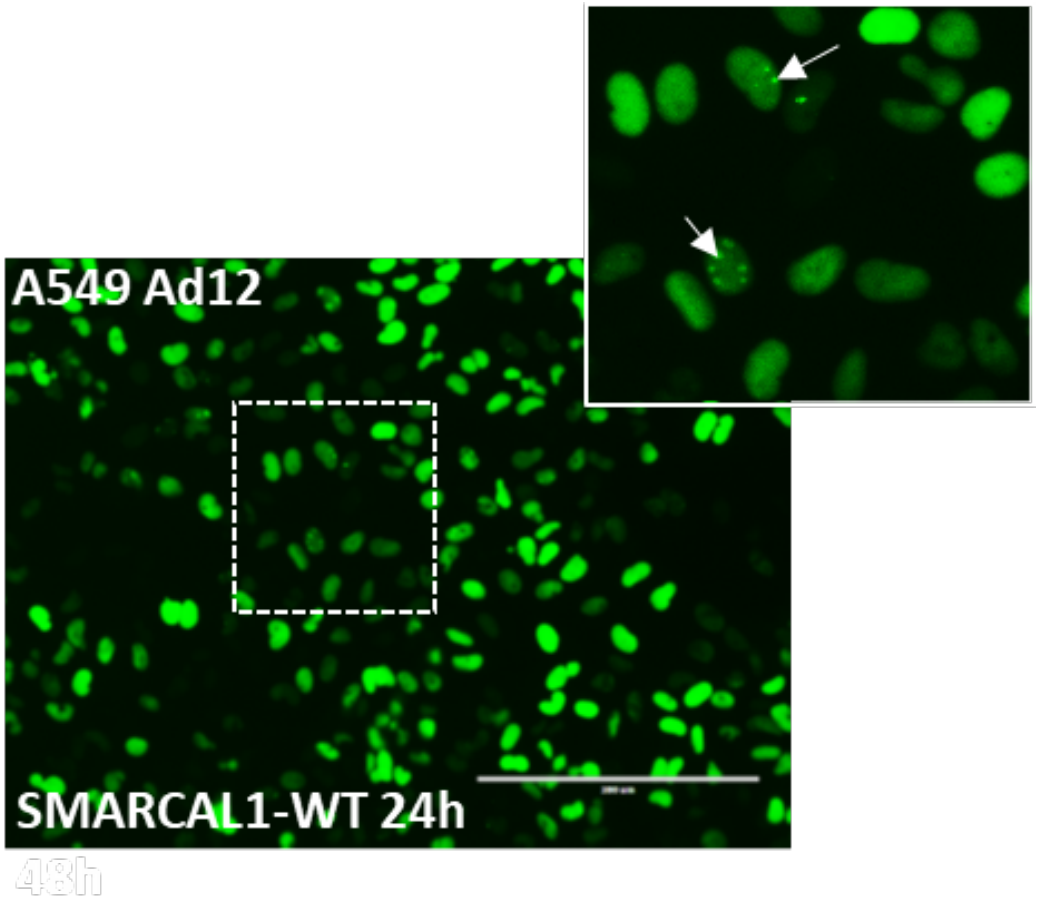

Figure 4.4. Expression and distribution of GFP-SMARCAL1 in WT GFP-SMARCAL1 expressing A549 clonal cell lines following Ad infection. WT GFP-SMARCAL1 expressing A549 cell lines were either mock infected or infected with WT Ad5 and WT Ad12 at 10 pfu/cell. Cells were visualised by live cell imaging fluorescence microscope. Arrows indicate Smarcal1 recruitment to VRCs at the times indicated.

4.2.3. Investigating the requirement for SMARCAL1 phosphorylation in the recruitment of SMARCAL1 to viral replication centres.

As we have established that w.t. GFP-SMARCAL1 is reorganised to VRCs in A549 cells (Figure 4.4) during both w.t. Ad5 and w.t. Ad12 infection we next decided to establish whether GFP-SMARCAL1 was also reorganised to VRCs in Ad-infected RPE-1 cells. To do this we infected clonal GFP-SMARCAL1- expressing RPE-1 cells with either w.t. Ad5 or w.t. Ad12 and analysed the cellular distribution of GFP-SMARCAL1 at 24h post-infection by immmunofluorescent live-cell imaging (Figure 4.5). In mock-infected cells GFP-SMARCAL1 was distributed throughout the nucleus, though there were noticeable differences in the protein levels of GFP-SMARCAL1 between individual cells (panel i, Figure 4.4). Following infection of RPE-1 cells with either Ad5 or Ad12, akin to the A549 studies, there was a noticeable increase in the level of GFP-SMARCAL1 protein expression, and GFP-SMARCAL1 was reorganized, typically to structures that resembled VRCs (cf panel i with panels ii and iii, Figure 4.5).

It was apparent that upon infection with either w.t. Ad5 or Ad12 that GFP-SMARCAL1 RPE-1 cells retained their, oval-shaped, nuclear integrity better than the Ad-infected GFP-SMARCAL1 A549 cells which often became crescent-shaped and distorted (RN and AST, unpublished observations). It was therefore easier using the GFP-SMARCAL1 RPE-1 cells, to record in which cells GFP-SMARCAL1 was redistributed to VRCs during Ad infection. We therefore chose to use these cells to determine whether ablation of SMARCAL1 phosphorylation acceptor sites affected the recruitment of GFP-SMARCAL1 to VRCs following Ad5 or Ad12 infection.

We first investigated whether phosphorylation-defective mutants in which one phospho-acceptor site was mutated to alanine affected the ability of w.t. Ad5 or Ad12 to induce the reorganization of GFP-SMARCAL1 to VRCs. To check this, we infected the relevant GFP-SMARCAL1 RPE-1 cell lines with w.t. Ad5 or w.t. Ad12 and analysed GFP-SMARCAL1 distribution to VRCs at 24h post-infection (Figure 4.6). Pertinently, in the mock-treated RPE-1 cells, the distribution of w.t. GFP-SMARCAL1, GFP-SMARCAL1 S123A, GFP-SMARCAL1 S129A and GFP-SMARCAL1 S173A were all observed to be pan-nuclear [panels i-iv, Figure 4.6A]. However, when GFP-SMARCAL1 RPE-1 cells were infected with either w.t. Ad5 or w.t. Ad12, GFP-SMARCAL1 levels increased, relative to mock-infected cells, though this was not as dramatic as observed for A549 cells [cf panels i-iv with panels v-xii, Figure 4.6A]. Interestingly, results of these analyses indicated that both w.t. and mutant GFP-SMARCAL1 species were redistributed to VRCs following Ad infection [panels v-xii, Figure 4.6A]. To determine whether there was any significant difference in the recruitment of w.t. or mutant GFP-SMARCAL1 species to VRCs following Ad infection we decided to quantify the proportion of mutant GFP-cells, relative to w.t. GFP-SMARCAL1 cells, which were recruited to VRCs following either w.t. Ad5, or w.t Ad12 infection. Analyses revealed that although there was a modest reduction in the recruitment of GFP-SMARCAL1 S123A, GFP-SMARCAL1 S129A and GFP-SMARCAL1 S173A, relative to w.t. GFP-SMARCAL1, following both w.t. Ad5 and w.t Ad12 infection, only the recruitment of GFP-SMARCAL1 S173A, relative to w.t. GFP-SMARCAL1, was reduced significantly following Ad5 infection [Figure 4.6B]. In all other instances, the recruitment of mutant GFP-SMARCAL1 species to VRCs did not differ significantly from the recruitment of w.t. GFP-SMARCAL1 species to VRCs,

although it appeared that the recruitment of S173A mutant to VRCs in Ad12-infected cells were reduced, relative to w.t. GFP-SMARCAL1 [Figure 4.6B].

Using an identical strategy, we next investigated whether the GFP-SMARCAL1 RPE-1 double phosphorylation-defective mutants, S123A/S129A, S123A/S173A and S129A/S173A were recruited to VRCs following Ad infection [Figure 4.7]. Visual inspection of mutant GFP-SMARCAL1 species cellular distribution revealed that, akin to w.t. GFP-SMARCAL1 species, they were recruited to VRCs following either w.t. Ad5 or w.t. Ad12 infection [cf panels i-iv with panels v-xii, Figure 4.7A]. Again, although there was a modest decrease in the recruitment of phosphorylation-defective mutants to VRCs following Ad infection this was not statistically significant for the majority of mutants [Figure 4.7B]. Only the distribution of GFP-SMARCAL1 mutant S129A/S173A to VRCs, was reduced significantly following Ad5 infection, relative to w.t. GFP-SMARCAL1 [Figure 4.7B].

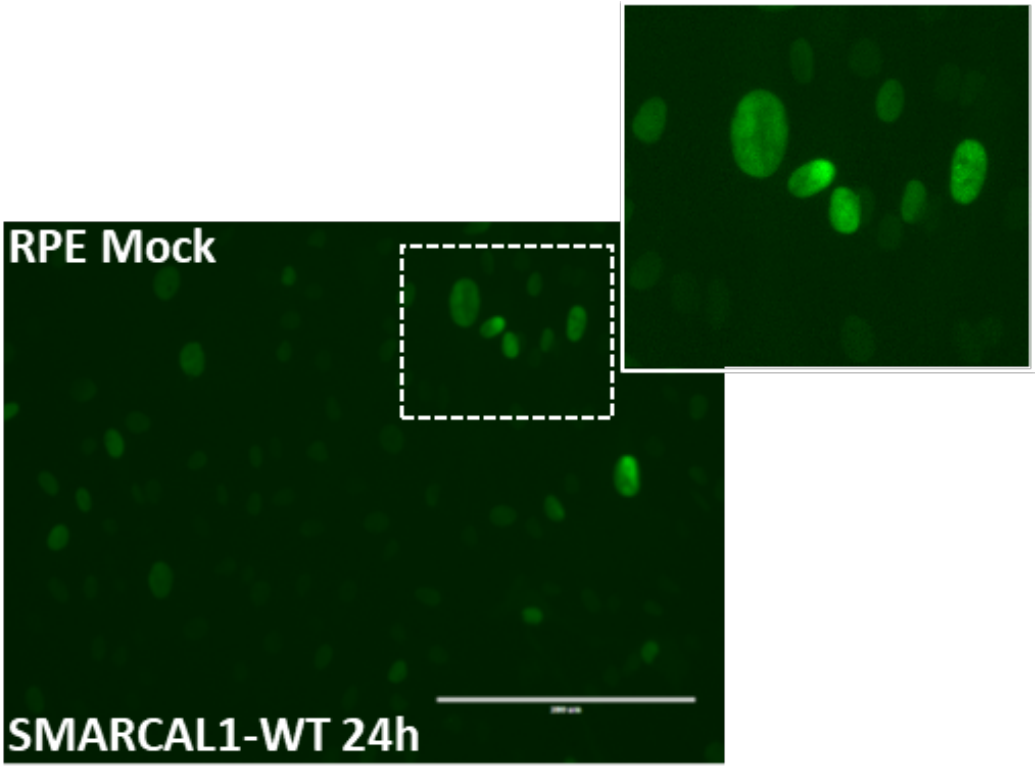

48h

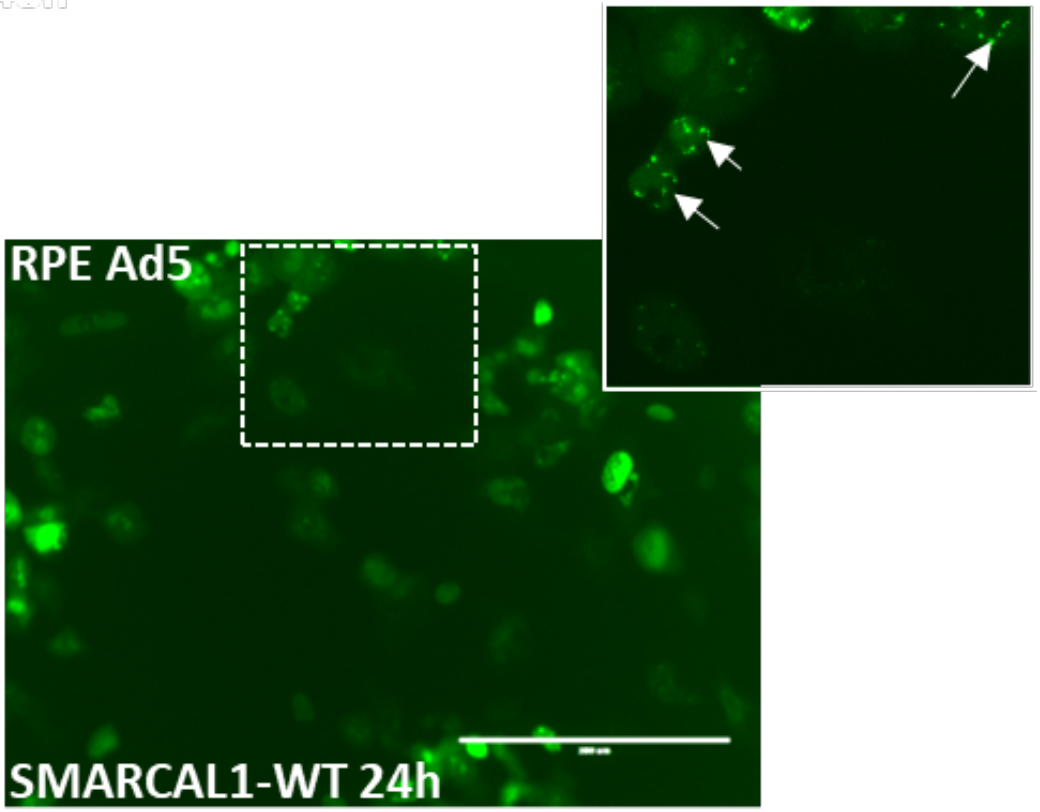

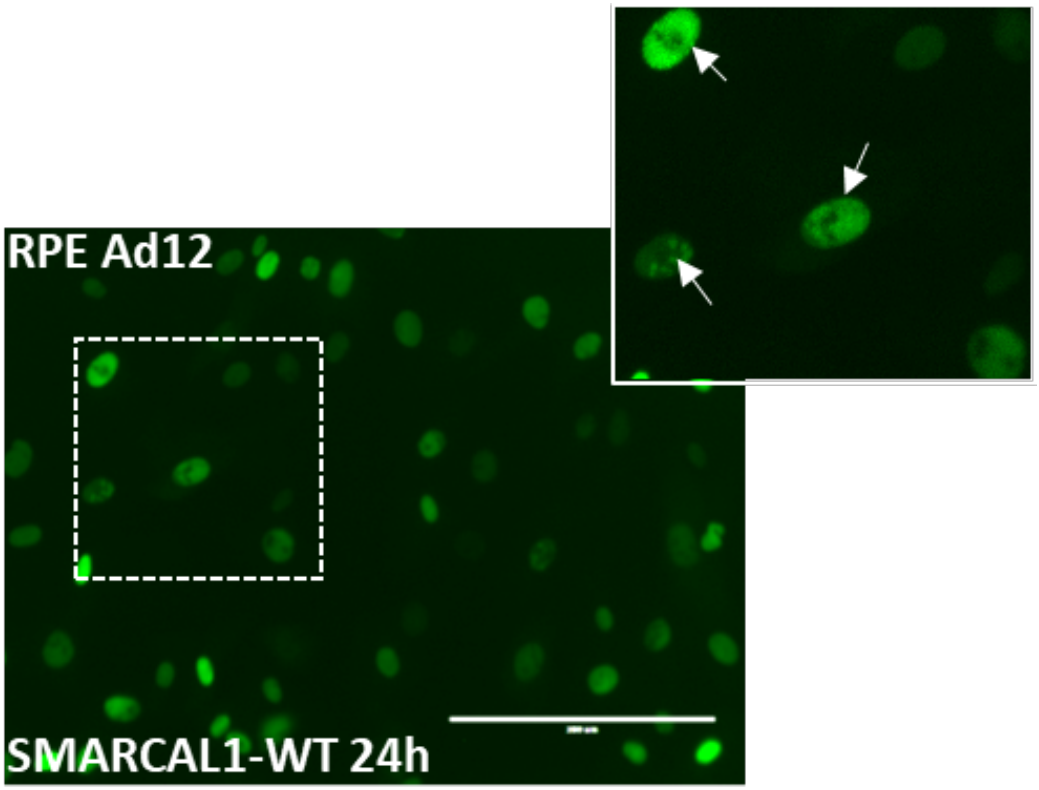

Figure 4.5. Expression and distribution of GFP-SMARCAL1 in WT GFP-SMARCAL1 expressing RPE-1 clonal cell lines following Ad infection. WT GFP-SMARCAL1 expressing A549 cell lines were either mock infected or infected with WT Ad5 and WT Ad12 at 10 pfu/cell. Cells were visualised by live cell imaging fluorescence microscope. Arrows indicate Smarcal1 recruitment to VRCs at the times indicated.

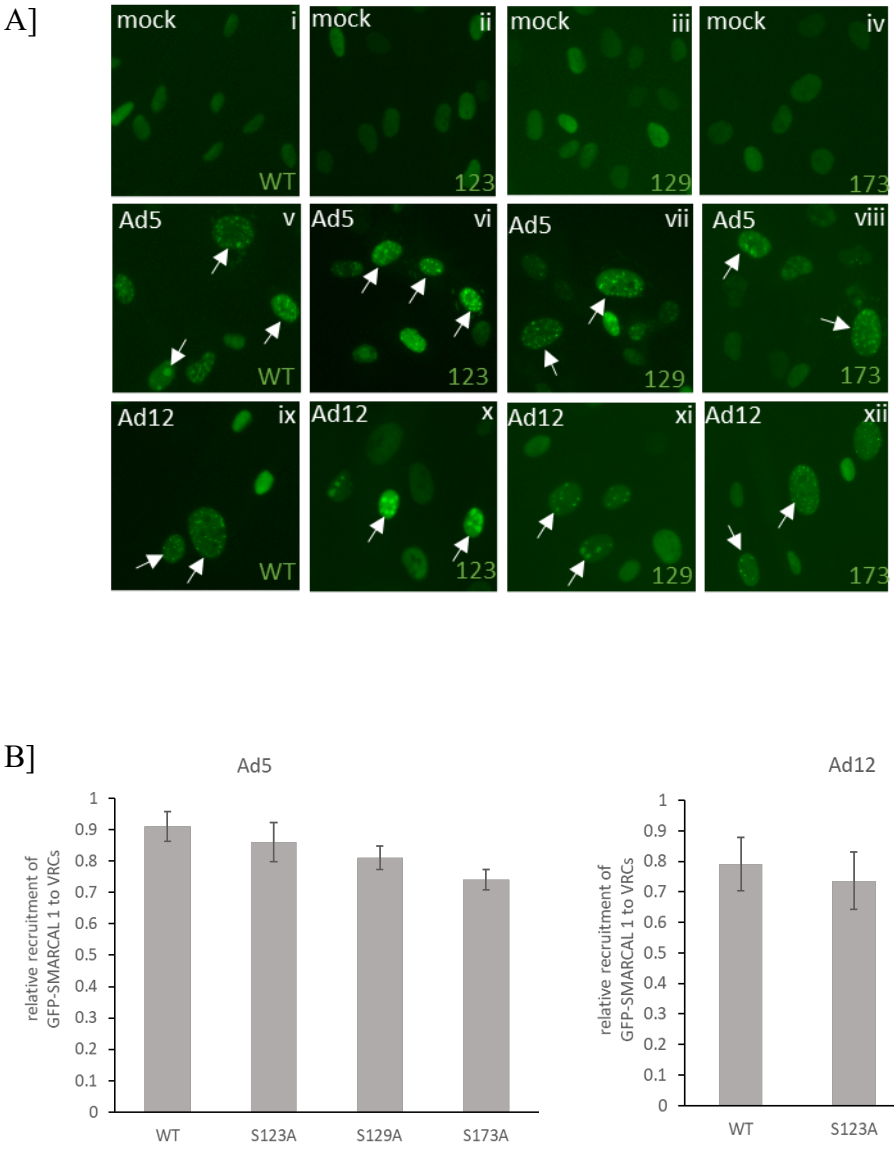

Figure 4.6. Quantification of SMARCAL1 recruitment to VRCs in GFP-Smarcal1 S123A, S129A and S173A expressing RPE-1 clonal cell lines. A] GFP-SMARCAL1 single mutants S123A, S129A and S173A expressing RPE-1 cell lines were either mock infected or infected with WT Ad5 and WT Ad12 at 10 pfu/cell. Cells were visualised by live cell imaging fluorescence microscopy at 24 h post-infection. B] The percentage of cells where GFP-SMARCAL1 was recruited to VRCs were recorded and analysed by (n=3, 200 cells per experiment). The data is expressed as mean +/- S.D.

A]

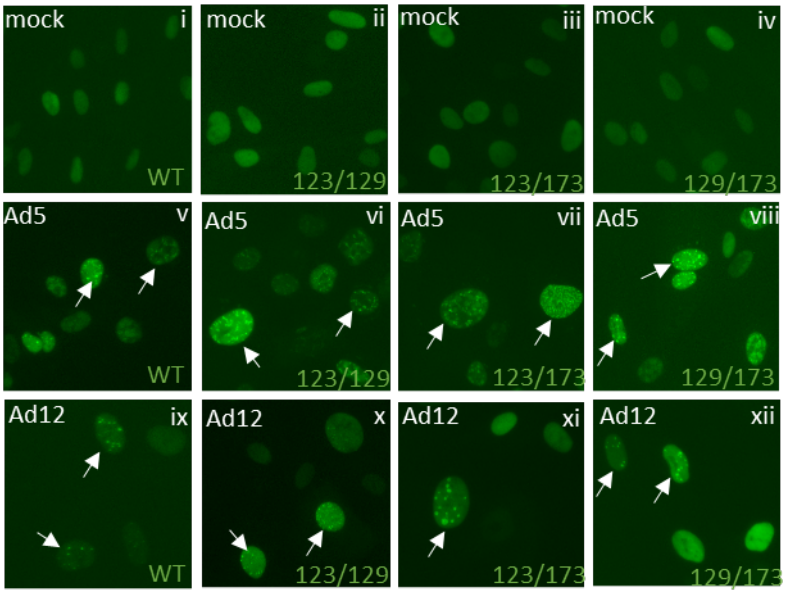

B]

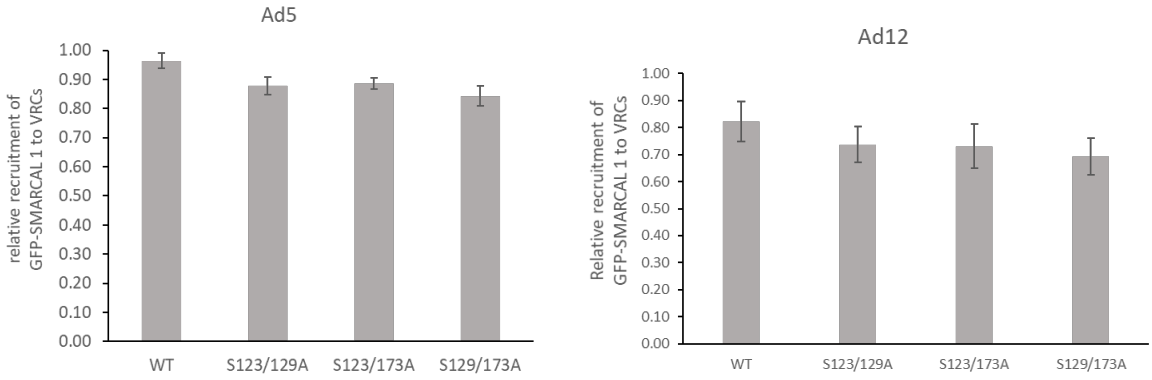

Figure 4.7. Quantification of SMARCAL1 recruitment to VRCs in GFP-Smarcal1 S123/S129A, S123/S173A and S129/S173A expressing RPE-1 clonal cell lines. A] GFP-SMARCAL1 double mutants S123/S129A, S123/S173A and S129/S173A expressing RPE-1 cell lines were either mock infected or infected with WT Ad5 and WT Ad12 at 10 pfu/cell. Cells were visualised by live cell imaging fluorescence microscopy at 24 h post-infection. B] The percentage of cells where GFP-SMARCAL1 was recruited to VRCs were recorded and analysed by (n=3, 200 cells per experiment). The data is expressed as mean +/- S.D.

4.2.4. GFP-SMARCAL1 recruitment to viral replication centres following Ad5 and Ad12 infection is dependent upon phosphorylation on S123, S129 and S173 and its association with the RPA complex.

To investigate the combined effect of CDK and ATR -directed phosphorylation upon SMARCAL1 localization to VRCs following Ad infection we utilized the RPE-1 cells that constitutively express the GFP-SMARCAL1 triple phosphorylation-defective mutant (S123A/S129A/S173A (ΔP) where S123, S129 and S173 are all mutated to A). Akin to w.t. GFP-SMARCAL1, GFP-SMARCAL1-ΔP was distributed evenly throughout the nucleus in mock-infected cells [cf panels i and ii with panels iv and v, and vii and viii, Figure 4.8A]. Interestingly, although GFP-SMARCAL1-ΔP was recruited to VRCs following both w.t. Ad5 and w.t. Ad12 infection, statistical analyses revealed that the recruitment of GFP-SMARCAL1-ΔP to VRCs, was attenuated significantly, relative to w.t. GFP-SMARCAL1 [Figure 4.7B]. In Ad5-infected cells, GFP-SMARCAL1-ΔP recruitment to VRCs was reduced by approximately 25% relative to w.t. GFP-SMARCAL1, whereas GFP-SMARCAL1-ΔP recruitment to VRCs was reduced by approximately 40% relative to w.t. GFP-SMARCAL1, following Ad12 infection [Figure 4.7B]. These data suggest that SMARCAL1 phosphorylation does contribute towards SMARCAL1 recruitment to VRCs following both Ad5 and Ad12 infection.

As the RPA complex has long been known to be recruited to VRCs, and SMARCAL1 associates with RPA at VRCs we were interested to establish whether SMARCAL1 recruitment to VRCs was dependent, or not, on its ability to bind RPA. We therefore took advantage of an N-terminal SMARCAL1 mutant that lacks the first 32 amino acids

that has previously been shown to define the binding site on SMARCAL1 for RPA (Bansbach, Bétous et al. 2009). As for other GFP-SMARCAL1 constructs we generated clonal RPE-1 cell lines that expresses constitutively, a GFP-SMARCAL1 species that does not bind RPA (data not shown; GFP-SMARCAL1-ΔRPA). Like w.t. GFP-SMARCAL1, GFP-SMARCAL1-ΔRPA was distributed throughout the nucleus in mock-infected cells [cf panel i with panel iii, Figure 4.8A]. In contrast to w.t. GFP-SMARCAL1 however, it was evident upon inspection of cells under the microscope that GFP-SMARCAL1-ΔRPA was not re-organised to VRCs efficiently following either w.t. Ad5 or w.t. Ad12 infection [cf panels iv and vii with panels v, vi, viii and ix, Figure 4.7A]. Analyses revealed that there was an approximately, two-thirds reduction in the recruitment of GFP-SMARCAL1-ΔRPA to VRCs, when compared directly to w.t. GFP-SMARCAL1 recruitment to VRCs [Figure 4.8B]. These data suggest that SMARCAL1 recruitment to VRCs following both Ad5 and Ad12 infection is largely dependent upon its ability to interact with the RPA complex.

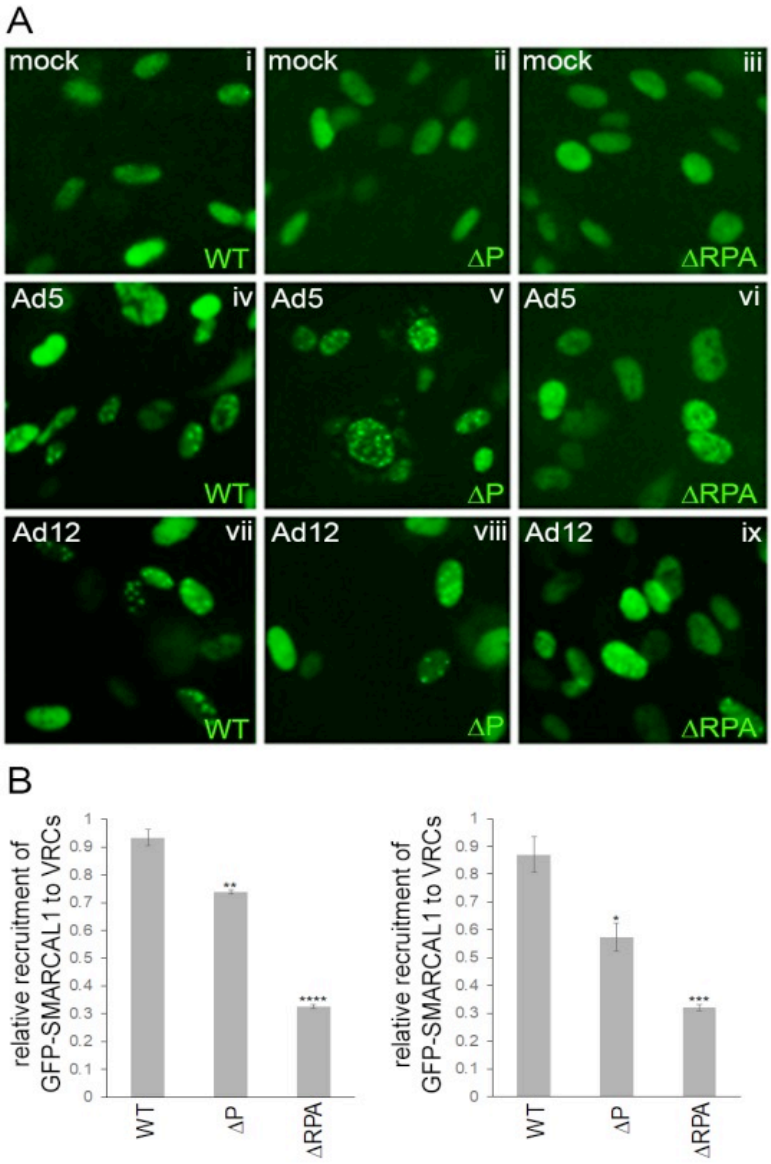

Figure 4.8. Quantification of SMARCAL1 recruitment to VRCs in WT GFP-Smarcal1, GFP-SMARCAL1 phosphorylation-defective triple mutant and GFP-SMARCAL1-ΔRPA mutant expressing RPE-1 clonal cell lines. A] WT GFP-Smarcal1, GFP-SMARCAL1-ΔP triple mutant and GFP-SMARCAL1-ΔRPA mutant expressing RPE-1 cell lines were either mock infected or infected with WT Ad5 and WT Ad12 at 10 pfu/cell. Cells were visualised by live cell imaging fluorescence microscopy at 24 h post-infection. B] The percentage of cells where GFP-SMARCAL1 was recruited to VRCs were recorded and analysed by (n=3, 200 cells per experiment). The data is expressed as mean +/- S.D. (Published in J.Virol 2019 by Nazeer et al).

4.3 Discussion.

In order to replicate successfully in the host cell, adenoviruses employ several strategies to neutralize host cell anti-viral proteins. In recent years, it has become evident that Ads target cellular proteins for degradation through the ubiquitin-proteasome system (Schreiner, Wimmer et al. 2012). It is also accepted that in this regard a number of anti-viral proteins are recruited to: VRCs through interaction with the RPA complex or E1B-55K; or nuclear tracks through interaction with E4orf3 prior to their degradation (Querido, Blanchette et al. 2001, Blackford, Bruton et al. 2008, Carson, Orazio et al. 2009, Blackford, Patel et al. 2010, Schreiner, Wimmer et al. 2011, Forrester, Patel et al. 2012, Bridges, Sohn et al. 2016). Alternatively, anti-viral host cell proteins have been suggested to be inactivated through sequestration, rather than undergo degradation, at these sites during infection (Nebenzahl-Sharon, Shalata et al. 2019). As we had shown in Chapter 3 that the combined actions of ATR and CDK inhibitors reduced substantially the ability of Ad to target SMARCAL1 for degradation (Figure 3.8), we wished to establish whether the phosphorylation of those specific SMARCAL1 residues targeted during Ad infection (S123, S129 and S173, Figure 3.3 , Chapter 3), contributed directly towards SMARCAL1 degradation during infection. This is an important question to resolve as phosphorylation has not been previously shown to modulate the degradation of host cell proteins during infection. To investigate this possibility we made A549 and RPE-1 cell lines that expressed constitutively w.t. GFP-SMARCAL1, and GFP-SMARCAL1 mutants where phospho-acceptor sites were inactivated through mutation (Figures 4.1 and 4.2).

Once generated, we intended to use these cell lines to establish whether these GFP-SMARCAL1 phosphorylation-defective mutants were degraded during Ad infection, or not. Unfortunately, our initial studies in A549 cells indicated that w.t. GFP-SMARCAL1 species were elevated, not reduced, following both w.t. Ad5 and w.t. Ad12 infection, suggesting that these cell lines were not a good model to investigate the role of phosphorylation in the degradation of SMARCAL1 (Figure 4.3). What is the explanation for our observations? It has long been known that the 13S E1A gene product serves to transactivate early region promoters during infection (e.g. (Berk, Lee et al. 1979, Jones and Shenk 1979, Bernards, Schrier et al. 1983, Bos and ten Wolde-Kraamwinkel 1983). In this regard the Zn-finger region of CR3 associates with host cell factors such as TBP, Sur2 and the proteasome (Geisberg, Lee et al. 1994, Liu and Green 1994, Boyer, Martin et al. 1999, Rasti, Grand et al. 2006), whilst the C-terminal region of CR3 targets E1A to promoter elements, through association with transcription factors such as ATF2, to stimulate transcription from viral early gene promoters (Liu and Green 1990). Crucially, it has also been shown that the 13S E1A gene product can transactivate heterologous promoters such as the CMV immediate early promoter (Metcalf, Monick et al. 1994). Unfortunately, mammalian expression vectors utilise constitutively active promoters such as the CMV promoter to induce the expression of exogenous gene products. In this regard, the retroviral pLEGFP vector utilised in this study uses a CMV promoter to induce the expression of the GFP construct [Clontech]. It is our expectation therefore that E1A stimulates the overexpression of GFP-SMARCAL1 species through transactivation of the CMV promoter in the pLEGFP vector. To overcome this problem in the future it might be worthwhile to express E1B-55K and E4orf6 as plasmids, or recombinant Ads, in the absence of E1A, in GFP-SMARCAL1 expressing cell lines to

see if we can establish whether E1B-55K and E4orf6 can drive the degradation of GFP-SMARCAL1 phospho-mutants.

As we have shown previously that SMARCAL1 is recruited to VRCs during infection, we next investigated, using our GFP-SMARCAL1 phospho-mutants, whether ATR and/or CDKs promote the recruitment of SMARCAL1 to VRCs. Our data indicated that GFP-SMARCAL1 recruitment to VRCs was dependent upon both ATR and CDKs, as only the triple phosphorylation-defective GFP-SMARCAL1 mutant was significantly, defective in its recruitment to VRCs (Figure 4.8). In this regard, the ability of w.t. Ad5 to promote the recruitment of the phosphorylation-defective GFP-SMARCAL1 mutant to VRCs was reduced by approximately 25%, relative to w.t. GFP-SMARCAL1 species, and the ability of w.t. Ad12 to promote recruitment of the phosphorylation-defective GFP-SMARCAL1 mutant to VRCs was reduced by approximately 40%, relative to w.t. GFP-SMARCAL1 species (Figure 4.8).

It is well established that ATR substrates and regulators, such as the RPA complex (including RPA32), ATRIP, RPA32, E1B-AP5 (hnRPUL1) and TopBP1 are all recruited to VRCs during Ad infection (Blackford, Bruton et al. 2008, Carson, Orazio et al. 2009, Blackford, Patel et al. 2010). Of these, only the RPA subunit, RPA32 is known to be phosphorylated by in an ATR-dependent manner during infection but that protein, unlike SMARCAL1, is not targeted for degradation [Blackford et al, 2008]. Given our analyses it would be interesting to determine whether ATR, and CDK, inhibitors similarly restrict the recruitment of these host cell proteins to VRCs. More generally, it would be of interest to establish whether the recruitment of any other host cell proteins (e.g. p53, MRN complex), or viral proteins (e.g. E1B-55K or E4orf6) is

dependent upon ATR or CDK activities. As RPA32 is known to be recruited to VRCs and is also a SMARCAL1-interacting protein where they co-localize at sites of ssDNA during cellular DNA replication or DNA damage (Bansbach, Bétous et al. 2009, Ciccia, Bredemeyer et al. 2009, Yusufzai, Kong et al. 2009) we investigated whether SMARCAL1 interaction with the RPA complex was important in its recruitment to VRCs. To do this we utilised a GFP-tagged N-terminal SMARCAL1 deletion mutant that does not interact with the RPA complex (Bansbach, Bétous et al. 2009). Interestingly, our analyses revealed that SMARCAL1 recruitment to VRCs was largely dependent upon its interaction with the RPA complex [Figure 4.8]. In this regard it would be interesting to see if the interaction between the RPA complex and SMARCAL1 is phosphorylation-dependent, or whether these two pathways function independently to recruit SMARCAL1 to VRCs.

Although the role of the RPA complex at VRCs is largely under-explored, our data suggest that it possesses pro-viral activities by promoting the recruitment, and subsequent degradation of SMARCAL1, at VRCs. Given these results, it would be interesting to establish whether other RPA complex-interacting proteins such as TopBP1 and E1B-AP5 are recruited to VRCs through their interaction with the RPA complex. Moreover, as both E1B-55K and E4orf6 are recruited to VRCs it would also be interesting to see if these proteins contribute towards the phosphorylation-dependent and/or RPA-dependent recruitment of SMARCAL1 to VRCs. As mentioned above the role of the RPA complex in Ad replication is not known. However, in some other viruses such as SV40, the large T-antigen (LT) -dependent replication of the viral genome is dependent upon the RPA complex (Wold, Li et al. 1987). It has been determined that LT functions as a replicative helicase and binds to the RPA complex through its origin

DNA-binding domain (Dornreiter, Erdile et al. 1992). It has been proposed that LT loads the RPA complex onto emerging ssDNA at the SV40 origin of DNA replication. In this regard, CDKs are implicated in the phosphorylation of the RPA32 subunit and the stimulation of DNA unwinding at origins of replication (Dutta and Stillman 1992). Given these data, it is highly likely that the RPA complex is pro-viral and associates with adenovirus ssDNA following unwinding at origins of replication within the 5' and 3' ITRs, and following Ad DNA replication, though its role in Ad replication awaits experimental confirmation. Given our findings it will also be interesting to determine whether SV40 similarly inhibits SMARCAL1 during infection, or whether it utilises SMARCAL1 for viral DNA replication. In this regard, SV40 is not known to engage with the ubiquitin-proteasome system to promote the degradation of DDR proteins, although LT has been shown to interact with CRL7 to inhibit the degradation of the insulin receptor substrate 1 (Hartmann, Xu et al. 2014).

In conclusion, results presented in this Chapter have demonstrated that SMARCAL1 recruitment to VRCs is complex, and relies upon both upon its phosphorylation by ATR and CDKs, and its association with the RPA complex. Further studies will be required to determine the molecular inter-relationship between these two pathways and SMARCAL1 recruitment to VRCs in Ad-infected cells.

CHAPTER 5

Modulation of cellular DNA replication by adenovirus E1B-55K

5.1. Introduction.

Adenovirus has evolved numerous strategies to counteract host cell defence mechanisms. For instance, the linear dsDNA genome of adenovirus, or adenovirus replication ssDNA intermediates, would ordinarily, be recognised as host cell DNA damage by the cellular DDR signalling cascades coordinated by ATM, ATR and DNA-PK. Adenoviruses have evolved to overcome the cellular DDR by inhibiting the activities of key components of these pathways (Turnell and Grand 2012, Weitzman and Fradet-Turcotte 2018). In this regard, the early region proteins play a key role in disrupting host cellular DDR signalling pathways that lead to cell cycle checkpoint activation and DNA repair, or apoptosis. Specifically, E1B-55K, E4orf3 and E4orf6 all participate in targeting the key cellular proteins involved in the DDR for degradation through the ubiquitin-proteasome system to usurp cell cycle checkpoints and cellular apoptotic programmes. Hence, understanding the biological activities of adenovirus early region proteins is key in the identification, and molecular characterization, of important DDR proteins that function as anti-viral agents, and discerning how adenovirus dysregulates their cellular functions.

The adenovirus early region protein, and oncoprotein, E1B-55K is a multifunctional protein that plays a major role in inhibiting the cellular DDR (see Introduction, section 1.3.6 and 1.6.2). In this regard, it associates with E4orf6 and recruits an E3 ubiquitin ligase complex consisting of CRLs (Cullin Ring Ligases), Elongins B and C and Rbx1 to target a number of cellular proteins involved in the DDR for degradation via the ubiquitin-proteasome system (Querido, Blanchette et al. 2001, Harada, Shevchenko et al. 2002, Stracker, Carson et al. 2002, Blackford, Patel et al. 2010, Orazio, Naeger et al.

2011). Apart from promoting viral replication, Ad E1B-55K is also involved in the transformation of mammalian cells with the co-operation of other E1, and E4 gene products, particularly E1A, E1B-19K, E4orf3 and E4orf6 (Yew and Berk 1992, Nevels, Täuber et al. 1999, Nevels, Täuber et al. 2001). Previous observations have shown that E1B-55K contributes to the transformation process through its ability to interact with the tumour suppressor protein, p53 and blocking the transcriptional activities of p53, to disable cell cycle checkpoint control and p53-dependent apoptosis (Yew and Berk 1992, Yew, Liu et al. 1994, Harada and Berk 1999).

Previously, we have shown that the RPA-interacting protein and ATR substrate SMARCAL1 is recruited to VRCs during infection and then targeted for proteasomal degradation in an E1B-55K and E4orf6 dependent manner (Figure 3.9; F.S.I Qashqari, PhD thesis, The University of Birmingham, 2017). As E1B-55K typically functions as a substrate adaptor for the Ad ubiquitin ligase through interaction with substrates such as p53 and MRE11, in the absence of E4orf6, we hypothesized that E1B-55K would also serve the same purpose for SMARCAL1. We wished therefore to establish whether E1B-55K associates with SMARCAL1 in the absence of E4orf6. Given that E1B-55K neutralizes p53 function through interaction, in the absence of E4orf6 (Yew and Berk 1992) we also hypothesized that E1B-55K could, in isolation, potentially modulate the cellular DNA replication functions of SMARCAL1. These hypotheses were tested experimentally, and the results of these studies are presented in this chapter.

5.2. Results.

5.2.1. Ad5 E1B-55K associates with SMARCAL1 in Ad5 transformed HEK 293 cells.

As previous observations have shown that E1B-55K associates with cellular proteins like MRE11 and p53 in Ad-transformed cells we wished to establish whether E1B-55K also associates with SMARCAL1 in Ad-transformed cells. To investigate this possibility, we performed reciprocal co-immunoprecipitation assays, and immunoprecipitated SMARCAL1 and E1B-55K from Ad5 E1-transformed HEK 293 cells using anti-E1B-55K and anti-SMARCAL1 antibodies [Figure 5.1]. Following incubation with anti-E1B-55K and anti-SMARCAL1 antibodies immunocomplexes were collected on protein G-sepharose beads, separated by SDS-PAGE and subjected to Western blot analyses. Co-immunoprecipitation studies revealed that the anti-Ad5 E1B-55K antibody co-immunoprecipitated SMARCAL1 and that the anti-SMARCAL1 antibody co-immunoprecipitated E1B-55K in Ad5 HEK 293 cells [Figure 5.1]. In this regard, it was evident that the anti-SMARCAL1 antibody was better at co-immunoprecipitation of E1B-55K than, the anti-E1B-55K antibody was at co-immunoprecipitating SMARCAL1 [Figure 3.1]. To validate the experimental approach taken we also showed by co-immunoprecipitation using anti-E1B-55K antibodies and anti-p53 antibodies that E1B-55K interacts p53 with in Ad5 HEK 293 cells [Figure 5.1].

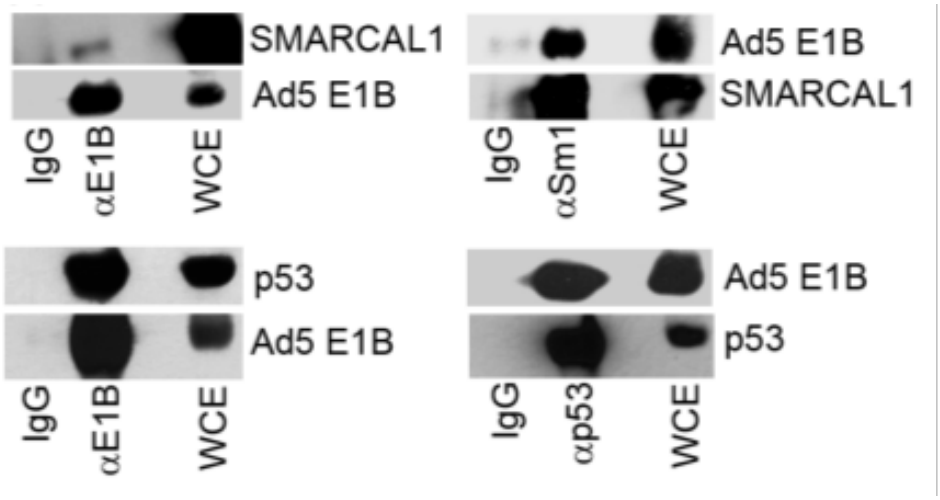

Figure 5.1: Ad5 E1B-55K associates with SMARCAL1 in Ad5 E1-transformed HEK 293 cells. Ad5 E1B-55K and SMARCAL1 were immunoprecipitated from Ad5 E1-transformed HEK 293 cells using the appropriate antibodies and subjected to Western blot analysis using anti-SMARCAL1 and anti- Ad5 E1B-55K antibodies. As p53 is a known Ad5 E1B-55K binding protein, reciprocal Ad5 E1B-55K and p53 IPs were performed as a positive control. Normal mouse IgG was used for control IPs to assess non-specific binding. Data presented is representative of three independent experiments. (Published in J.Virol 2019 by Nazeer et al).

5.2.2. Ad12 E1B-55K association with SMARCAL1 in Ad12 transformed HER2 cells.

After confirmation that Ad5 E1B-55K associates with SMARCAL1 *in vivo*, we wished to investigate whether Ad12 E1B-55K similarly interacts with SMARCAL1 *in vivo* in Ad12 E1-transformed HER2 cells. We therefore carried out reciprocal co-immunoprecipitation assays in Ad12 E1 transformed HER2 cell lysates using anti-SMARCAL1 and anti-E1B-55K antibodies. Consistent with the Ad5 studies, an anti-Ad12 E1B-55K antibody co-immunoprecipitated SMARCAL1, and moreover, an anti-SMARCAL1 antibody co-immunoprecipitated Ad12 E1B-55K [Figure 5.2]. In this regard the Ad12 E1B-55K antibody was more efficient than the Ad5 E1B-55K antibody at co-immunoprecipitation of SMARCAL1 [cf Figures 5.1 and 5.2]. Again, we further validated our findings by demonstrating that E1B-55K associates with p53 in Ad12 E1-transformed HER2 cells [Figure 5.2].

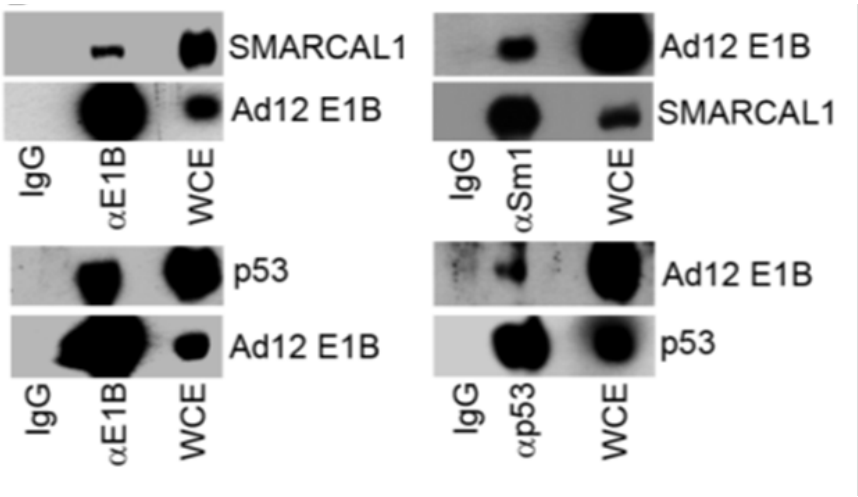

Figure 5.2: Ad5 E1B-55K associates with SMARCAL1 in Ad12 E1-transformed HER2 cells. Ad12 E1B-55K and SMARCAL1 were immunoprecipitated from Ad12 E1-transformed HER2 cells using the appropriate antibodies and subjected to Western blot analysis using anti-SMARCAL1 and anti- Ad12 E1B-55K antibodies. As p53 is a known Ad12 E1B-55K binding protein, reciprocal Ad5 E1B-55K and p53 IPs were performed as a positive control. Normal mouse IgG was used for control IPs to assess non-specific binding. Data presented is representative of three independent experiments. (Published in J.Virol 2019 by Nazeer et al).

5.2.3. Validation of TET-inducible Ad5 and Ad12 E1B-55K U2OS cell lines.

After establishing that Ad5 and Ad12 E1B-55K interact with SMARCAL1 in Ad E1-transformed HEK-293 and HER2 cells, respectively [Figure 5.1 and 5.2], we next wished to investigate whether E1B-55K modulates the cellular activities of SMARCAL1. To do this we took advantage of TET-inducible Ad5 and Ad12 E1B-55K U2OS cell lines that had been generated in our laboratory specifically as an experimental tool to study E1B-55K function [A Albalawi and AS Turnell, unpublished data]. To validate the usefulness of these experimental systems we first, assessed the expression of Ad5 and Ad12 E1B-55K in these cell lines, before and after, doxycycline induction by Western blot analysis [panels iv and v, Figure 5.3]. Moreover, given that both Ad5 and Ad12 E1B-55K are known to stabilise (increase the levels of) the p53 protein by inhibiting the Mdm2-mediated degradation of p53 (Querido, Blanchette et al. 2001), we also performed Western blot analyses for p53 in the absence and presence of doxycycline induction [panel ii, Figure 5.3]. Consistent with previous observations the levels of p53 were increased following the expression of Ad5 and Ad12 E1B-55K, suggesting that E1B-55K is functional in these cells [panel ii, Figure 5.3]. However, the levels of E1B-55K binding partners MRE11 and SMARCAL1 were not altered following Ad5 and Ad12 E1B-55K induction [panels i and iii, Figure 5.3]. Taken together, these data indicate that the TET-inducible Ad5 and Ad12 E1B-55K U2OS cell lines express functional E1B-55K that can be used to investigate the specific effects of E1B-55K expression upon SMARCAL1 function.

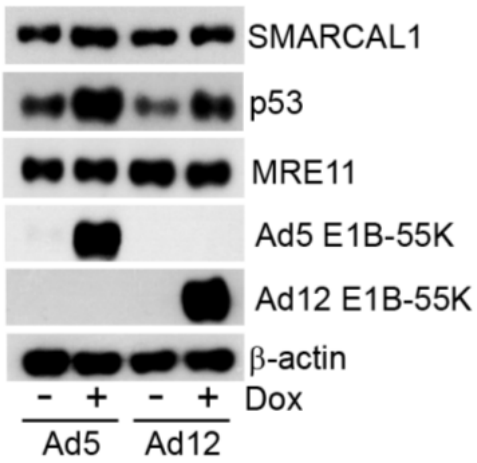

Figure 5.3: Validation of Ad5 and Ad12 E1B-55K TET-inducible U2OS FlpIn cells. Ad5 E1B-55K and Ad12 E1B-55K TET-inducible U2OS cell lines were induced to express in E1B-55K in the presence of 0.1μg/ml doxycycline. Cells were harvested 24h post-induction and the lysates were subjected for SDS-PAGE analysis for Ad5 and Ad12 E1B-55K, p53, MRE11 and β-actin using appropriate antibodies. Data presented is representative of two independent experiments. (Published in J.Virol 2019 by Nazeer et al).

5.2.4. Investigating the effects of E1B-55K on cellular DNA replication.

It is well established that SMARCAL1 is a DNA helicase that helps to prevent replication fork collapse in unperturbed S-phase and promotes replication restart after fork collapse during replication stress (Postow, Woo et al. 2009, Poole and Cortez 2017). Akin to the ability of E1B-55K to inhibit p53 functions (Boyer, Martin et al. 1999) we wished to establish whether Ad5 and/or Ad12 E1B-55K modulated cellular DNA replication through its ability to interact with SMARCAL1. To investigate whether Ad E1B-55K regulated cellular DNA replication during S-phase we performed DNA fibre analyses. The principle of the DNA Fibre analysis is to incorporate nucleotide analogues CldU and IdU into newly synthesized DNA for a pre-determined time and then detect these two analogues on individual DNA molecules by immunofluorescence in order to determine the rate of DNA synthesis. To do this we first pulse-labelled both Ad5 and Ad12 E1B-55K U2OS cells (+/- doxycycline) for 20 minutes each in CldU and IdU, lysed the cells, and then spread the DNA fibres onto glass slides where they were fixed in methanol/acetic acid and then denatured in HCl. Newly synthesized DNA was then detected with primary antibodies that recognise CldU and IdU nucleotide analogues specifically and visualized with the appropriate Alexa 488 and 594 secondary antibodies, after which images were acquired using the Nikon E600 microscope with an Nikon Plan Apo 60x (1.3 NA) oil lens and Hamamatsu digital camera (C4742-95) and by using Velocity acquisition software (Perkin Elmer) [Figure 5.4] and fork length determined using Image J.

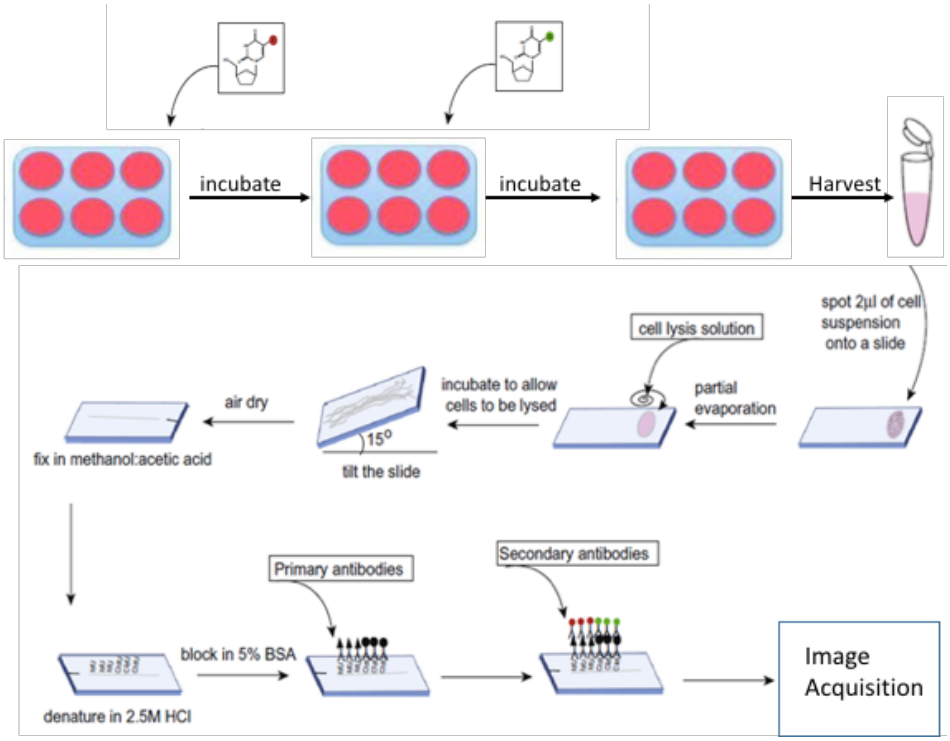

Figure adapted from: (Nieminuszczy, Schwab et al. 2016)

Figure 5.4: Principle of the DNA Fibre Assay. Cellular DNA replication was analyzed using the DNA Fibre Assay. Cells were pulse-labelled, in turn, with two nucleotide analogues CldU (25 µM) and IdU (250 µM) for 20 minutes each. Cells were harvested and spread onto glass slides, whereupon they were air dried, fixed in methanol-acetic acid and denatured with 2.5 M HCl. DNA fibres were then labelled with appropriate primary and secondary antibodies and fibres were visualized using high resolution microscope.

5.2.5. Ad5 and Ad12 E1B-55K dysregulate DNA replication fork speed.

Using the protocol outlined above we were able to analyse DNA replication fork speed in S-phase in the absence, or presence of Ad5 and Ad12 E1B-55K. Strikingly, analysis of the data revealed that CldU-labelled tracks were significantly longer in both Ad5 and Ad12 EB-55K induced cells compared to cells that did not express these viral proteins [Figure 5.5A and 5.6A]. Indeed, the initial average fork speed in Ad5 E1B-55K expressing cells was 2.27kb/min whilst average fork speed in the cells not expressing Ad5 E1B-55K was 1.66kb/min [Figure 5.5A]. Similarly, the initial average fork speed in Ad12 E1B-55K expressing cells was 1.68kb/min whilst average fork speed in the cells not expressing Ad12 E1B-55K was 1.04kb/min [Figure 5.6A]. When the data was plotted as a bar graph showing the distribution of CldU fork speeds +/- Ad5 or Ad12 E1B-55K it was evident that there was a greater proportion of cells expressing Ad E1B 55K that had increased, initial fork speeds (Figures 5.5B and 5.6B). These data indicate that Ad5 and Ad12 E1B-55K expression, initially led to a significant acceleration of replication fork speed. However, when we analysed the speed of on-going forks by measuring the length of the IdU-labelled tracts it was apparent that IdU fork speeds +/- Ad5 and Ad12 E1B-55K cells were very similar and that accelerated fork speed was not maintained in on-going forks [Figures 5.5A and 5.6A]. As such the average on-going fork speed in Ad5 E1B-55K expressing cells was 1.49kb/min whilst average on-going fork speed in the cells not expressing Ad5 E1B-55K was 1.46kb/min [Figure 5.5A]. Moreover, the average on-going fork speed in Ad12 E1B-55K expressing cells was 1.03kb/min whilst average fork speed in the cells not expressing Ad12 E1B-55K was 0.91kb/min [Figure 5.6A]. Closer inspection of the distribution of IdU fork speeds revealed that they were very similar +/- Ad5 or Ad12 E1B-55K [Figure 5.5B and 5.6B]. We next measured the distribution of combined fork speeds (CldU + IdU), which very

verified that cells expressing Ad5 or Ad12 E1B-55K had increased overall fork speeds [Figure 5.5C and 5.6C].

5.2.6. Ad5 and Ad12 E1B-55K expression increases CldU/IdU fork speed ratios.

Individual CldU and IdU fork speeds were then plotted as a dot plot in order to establish the mean CldU and IdU fork speeds +/-Ad5 and Ad12 E1B-55K. These results confirmed our expectations that both Ad5 and Ad12 E1B-55K enhanced significantly CldU fork speeds, but that IdU fork speeds +/- Ad E1B-55K were not significantly different from each other [Figures 5.7 and 5.8]. However, when we plotted CldU/IdU ratios for individual DNA fibres it was clear that CldU/IdU ratios were significantly higher for cells that expressed Ad E1B-55K, relative to cells that did not express these proteins [Figures 5.7 and 5.8]. These data are important, as it has previously been shown that cells that display increased CldU/IdU ratios have a tendency to undergo replication fork stalling and collapse (Petermann, Maya-Mendoza et al. 2006).

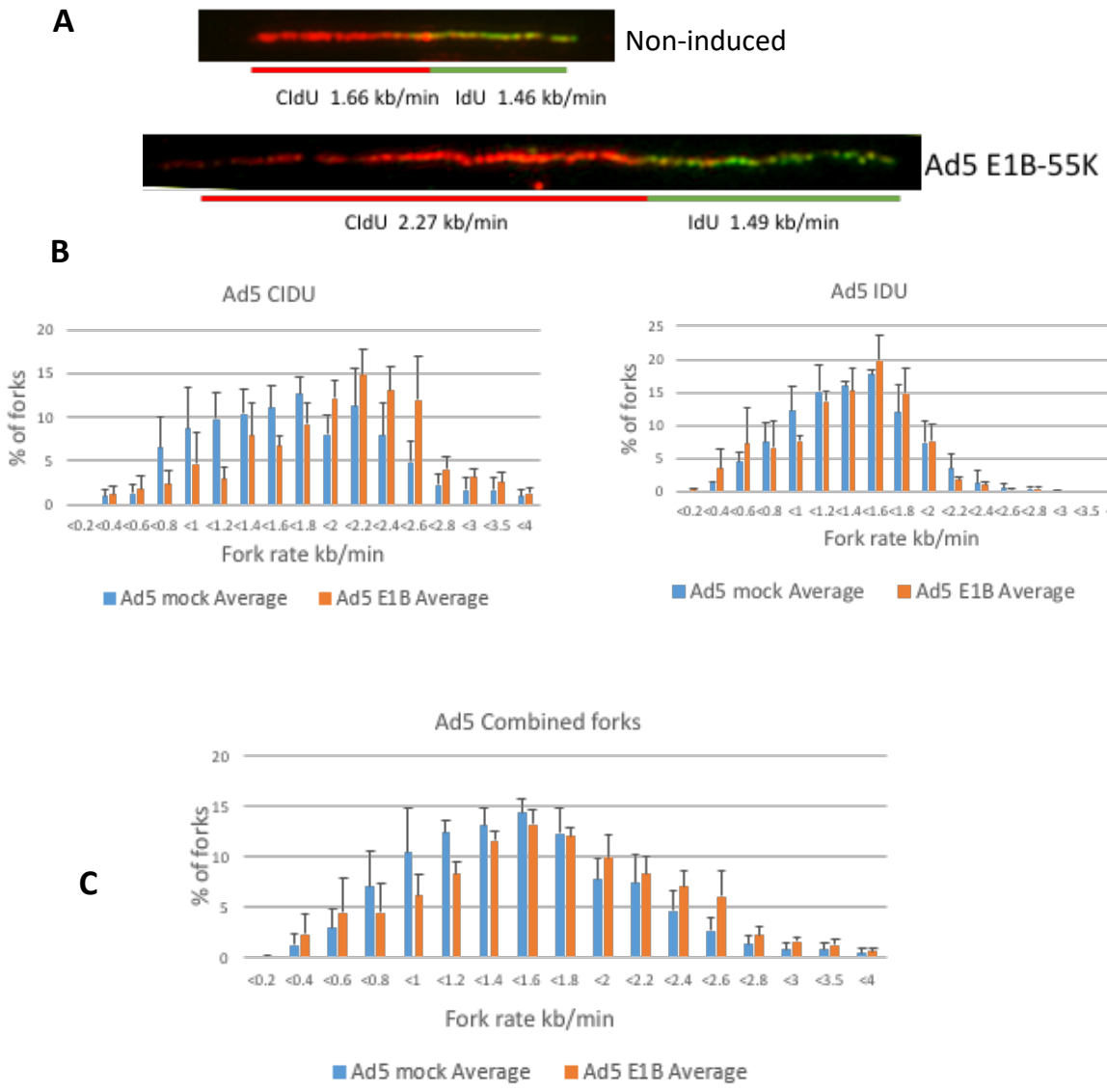

Figure 5.5: Effect of Ad5 E1B-55K on cellular DNA replication speed. (**A**) Representative DNA spreads taken from non-induced and Ad5 E1B-55K expressing cells illustrating cellular DNA replication fork speeds in CldU and IdU -labelled DNA (**B**) Bar graph illustrating the effect of Ad5 E1B-55K expression, relative to mock (non-induced) cells not expressing Ad5 E1B-55K, on individual replication fork speeds (kb/min) as judged by the incorporation of CldU and IdU into newly synthesized DNA. (**C**) Distribution of combined CldU and IdU fork rates in Ad5 E1B-55K induced cells and mock (non-induced) cells is shown, each panel showing the combined CldU + IdU labelling fork rates. Data is taken from three independent experiments (Total number of mock (non-induced) cells = 370; Ad5 E1B-55K cells = 364) +/- standard deviation.

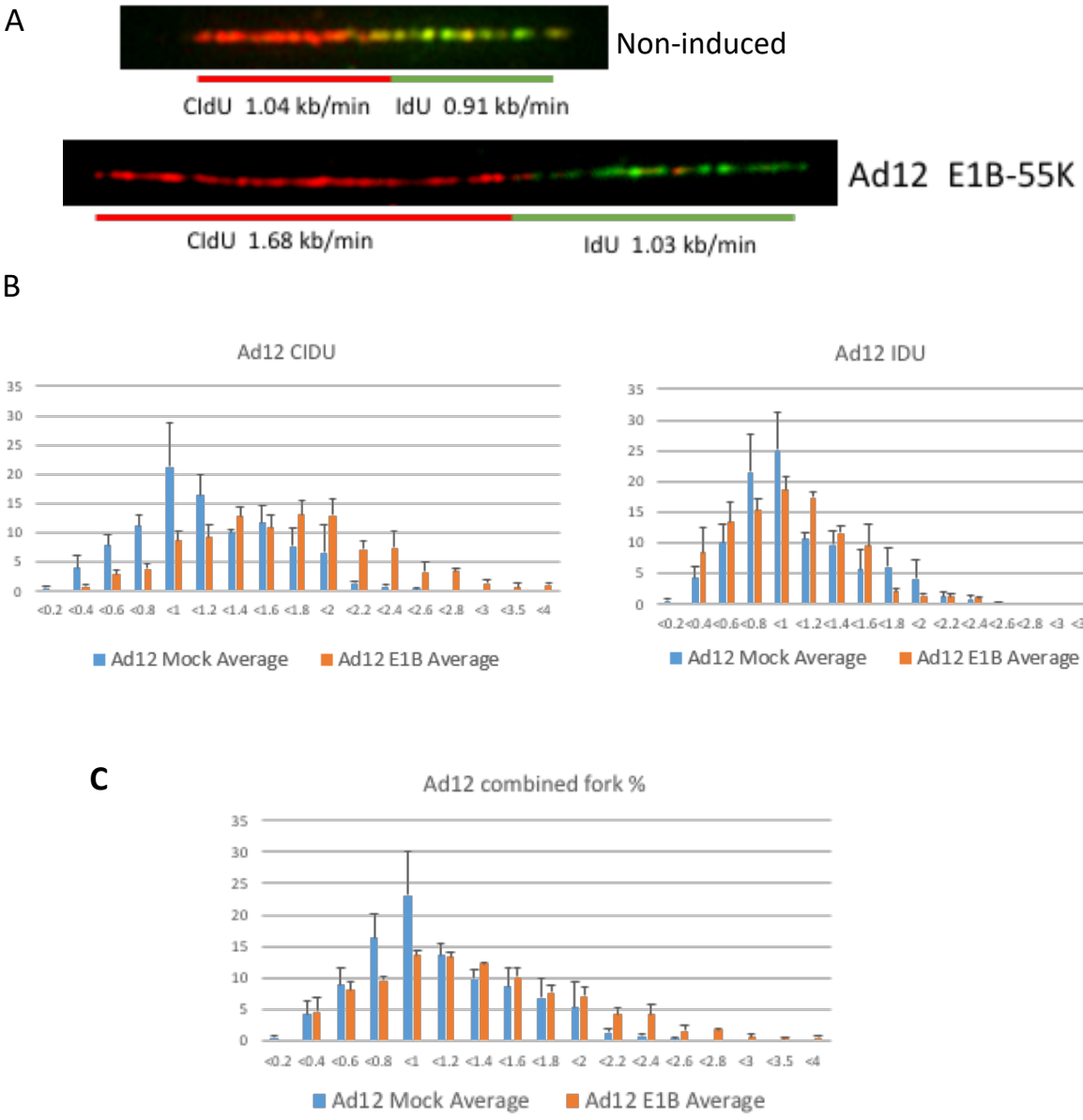

Figure 5.6: Effect of Ad12 E1B-55K on cellular DNA replication speed. (**A**) Representative DNA spreads taken from non-induced and Ad12 E1B-55K expressing cells illustrating cellular DNA replication fork speeds in CldU and IdU -labelled DNA (**B**) Bar graph illustrating the effect of Ad12 E1B-55K expression, relative to mock (non-induced) cells not expressing Ad12 E1B-55K, on individual replication fork speeds (kb/min) as judged by the incorporation of CldU and IdU into newly synthesized DNA. (**C**) Distribution of combined CldU and IdU fork rates in Ad12 E1B-55K induced cells and mock (non-induced) cells is shown, each panel showing the combined CldU + IdU labelling fork rates. Data is taken from three independent experiments (Total number of mock cells = 347; Ad12 E1B-55K cells = 368) +/- standard deviation.

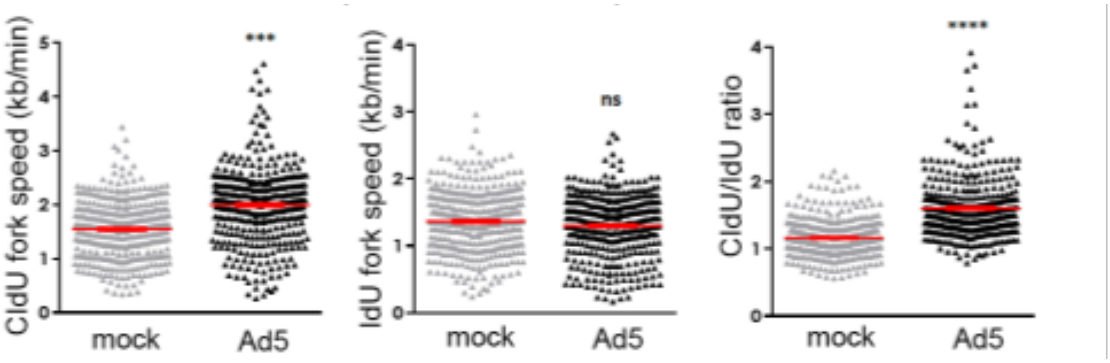

Figure 5.7: Modulation of cellular DNA replication fork speeds by Ad5 E1B-55K. Distribution of fork speeds and CldU/IdU ratios in Ad5 E1B-55K expressing cells relative to mock (non-induced) cells is shown as dot plots +/- standard deviation with the red bar representing the mean fork speed from three individual experiments. Total number of Ad5 mock (non-induced) fibres analyzed was 347 and the total number of fibres analyzed from Ad5 E1B-55K expressing cells 368. The data was subjected to an ANOVA two-tailed t-test. Ad5 E1B-55K CldU tract length relative to the mock (non-induced) CldU tract length, P=4.8E-20 (***); Ad5 E1B-55K CldU/IdU ratio relative to the mock (non-induced) CldU tract length, P=9.44E-45 (****); ns, not significant. (Published in J.Virol 2019 by Nazeer et al).

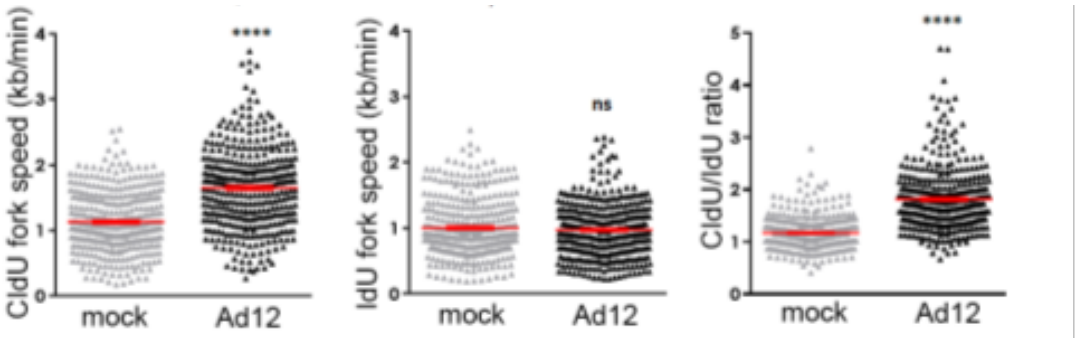

Figure 5.8: Modulation of cellular DNA replication fork speeds by Ad12 E1B-55K. Distribution of fork speeds and CldU/IdU ratios in Ad12 E1B-55K expressing cells relative to mock (non-induced) cells is shown as dot plots +/- standard deviation with the red bar representing the mean fork speed from three individual experiments. Total number of Ad12 mock (non-induced) fibres analyzed was 370 and the total number of fibres analyzed from Ad12 E1B-55K expressing cells was 364. The data was subjected to an ANOVA two-tailed t-test. Ad12 E1B-55K CldU tract length relative to the mock (non-induced) CldU tract length, P=1.29E-32 (****); Ad12 E1B-55K CldU/IdU ratio relative to the mock (non-induced) CldU tract length, P=6.32E-61 (****); ns, not significant. (Published in J.Virol 2019 by Nazeer et al).

5.2.7. Ad5 and Ad12 E1B-55K promote fork stalling during cellular DNA replication.

As the frequency of replication stalling depends on increased fork speed (Petermann, Maya-Mendoza et al. 2006, Quinet and Vindigni 2018), we next re-analysed our DNA fibre spreads to quantify the number of stalled replication forks in the absence or presence of Ad5 and Ad12 E1B-55K expression. To do this we counted the number of CldU-only tracts that did not label with IdU. CldU-only labelled tracts are indicative of replication stalling [Figures 5.9 and 5.10]. It was clear upon inspection of our slides that there was clearly an increased number of stalled replication forks (CldU-only tracts) in those cells that expressed Ad5 or Ad12 E1B-55K, relative to cells that did not [Figures 5.9A and 5.10A]. More detailed analyses revealed that Ad5 and Ad12 E1B-55K expression led to an approximately three-fold increase in the number of stalled replication forks, relative to cells that did not express these proteins [Figures 5.9B and 5.10B].

Overall, these data indicate that expression of Ad5 and Ad12 E1B-55K initially enhances cellular DNA replication fork speed which ultimately leads to DNA replication fork stalling. Taken together these data indicate that both Ad5 and Ad12 E1B-55K have the intrinsic ability to modulate cellular DNA replication. In consideration of the fact that a main function of SMARCAL1 is to promote replication restart after fork collapse during replication stress (Couch, Bansbach et al. 2013), our data suggests that Ad E1B-55K inhibits SMARCAL1 activity in vivo leading to dysregulated cellular DNA replication and fork stalling.

A

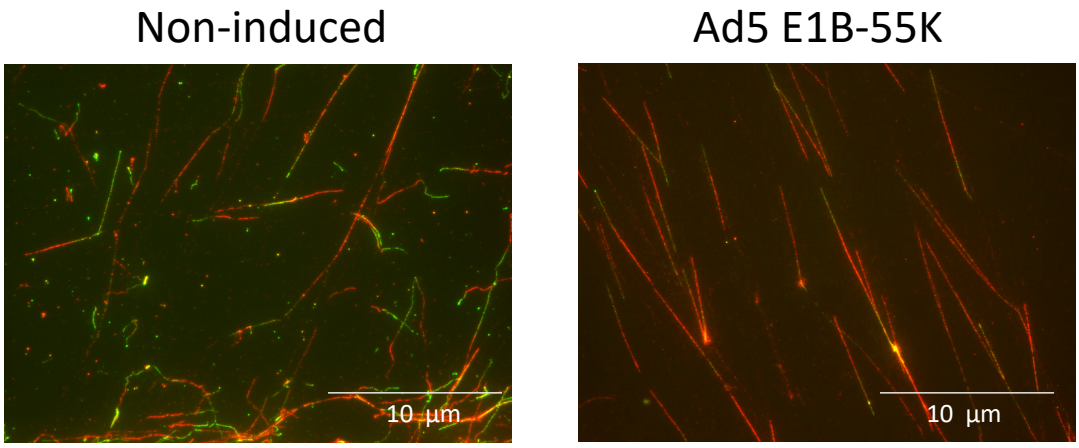

B

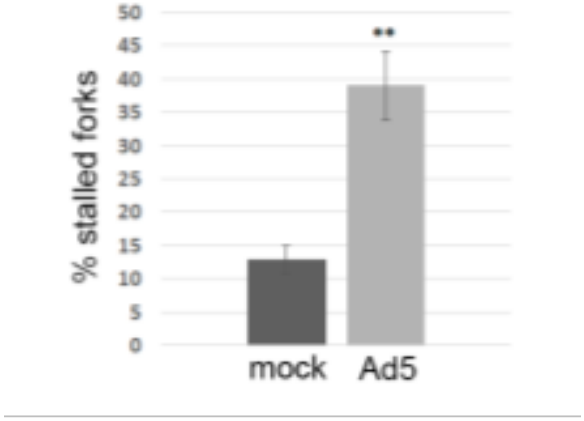

Figure 5.9: Effect of Ad5 E1B-55K expression on replication fork stalling. (**A**) Representative images of dual CldU and IdU-labelled DNA fibres in the absence or presence of Ad5 E1B-55K showing an increased number of CldU-only labelled fibres relative to mock cells (B). Bar graph illustrating percentage of stalled forks in Ad5 E1B-55K induced cells relative to mock cells +/- standard deviation, with the error bar representing three experimental repeats. The data was subjected to an ANOVA two-tailed t-test. P = 0.009 (**). (Published in J.Virol 2019 by Nazeer et al).

A

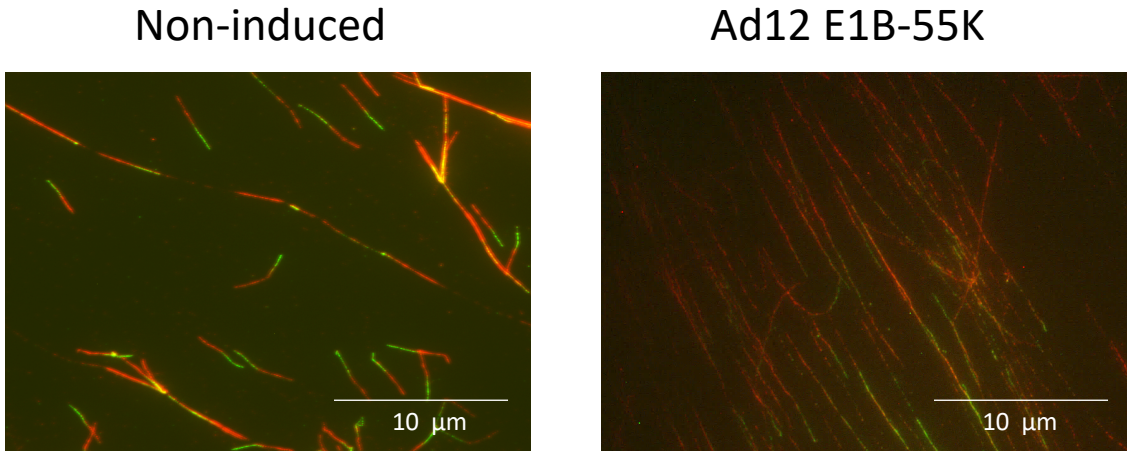

B

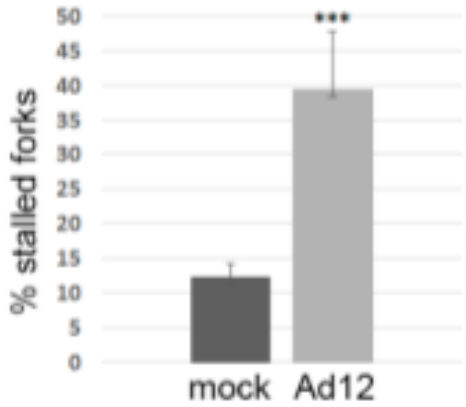

Figure 5.10: Effect of Ad12 E1B-55K expression on replication fork stalling. (**A**) Representative images of dual CldU and IdU-labelled DNA fibres in the absence or presence of Ad12 E1B-55K showing an increased number of CldU-only labelled fibres relative to mock cells (B). Bar graph illustrating percentage of stalled forks in Ad12 E1B-55K induced cells relative to mock cells +/- standard deviation, with the error bar representing three experimental repeats. The data was subjected to an ANOVA two-tailed t-test. P = 0.002 (**). (Published in J.Virol 2019 by Nazeer et al).

5.3. Discussion.

It is well established that the adenovirus early region protein, E1B-55K often functions as a substrate adaptor and serves to recruit cellular proteins involved in the DDR, such as p53, MRE11 and BLM, to CRLs, through interaction with E4orf6, for ubiquitin-mediated proteolysis (Turnell and Grand 2012, Weitzman and Fradet-Turcotte 2018). Ad E1B-55K is a multifunctional protein that cooperates with E4 early region proteins, including E4orf6, to regulate host cell shut-off of cellular metabolism. In this regard, E1B-55K and E4orf6 inhibit cellular mRNA transport into the cytoplasm and inhibit cellular mRNA translation, whilst promoting viral mRNA accumulation in the cytoplasm (Babich, Feldman et al. 1983, Babiss, Ginsberg et al. 1985, Halbert, Cutt et al. 1985). More recently it has been determined that the ability of E1B-55K and E4orf6 to promote viral mRNA export to the cytoplasm is dependent upon the ubiquitin ligase activity of the E1B-55K-E4orf6-CRL complex (Blanchette, Kindsmüller et al. 2008). In addition to these properties E1B-55K also promotes adenovirus-mediated transformation of human and rodent cells, in cooperation with E1A, E1B-19K and E4 proteins (Yew, Liu et al. 1994, Nevels, Täuber et al. 1999). In this regard, it is thought that E1B-55K contributes to the transformation process through its ability to interact with p53 and inhibit its transcriptional activities (Yew and Berk 1992, Boyer, Martin et al. 1999).

Given the properties of E1B-55K and E4orf6 in host cell shut-off and cellular transformation, we wondered whether E1B-55K functions as a substrate adaptor for SMARCAL1 in the Ad-induced targeting of SMARCAL1 for proteasome-mediated degradation. Co-immunoprecipitation data presented in this chapter indicated that E1B-

55K from both Ad5 and Ad12 -transformed human cells possessed the capacity to interact with SMARCAL1 suggesting that E1B-55K, consistent with the data presented in Chapter 3, does most-likely function as a substrate adaptor for SMARCAL1 (Figures 5.1 and 5.2; Figures 3.9). As we have indicated previously that SMARCAL1 is phosphorylated during the early stages of Ad infection, prior to its degradation, it would be extremely interesting to see if E1B-55K binds preferentially to phosphorylated SMARCAL1. This would be interesting as E1B-55K has not been shown, as yet, to interact with any of its binding partners in a phospho-dependent manner. As we showed that E1B-55K bound to SMARCAL1 we next wished to establish whether E1B-55K could modulate the cellular function of SMARCAL1, as it does for p53. To do this we took advantage of our TET-inducible Ad5 and Ad12 E1B-55K U2OS cell lines generated in our laboratory to investigate the individual activities of adenovirus early region proteins [Albalawi and Turnell, unpublished data; Figure 5.3].

As described previously SMARCAL1 functions as an annealing helicase in cellular DNA replication that is involved in promoting cellular DNA replication restart after fork collapse and maintaining replication forks in unperturbed S-phase (Postow, Woo et al. 2009, Poole and Cortez 2017). SMARCAL1 activity is inhibited in response to activation of the DDR, in an ATR-dependent manner, to ensure that cellular replication is inhibited in response to DNA damage (Bansbach, Bétous et al. 2009, Couch, Bansbach et al. 2013).To investigate whether E1B-55K modulated cellular DNA replication, through interaction with SMARCAL1, we performed DNA fibre analyses where we observed the effects of E1B-55K expression upon the synthesis of new individual, DNA replication strands [(Petermann, Woodcock et al. 2010); Figure 5.4]. Our results demonstrated clearly that the expression of either Ad5 or Ad12 E1B-55K,

initially promoted accelerated cellular DNA replication [Figures 5.5- 5.8]. Strikingly, however, the increased cellular DNA replication rates induced by Ad5 and Ad12 E1B-55K expression ultimately resulted cellular DNA replication fork stalling [Figures 5.9 and 5.10]. In this regard, it has been shown previously that replication stress by oncogene products can lead, initially, to accelerated DNA replication that is ultimately followed by the destabilization of cellular DNA replication and fork collapse (Quinet and Vindigni 2018). As SMARCAL1 is recruited to stalled replication forks during replication stress, through its interaction of RPA, to promote fork re-start and prevent fork collapse (Bansbach, Bétous et al. 2009, Ciccia, Bredemeyer et al. 2009, Postow, Woo et al. 2009, Yusufzai, Kong et al. 2009), we hypothesize that E1B-55K expression induces replication stress to promote accelerated DNA synthesis, and moreover, inhibits SMARCAL1 activity to prevent replication restart after fork collapse. Consistent with this idea, the ATR-dependent inactivation of SMARCAL1 during DNA damage leads to the inhibition of replication restart and results in stalled fork replication (Couch, Bansbach et al. 2013).

Interestingly, the inhibition of MRE11 and p53 also results in cellular DNA replication stalling (Bryant, Petermann et al. 2009, Klusmann, Rodewald et al. 2016). Given that E1B-55K also interacts with these proteins, it is possible therefore that the effects of E1B-55K on cellular DNA replication are dependent upon its abilities to interact with SMARCAL1, MRE11 and p53, and potentially other cellular E1B-55K partner proteins. To distinguish the relative contribution of SMARCAL1, MRE11 and p53, in the E1B-55K dependent modulation of cellular DNA replication It would be interesting to make multiple E1B-55K mutants that possess selective binding capacity for SMARCAL1, MRE11 and p53. In this regard, E1B-55K mutants have been made that purportedly

distinguish between p53 and MRE11 binding, although close inspection of the data suggests that these mutants do retain at least, some, binding activity for both proteins (Carson, Schwartz et al. 2003, Härtl, Zeller et al. 2008).

In conclusion, we speculate that Ad E1B-55K creates a replication stress environment in the Ad infected cells by interacting with proteins such as SMARCAL1, MRE11 and p53 that results perturbed cellular DNA replication and fork stalling. Given the known role of E1B-55K and E4orf6 in host protein shut-off, as described earlier, we speculate that Ad E1B-55K and E4orf6 also promote the shut-off of host cell DNA replication and promote viral DNA replication through the targeting of SMARCAL1 and other cellular proteins for proteasome-mediated degradation during infection.

CHAPTER 6

Final Discussion

6.1. Regulation of ATR signalling pathways during adenovirus infection.

The work presented in this thesis has helped to determine that SMARCAL1 is targeted by adenoviruses for degradation in an E1B-55K/E4orf6 and CRL -dependent manner (Figure 3.1and 3.12, Chapter 3) and that E1B-55K expression modulates cellular DNA replication (Chapter 5). We also presented data to indicate that SMARCAL1 was phosphorylated by ATR and a CDK prior to degradation and that ATR and CDK1 inhibitors attenuated the Ad-mediated degradation of SMARCAL1 (Figure 3.8, Chapter 3). In this regard, we were able to show that the recruitment of SMARCAL1 to VRCs was to some extent dependent upon ATR and CDK -targeted phosphorylation of SMARCAL1, but SMARCAL1 association with the RPA complex was the major determining factor in facilitating SMARCAL1 recruitment to VRCs (Figure 4.8, Chapter 4). Although we determined that SMARCAL1 was phosphorylated at residues S123, S129 and S173 by ATR and CDK kinases during infection (Figure 3.3, Chapter 3) we were not able to experimentally investigate whether inactivation of these phosphorylation sites by mutation affected the Ad-mediated degradation of SMARCAL1 (Chapter 4). It will be important in the future to establish, without doubt, that phosphorylation at S123, S129 and S173 promote SMARCAL1 degradation.

The primary reason we could not determine whether phosphorylation at these sites was required for SMARCAL1 degradation in Ad-infected cells was because we made the phospho-inhibitory mutants in GFP-SMARCAL1 cDNA cloned into the retroviral, pLEGFP vector, which uses the constitutively active CMV promoter. It is well established that the 13S E1A gene transactivates the CMV promoter, such that upon Ad

infection GFP-SMARCAL1 levels were elevated and not reduced. To overcome this in the future we could try to co-express E1B-55K and E4orf6 plasmids or infect with E1B-55K and E4orf6 recombinant adenoviruses, in the absence of E1A, into the GFP-SMARCAL1 cell lines. However, it is also known that in the absence of E1A, E1B-55K and E4orf6 mimic many of the E1A like transactivation properties and enhance E1A functionality (Dallaire, Schreiner et al. 2015, Dallaire, Schreiner et al. 2016). Indeed, E1B-55K and E4orf6 stimulate viral early and late gene expression, in the absence of E1A and disrupt E2F-pRB interaction to drive viral and cellular DNA synthesis, such that this approach might not be useful either. CRISPR gene editing is a powerful new technique that can introduce specific mutations in the genome (Gilani, Shaukat et al. 2019). It would be interesting to introduce SA phospho-inhibitory mutations into the endogenous SMARCAL1 gene loci, to determine whether phosphorylation at these sites do promote SMARCAL1 degradation in Ad-infected cells. These studies might also determine whether these phosphorylation sites contribute towards regulating the protein levels of SMARCAL1 in replicating cells and in cells following replication stress, in the absence of Ad infection. Although there are not many published publications attempting to investigate the role of specific phosphorylation sites in biological processes it has been established that introduction of T25A mutation at the genomic level with CRISPR into the proteasome subunit, Rpt3, impairs proteasome activity and reduces the rate of cellular proliferation (Guo, Wang et al. 2016).

It is well established that many cellular DDR and replication proteins are recruited to VRCs and/or viral DNA during infection, some of which will be pro-viral and some anti-viral. The identification of new cellular factors that are recruited to VRCs or viral DNA will help establish a molecular profile of those factors that possess pro-viral or

anti-viral activity. In this context, Matthew Weitzman's group has recently utilised iPOND (isolation of proteins on nascent DNA), to identify cellular factors that associate with, or are excluded from the Ad5 genome during Ad5 DNA replication; the study also utilised iPOND to investigate those cellular proteins that associated with replicating HSV-1 and VACV DNA (Reyes, Kulej et al. 2017). Several host replication factors and DDR factors that are known to be recruited to VRCs, such as the MRN complex, BLM, ATR and SMARCAL1 were under-represented on replicating Ad5 DNA, relative to host cell DNA, suggesting that these factors all possess ant-viral activities (Reyes, Kulej et al. 2017). Interestingly, they also determined that ATR regulators such as Claspin and Timeless were excluded from Ad5 DNA during viral DNA replication, suggesting that ATR signalling is generally detrimental to Ad DNA replication. In order to identify other anti-viral host cell factors that are recruited to VRCs and potentially function in ATR signalling pathways our laboratory is currently using a proteomic approach to identify host cell proteins that associate with the RPA complex during infection. In this regard, it would also be worthwhile to investigate systematically all proteins known to function in the ATR pathway to determine if they are recruited to VRCs and/or degraded during Ad infection. If candidate proteins are identified using these approaches we could over-express or deplete these proteins and investigate the ability of Ad to replicate its DNA and produce new virions.

It is very well established that the adenovirus oncoprotein, E1B-55K interacts with p53 to inhibit its transcriptional activities (Yew and Berk 1992). It also known to serve as a substrate adaptor, for proteins like MRE11, when targeting it for degradation in an E1B-55K/E4orf6 and CRL-dependent manner (Stracker, Carson et al. 2002). As we determined that E1B-55K interacts with SMARCAL1 (Figure 5.1 and 5.2, Chapter 5),

we investigated whether E1B-55K could modulate the function of SMARCAL1 in cellular DNA replication. Using the DNA fibre analysis technique, we determined that both Ad5 and Ad12 E1B-55K promoted accelerated cellular DNA fork speed that ultimately led to DNA fork stalling (Figures 5.5 to 5.10, Chapter 5). It is also known however, that depletion of p53 and MRE11 also result in replication fork stalling (Bryant, Petermann et al. 2009, Klusmann, Rodewald et al. 2016). Hence, it will be interesting to establish in the future whether the ability of E1B-55K to promote accelerated replication fork speed that results in fork stalling is due to the combined action of E1B-55K on SMARCAL1, p53 and MRE11, or whether these activities are separable. As such, depending on where these proteins bind to E1B-55K, it would be of value to identify E1B-55K point mutations that discriminate between SMARCAL1, p53 and MRE11 binding so that we can investigate how these E1B-55K mutants affect cellular DNA replication and ATR signalling pathways activated in response to DNA damage. Moreover, as E1B-55K is known to cooperate with E4orf3 and E4orf6 in the inactivation of p53 and the MRN complex during infection and transformation (Yew and Berk 1992, Nevels, Täuber et al. 1999, Nevels, Täuber et al. 2001, Soria, Estermann et al. 2010), as well as during host-cell shutoff (Babich, Feldman et al. 1983, Babiss, Ginsberg et al. 1985, Halbert, Cutt et al. 1985), it will be worthwhile to investigate whether E4orf3 and E4orf6 target SMARCAL1, independent of E1B-55K and also modulate cellular DNA replication. These studies are currently on-going in our laboratory.

It is now established that SMARCAL1 maintains telomere integrity through modulation of the ALT pathway (Poole, Zhao et al. 2015, Cox, Maréchal et al. 2016). As such, SMARCAL1 associates with ALT telomeres and resolves replication stress, whilst in

the absence of SMARCAL1, DSBs accumulate at ALT telomere DNA, which promotes the formation of both chromosome fusions and extrachromosomal telomeric DNA (Poole, Zhao et al. 2015, Cox, Maréchal et al. 2016). Interestingly, Ad12 E1B-55K is known to extend the life-span of normal human skin fibroblasts in culture, such that cells escape cellular mortality-stage 1, senescence (Gallimore, Lecane et al. 1997). These cells do eventually enter crisis (mortality-stage 2) but this is not due to telomere-erosion or the activation of p53 (p21) or p16 pathways. Indeed, telomeric length was maintained in Ad12 E1B-55K-expressing fibroblasts in the absence of telomerase activation (Gallimore, Lecane et al. 1997), suggestive of the idea that Ad12 E1B-55K activates the ALT pathway. It would be very interesting to establish if Ad12 E1B-55K modulates SMARCAL1 activity to promote ALT or induces/inhibits DNA damage at ALT telomeres or the formation of extrachromosomal telomeric DNA.

Conditionally-replicating adenoviruses are an important therapeutic strategy for a number of human cancers (Rein, Breidenbach et al. 2006, Baker, Aguirre-Hernández et al. 2018). Interestingly, it has been determined that the killing of pancreatic adenocarcinoma cell lines with cytotoxic drugs is enhanced by infection with an E1B-19K deficient adenovirus (Pantelidou, Cherubini et al. 2016), which promotes the down-regulation of DDR proteins, MRE11 and Claspin. As such, it was postulated that the targeted knockdown, or inhibition of Claspin or MRE11 with selective drugs, could be used in combination with oncolytic adenoviruses to enhance cancer cell killing (Pantelidou, Cherubini et al. 2016). Given that some oncolytic viruses have deletions in the E1B region and that E1B-55K helps to inactivate SMARCAL1 during infection it would be worthwhile to use shRNAs/siRNAs against SMARCAL1, or selective drugs

for SMARCAL1,that do not exist currently, in combination with E1B-55K-deleted adenoviruses to see if cancer cell killing is enhanced in the absence of SMARCAL1.

The work presented in this thesis highlights the complex relationship between adenoviruses and host cell DDR pathways. It also re-emphasises the importance of studies with adenovirus to identify and dissect the molecular events that regulate host cell DDR pathways. Given that genome stability is currently a major, global research theme, particularly in relation to cancer research, and that adenoviruses are known to target key players in DDR pathways, research into adenovirus biology will continue to provide important insight into the fundamental processes that govern genome stability, and provide new opportunities to exploit DDR pathways for therapeutic intervention.

7. References

Abraham, R. T. (2001). "Cell cycle checkpoint signaling through the ATM and ATR kinases." Genes & development **15**(17): 2177-2196.

Abraham, R. T. (2004). "PI 3-kinase related kinases:'big'players in stress-induced signaling pathways." DNA repair **3**(8-9): 883-887.

Ali, S. H. and J. A. DeCaprio (2001). Cellular transformation by SV40 large T antigen: interaction with host proteins. Seminars in cancer biology, Elsevier.

Araujo, F. D., et al. (2005). "Adenovirus type 5 E4orf3 protein targets the Mre11 complex to cytoplasmic aggresomes." Journal of virology **79**(17): 11382-11391.

Babich, A., et al. (1983). "Effect of adenovirus on metabolism of specific host mRNAs: transport control and specific translational discrimination." Molecular and cellular biology **3**(7): 1212-1221.

Babiss, L., et al. (1985). "Adenovirus E1B proteins are required for accumulation of late viral mRNA and for effects on cellular mRNA translation and transport." Molecular and cellular biology **5**(10): 2552-2558.

Baker, A., et al. (2007). "Adenovirus E4 34k and E1b 55k oncoproteins target host DNA ligase IV for proteasomal degradation." Journal of virology **81**(13): 7034-7040.

Baker, A. T., et al. (2018). "Designer oncolytic adenovirus: coming of age." Cancers **10**(6): 201.

Bansbach, C. E., et al. (2009). "The annealing helicase SMARCAL1 maintains genome integrity at stalled replication forks." Genes & development **23**(20): 2405-2414.

Bansbach, C. E., et al. (2010). "SMARCAL1 and replication stress: an explanation for SIOD?" Nucleus **1**(3): 245-248.

Barker, D. D. and A. J. Berk (1987). "Adenovirus proteins from both E1B reading frames are required for transformation of rodent cells by viral infection and DNA transfection." Virology **156**(1): 107-121.

Bergonzini, V., et al. (2010). "View and review on viral oncology research." Infectious agents and cancer **5**(1): 11.

Berk, A. J. (2005). "Recent lessons in gene expression, cell cycle control, and cell biology from adenovirus." Oncogene **24**(52): 7673-7685.

Berk, A. J., et al. (1979). "Pre-early adenovirus 5 gene product regulates synthesis of early viral messenger RNAs." Cell **17**(4): 935-944.

Berk, A. J. and P. A. Sharp (1977). "Sizing and mapping of early adenovirus mRNAs by gel electrophoresis of S1 endonuclease-digested hybrids." Cell **12**(3): 721-732.

Bernards, R., et al. (1983). "Role of adenovirus types 5 and 12 early region 1 b tumor antigens in oncogenic transformation." Virology **127**(1): 45-53.

Bhat, K. P., et al. (2015). "High-affinity DNA-binding domains of replication protein A (RPA) direct SMARCAL1-dependent replication fork remodeling." Journal of Biological Chemistry **290**(7): 4110-4117.

Binz, S. K., et al. (2004). "Replication protein A phosphorylation and the cellular response to DNA damage." DNA repair **3**(8-9): 1015-1024.

Bischof, O., et al. (2005). "Human papillomavirus oncoprotein E7 targets the promyelocytic leukemia protein and circumvents cellular senescence via the Rb and p53 tumor suppressor pathways." Molecular and cellular biology **25**(3): 1013-1024.

Bischoff, J. R., et al. (1996). "An adenovirus mutant that replicates selectively in p53-deficient human tumor cells." science **274**(5286): 373-376.

Bitner, J. (1936). "Some possible effects of nursing on the mammary gland tumor incidence in mice." science **84**(2172): 1962.

Blackford, A. N., et al. (2008). "A role for E1B-AP5 in ATR signaling pathways during adenovirus infection." Journal of virology **82**(15): 7640-7652.

Blackford, A. N. and R. J. Grand (2009). "Adenovirus E1B 55-kilodalton protein: multiple roles in viral infection and cell transformation." Journal of virology **83**(9): 4000-4012.

Blackford, A. N. and S. P. Jackson (2017). "ATM, ATR, and DNA-PK: the trinity at the heart of the DNA damage response." Molecular cell **66**(6): 801-817.

Blackford, A. N., et al. (2010). "Adenovirus 12 E4orf6 inhibits ATR activation by promoting TOPBP1 degradation." Proceedings of the National Academy of Sciences **107**(27): 12251-12256.

Blanchette, P., et al. (2004). "Both BC-box motifs of adenovirus protein E4orf6 are required to efficiently assemble an E3 ligase complex that degrades p53." Molecular and cellular biology **24**(21): 9619-9629.

Blanchette, P., et al. (2008). "Control of mRNA export by adenovirus E4orf6 and E1B55K proteins during productive infection requires E4orf6 ubiquitin ligase activity." Journal of virology **82**(6): 2642-2651.

Block, W. D., et al. (2004). "Selective inhibition of the DNA-dependent protein kinase (DNA-PK) by the radiosensitizing agent caffeine." Nucleic acids research **32**(6): 1967-1972.

Blumberg, B. S., et al. (1967). "A serum antigen (Australia antigen) in Down's syndrome, leukemia, and hepatitis." Annals of internal medicine **66**(5): 924-931.

Boerkoel, C. F., et al. (2002). "Mutant chromatin remodeling protein SMARCAL1 causes Schimke immuno-osseous dysplasia." Nature genetics **30**(2): 215.

Bos, J. and H. ten Wolde-Kraamwinkel (1983). "The E1b promoter of Ad12 in mouse L tk- cells is activated by adenovirus region E1a." The EMBO journal **2**(1): 73-76.

Boshart, M., et al. (1984). "A new type of papillomavirus DNA, its presence in genital cancer biopsies and in cell lines derived from cervical cancer." The EMBO journal **3**(5): 1151-1157.

Boulanger, P. A. and G. E. Blair (1991). "Expression and interactions of human adenovirus oncoproteins." Biochemical journal **275**(Pt 2): 281.

Boyer, J., et al. (1999). "Adenovirus E4 34k and E4 11k inhibit double strand break repair and are physically associated with the cellular DNA-dependent protein kinase." Virology **263**(2): 307-312.

Boyer, T. G., et al. (1999). "Mammalian Srb/Mediator complex is targeted by adenovirus E1A protein." Nature **399**(6733): 276.

Brady, H. A. and W. Wold (1988). "Competition between splicing and polyadenylation reactions determines which adenovirus region E3 mRNAs are synthesized." Molecular and cellular biology **8**(8): 3291-3297.

Bremner, K. H., et al. (2009). "Adenovirus transport via direct interaction of cytoplasmic dynein with the viral capsid hexon subunit." Cell host & microbe **6**(6): 523-535.

Brenner, S. and R. Horne (1959). "A negative staining method for high resolution electron microscopy of viruses." Biochimica et biophysica acta **34**: 103-110.

Brestovitsky, A., et al. (2016). "The adenovirus E4orf4 protein provides a novel mechanism for inhibition of the DNA damage response." PLoS pathogens **12**(2): e1005420.

Bridges, R. G., et al. (2016). "The adenovirus E4-ORF3 protein stimulates SUMOylation of general transcription factor TFII-I to direct proteasomal degradation." MBio **7**(1): e02184-02115.

Brown, E. J. and D. Baltimore (2000). "ATR disruption leads to chromosomal fragmentation and early embryonic lethality." Genes & development **14**(4): 397-402.

Bryant, H. E., et al. (2009). "PARP is activated at stalled forks to mediate Mre11-dependent replication restart and recombination." The EMBO journal **28**(17): 2601-2615.

Byrd, P., et al. (1982). "Malignant transformation of human embryo retinoblasts by cloned adenovirus 12 DNA."

Byrd, P., et al. (1988). "Differential transformation of primary human embryo retinal cells by adenovirus E1 regions and combinations of E1A+ ras." Oncogene **2**(5): 477-484.

Byun, T. S., et al. (2005). "Functional uncoupling of MCM helicase and DNA polymerase activities activates the ATR-dependent checkpoint." Genes & development **19**(9): 1040-1052.

Carrassa, L. and G. Damia (2017). "DNA damage response inhibitors: Mechanisms and potential applications in cancer therapy." Cancer treatment reviews **60**: 139-151.

Carroll, C., et al. (2013). "Phosphorylation of a C-terminal auto-inhibitory domain increases SMARCAL1 activity." Nucleic acids research **42**(2): 918-925.

Carson, C. T., et al. (2009). "Mislocalization of the MRN complex prevents ATR signaling during adenovirus infection." The EMBO journal **28**(6): 652-662.

Carson, C. T., et al. (2003). "The Mre11 complex is required for ATM activation and the G2/M checkpoint." The EMBO journal **22**(24): 6610-6620.

Carvalho, T., et al. (1995). "Targeting of adenovirus E1A and E4-ORF3 proteins to nuclear matrix-associated PML bodies." The Journal of cell biology **131**(1): 45-56.

Cesarman, E., et al. (2019). "Kaposi sarcoma." Nature Reviews Disease Primers **5**(1): 9.

Chang, L.-S. and T. Shenk (1990). "The adenovirus DNA-binding protein stimulates the rate of transcription directed by adenovirus and adeno-associated virus promoters." Journal of virology **64**(5): 2103-2109.

Chang, Y., et al. (1994). "Identification of herpesvirus-like DNA sequences in AIDS-associated Kaposi's sarcoma." science **266**(5192): 1865-1869.

Chen, R. and M. S. Wold (2014). "Replication protein A: Single-stranded DNA's first responder." Bioessays **36**(12): 1156-1161.

Chow, L. T., et al. (1977). "A map of cytoplasmic RNA transcripts from lytic adenovirus type 2, determined by electron microscopy of RNA: DNA hybrids." Cell **11**(4): 819-836.

Ciccia, A., et al. (2009). "The SIOD disorder protein SMARCAL1 is an RPA-interacting protein involved in replication fork restart." Genes & development **23**(20): 2415-2425.

Ciccia, A. and S. J. Elledge (2010). "The DNA damage response: making it safe to play with knives." Molecular cell **40**(2): 179-204.

Cimprich, K. A. and D. Cortez (2008). "ATR: an essential regulator of genome integrity." Nature reviews Molecular cell biology **9**(8): 616.

Cohen, M., et al. (2013). "Dissection of the C-terminal region of E1A redefines the roles of CtBP and other cellular targets in oncogenic transformation." Journal of virology **87**(18): 10348-10355.

Cohen, P. (2002). "Protein kinases—the major drug targets of the twenty-first century?" Nature reviews Drug discovery **1**(4): 309.

Cortez, D. (2015). "Preventing replication fork collapse to maintain genome integrity." DNA repair **32**: 149-157.

Couch, F. B., et al. (2013). "ATR phosphorylates SMARCAL1 to prevent replication fork collapse." Genes & development **27**(14): 1610-1623.

Coussens, P., et al. (1985). "Restriction of the in vitro and in vivo tyrosine protein kinase activities of pp60c-src relative to pp60v-src." Molecular and cellular biology **5**(10): 2753-2763.

Cox, K. E., et al. (2016). "SMARCAL1 resolves replication stress at ALT telomeres." Cell reports **14**(5): 1032-1040.

Dallaire, F., et al. (2009). "Identification of integrin α3 as a new substrate of the adenovirus E4orf6/E1B 55-kilodalton E3 ubiquitin ligase complex." Journal of virology **83**(11): 5329-5338.

Dallaire, F., et al. (2015). The human adenovirus type 5 E4orf6/E1B55K E3 ubiquitin ligase complex enhances E1A functional activity. mSphere 1 (1): e00015-15.

Dallaire, F., et al. (2016). "The human adenovirus type 5 E4orf6/E1B55K E3 ubiquitin ligase complex can mimic E1A effects on E2F." mSphere **1**(1): e00014-00015.

Dane, D., et al. (1970). "Virus-like particles in serum of patients with Australia-antigen-associated hepatitis." The lancet **295**(7649): 695-698.

de Jong, R. N., et al. (2003). Adenovirus DNA replication: protein priming, jumping back and the role of the DNA binding protein DBP. Adenoviruses: Model and Vectors in Virus-Host Interactions, Springer**:** 187-211.

de Lange, T. (2018). "Shelterin-mediated telomere protection." Annual review of genetics **52**: 223-247.

Delacroix, S., et al. (2007). "The Rad9–Hus1–Rad1 (9–1–1) clamp activates checkpoint signaling via TopBP1." Genes & development **21**(12): 1472-1477.

DeLeo, A. B., et al. (1979). "Detection of a transformation-related antigen in chemically induced sarcomas and other transformed cells of the mouse." Proceedings of the National Academy of Sciences **76**(5): 2420-2424.

Dhingra, A., et al. (2019). "Molecular Evolution of Human Adenovirus (HAdV) Species C". Scientific Reports 9: 1039.

Dobner, T., et al. (1996). "Blockage by adenovirus E4orf6 of transcriptional activation by the p53 tumor suppressor." science **272**(5267): 1470-1473.

Doerfler, W. (2007). "Human Adenovirus Type 12". SpringerLink, 131: 197-211.

Dornreiter, I., et al. (1992). "Interaction of DNA polymerase alpha-primase with cellular replication protein A and SV40 T antigen." The EMBO journal **11**(2): 769-776.

Downey, J., et al. (1983). "Mapping of a 14,000-dalton antigen to early region 4 of the human adenovirus 5 genome." Journal of virology **45**(2): 514-523.

Duda, D. M., et al. (2008). "Structural insights into NEDD8 activation of cullin-RING ligases: conformational control of conjugation." Cell **134**(6): 995-1006.

Dürst, M., et al. (1983). "A papillomavirus DNA from a cervical carcinoma and its prevalence in cancer biopsy samples from different geographic regions." Proceedings of the National Academy of Sciences **80**(12): 3812-3815.

Dutta, A. and B. Stillman (1992). "cdc2 family kinases phosphorylate a human cell DNA replication factor, RPA, and activate DNA replication." The EMBO journal **11**(6): 2189-2199.

Echavarria, M. (2008). "Adenoviruses in immunocompromised hosts." Clinical microbiology reviews **21**(4): 704-715.

Eddy, B. E., et al. (1962). "Identification of the oncogenic substance in rhesus monkey kidney cell cultures as simian virus 40." Virology **17**(1): 65-75.

Engels, E. A., et al. (2005). "Antibody responses to simian virus 40 T antigen: a case-control study of non-Hodgkin lymphoma." Cancer Epidemiology and Prevention Biomarkers **14**(2): 521-524.

Engels, E. A., et al. (2003). "Cancer incidence in Denmark following exposure to poliovirus vaccine contaminated with simian virus 40." Journal of the National Cancer Institute **95**(7): 532-539.

Epstein, M., et al. (1964). "VIRUS PARTICLES IN CULTURED LYMPHOBLASTS FROM BURKITT'S LYMPHOMA." The lancet **283**(7335): 702-703.

Faulds, D. and R. C. Heel (1990). "Ganciclovir." Drugs **39**(4): 597-638.

Feling, R. H., et al. (2003). "Salinosporamide A: a highly cytotoxic proteasome inhibitor from a novel microbial source, a marine bacterium of the new genus Salinospora." Angewandte Chemie International Edition **42**(3): 355-357.

Feng, H., et al. (2008). "Clonal integration of a polyomavirus in human Merkel cell carcinoma." science **319**(5866): 1096-1100.

Ferrari, R., et al. (2014). "Adenovirus small E1A employs the lysine acetylases p300/CBP and tumor suppressor Rb to repress select host genes and promote productive virus infection." Cell host & microbe **16**(5): 663-676.

Ferrari, R., et al. (2008). "Epigenetic reprogramming by adenovirus e1a." science **321**(5892): 1086-1088.

Field, J., et al. (1984). "Properties of the adenovirus DNA polymerase." Journal of Biological Chemistry **259**(15): 9487-9495.

Flaus, A., et al. (2006). "Identification of multiple distinct Snf2 subfamilies with conserved structural motifs." Nucleic acids research **34**(10): 2887-2905.

Forrester, N. A., et al. (2012). "Adenovirus E4orf3 targets transcriptional intermediary factor 1γ for proteasome-dependent degradation during infection." Journal of virology **86**(6): 3167-3179.

Forrester, N. A., et al. (2011). "Serotype-specific inactivation of the cellular DNA damage response during adenovirus infection." Journal of virology **85**(5): 2201-2211.

Frisch, S. M. and J. S. Mymryk (2002). "Adenovirus-5 E1A: paradox and paradigm." Nature reviews Molecular cell biology **3**(6): 441-452.

Fu, Y. R., et al. (2017). "Comparison of protein expression during wild-type, and E1B-55k-deletion, adenovirus infection using quantitative time-course proteomics." The Journal of general virology **98**(6): 1377.

Fuchs, M., et al. (2001). "The p400 complex is an essential E1A transformation target." Cell **106**(3): 297-307.

Gallimore, P. H., et al. (1997). "Adenovirus type 12 early region 1B 54K protein significantly extends the life span of normal mammalian cells in culture." Journal of virology **71**(9): 6629-6640.

Gallimore, P. H. and A. S. Turnell (2001). "Adenovirus E1A: remodelling the host cell, a life or death experience." Oncogene **20**(54).

Gaurab Karki (2018). "Adenovirus: Structure and genome, Replication, Pathogenesis, Infection, laboratory diagnosis, Prevention and Treatment." from https://www.onlinebiologynotes.com/adenovirus-structure-genome-replication-pathogenesis-infection-laboratory-diagnosis-prevention-treatment/.

Geisberg, J. V., et al. (1994). "The zinc finger region of the adenovirus E1A transactivating domain complexes with the TATA box binding protein." Proceedings of the National Academy of Sciences **91**(7): 2488-2492.

Ghosal, G., et al. (2011). "The HARP domain dictates the annealing helicase activity of HARP/SMARCAL1." EMBO reports **12**(6): 574-580.

Gilani, U., et al. (2019). "The implication of CRISPR/Cas9 genome editing technology in combating human oncoviruses." Journal of medical virology **91**(1): 1-13.

Gilson, T., et al. (2012). "The α2 helix in the DNA ligase IV BRCT-1 domain is required for targeted degradation of ligase IV during adenovirus infection." Virology **428**(2): 128-135.

Gissmann, L., et al. (1983). "Human papillomavirus types 6 and 11 DNA sequences in genital and laryngeal papillomas and in some cervical cancers." Proceedings of the National Academy of Sciences of the United States of America **80**(2): 560.

Gorgoulis, V. G., et al. (2005). "Activation of the DNA damage checkpoint and genomic instability in human precancerous lesions." Nature **434**(7035): 907.

Graham, F., et al. (1977). "Characteristics of a human cell line transformed by DNA from human adenovirus type 5." Journal of General Virology **36**(1): 59-72.

Graham, F. L., et al. (1977). "Characteristics of a human cell line transformed by DNA from human adenovirus type 5." Journal of General Virology **36**(1): 59-72.

Grand, R. J., et al. (1998). "Human cells arrest in S phase in response to adenovirus 12 E1A." Virology **244**(2): 330-342.

Gross, L. (1953). "A filterable agent, recovered from Ak leukemic extracts, causing salivary gland carcinomas in C3H mice." Proceedings of the Society for Experimental Biology and Medicine **83**(2): 414-421.

Gulder, T. A. and B. S. Moore (2010). "Salinosporamide natural products: Potent 20 S proteasome inhibitors as promising cancer chemotherapeutics." Angewandte Chemie International Edition **49**(49): 9346-9367.

Guo, X., et al. (2016). "Site-specific proteasome phosphorylation controls cell proliferation and tumorigenesis." Nature cell biology **18**(2): 202.

Halbert, D., et al. (1985). "Adenovirus early region 4 encodes functions required for efficient DNA replication, late gene expression, and host cell shutoff." Journal of virology **56**(1): 250-257.

Hall, K., et al. (2010). "Unity and diversity in the human adenoviruses: exploiting alternative entry pathways for gene therapy." Biochemical Journal **431**(3): 321-336.

Harada, J. N. and A. J. Berk (1999). "p53-Independent and-dependent requirements for E1B-55K in adenovirus type 5 replication." Journal of virology **73**(7): 5333-5344.

Harada, J. N., et al. (2002). "Analysis of the adenovirus E1B-55K-anchored proteome reveals its link to ubiquitination machinery." Journal of virology **76**(18): 9194-9206.

Härtl, B., et al. (2008). "Adenovirus type 5 early region 1B 55-kDa oncoprotein can promote cell transformation by a mechanism independent from blocking p53-activated transcription." Oncogene **27**(26): 3673.

Hartlerode, A. J., et al. (2015). "Recruitment and activation of the ATM kinase in the absence of DNA-damage sensors." Nature structural & molecular biology **22**(9): 736.

Hartmann, T., et al. (2014). "Inhibition of Cullin-RING E3 ubiquitin ligase 7 by simian virus 40 large T antigen." Proceedings of the National Academy of Sciences **111**(9): 3371-3376.

Heise, C., et al. (1997). "ONYX-015, an E1B gene-attenuated adenovirus, causes tumor-specific cytolysis and antitumoral efficacy that can be augmented by standard chemotherapeutic agents." Nature medicine **3**(6): 639.

Helin, K. and E. Harlow (1994). "Heterodimerization of the transcription factors E2F-1 and DP-1 is required for binding to the adenovirus E4 (ORF6/7) protein." Journal of virology **68**(8): 5027-5035.

Hickson, I., et al. (2004). "Identification and characterization of a novel and specific inhibitor of the ataxia-telangiectasia mutated kinase ATM." Cancer research **64**(24): 9152-9159.

Hirao, A., et al. (2000). "DNA damage-induced activation of p53 by the checkpoint kinase Chk2." science **287**(5459): 1824-1827.

Hoeben, R. C. and T. G. Uil (2013). "Adenovirus DNA replication." Cold Spring Harbor perspectives in biology **5**(3): a013003.

Holm, P. S., et al. (2002). "YB-1 relocates to the nucleus in adenovirus-infected cells and facilitates viral replication by inducing E2 gene expression through the E2 late promoter." Journal of Biological Chemistry **277**(12): 10427-10434.

Horwitz, G. A., et al. (2008). "Adenovirus small e1a alters global patterns of histone modification." science **321**(5892): 1084-1085.

Huang, M.-M. and P. Hearing (1989). "Adenovirus early region 4 encodes two gene products with redundant effects in lytic infection." Journal of virology **63**(6): 2605-2615.

Hunter, T. (1995). "Protein kinases and phosphatases: the yin and yang of protein phosphorylation and signaling." Cell **80**(2): 225-236.

Imelli, N., et al. (2004). "Cholesterol is required for endocytosis and endosomal escape of adenovirus type 2." Journal of virology **78**(6): 3089-3098.

Jackson, S. P. and J. Bartek (2009). "The DNA-damage response in human biology and disease." Nature **461**(7267): 1071.

Jelsma, T. N., et al. (1989). "Sequences in E1A proteins of human adenovirus 5 required for cell transformation, repression of a transcriptional enhancer, and induction of proliferating cell nuclear antigen." Virology **171**(1): 120-130.

Johnson, L., et al. (2002). "Selectively replicating adenoviruses targeting deregulated E2F activity are potent, systemic antitumor agents." Cancer cell **1**(4): 325-337.

Jones, N. and T. Shenk (1979). "Isolation of adenovirus type 5 host range deletion mutants defective for transformation of rat embryo cells." Cell **17**(3): 683-689.

Kabeche, L., et al. (2018). "A mitosis-specific and R loop–driven ATR pathway promotes faithful chromosome segregation." science **359**(6371): 108-114.

Kastan, M. B. and J. Bartek (2004). "Cell-cycle checkpoints and cancer." Nature **432**(7015): 316.

Kleinberger, T. (2015). "Mechanisms of cancer cell killing by the adenovirus E4orf4 protein." Viruses **7**(5): 2334-2357.

Kleinberger, T. and T. Shenk (1993). "Adenovirus E4orf4 protein binds to protein phosphatase 2A, and the complex down regulates E1A-enhanced junB transcription." Journal of virology **67**(12): 7556-7560.

Klusmann, I., et al. (2016). "p53 activity results in DNA replication fork processivity." Cell reports **17**(7): 1845-1857.

König, C., et al. (1999). "Adenovirus type 5 E4orf3 protein relieves p53 inhibition by E1B-55-kilodalton protein." Journal of virology **73**(3): 2253-2262.

Krajcsi, P., et al. (1996). "The adenovirus E3-14.7 K protein and the E3-10.4 K/14.5 K complex of proteins, which independently inhibit tumor necrosis factor (TNF)-induced apoptosis, also independently inhibit TNF-induced release of arachidonic acid." Journal of virology **70**(8): 4904-4913.

Kress, M., et al. (1979). "Simian virus 40-transformed cells express new species of proteins precipitable by anti-simian virus 40 tumor serum." Journal of virology **31**(2): 472-483.

Kumagai, A., et al. (2006). "TopBP1 activates the ATR-ATRIP complex." Cell **124**(5): 943-955.

Kuper, H., et al. (2001). "The risk of liver and bile duct cancer in patients with chronic viral hepatitis, alcoholism, or cirrhosis." Hepatology **34**(4): 714-718.

Lan, H., et al. (2016). "Neddylation inhibitor MLN4924 suppresses growth and migration of human gastric cancer cells." Scientific reports **6**: 24218.

Lane, D. P. and L. V. Crawford (1979). "T antigen is bound to a host protein in SY40-transformed cells." Nature **278**(5701): 261.

Lee, D. H. and A. L. Goldberg (1996). "Selective inhibitors of the proteasome-dependent and vacuolar pathways of protein degradation in Saccharomyces cerevisiae." Journal of Biological Chemistry **271**(44): 27280-27284.

Lee, W. S., et al. (1991). "Adenovirus E1A activation domain binds the basic repeat in the TATA box transcription factor." Cell **67**(2): 365-376.

Linzer, D. I. and A. J. Levine (1979). "Characterization of a 54K dalton cellular SV40 tumor antigen present in SV40-transformed cells and uninfected embryonal carcinoma cells." Cell **17**(1): 43-52.

Liu, F. and M. R. Green (1990). "A specific member of the ATF transcription factor family can mediate transcription activation by the adenovirus E1a protein." Cell **61**(7): 1217-1224.

Liu, F. and M. R. Green (1994). "Promoter targeting by adenovirus E1a through interaction with different cellular DNA-binding domains." Nature **368**(6471): 520.

Liu, H., et al. (2003). Adenovirus DNA replication. Adenoviruses: Model and Vectors in Virus-Host Interactions, Springer**:** 131-164.

Lyle, C. and F. McCormick (2010). "Integrin αvβ5 is a primary receptor for adenovirus in CAR-negative cells." Virology journal **7**(1): 148.

Madisch, I., et al. (2005). "Phylogenetic analysis of the main neutralization and hemagglutination determinants of all human adenovirus prototypes as a basis for molecular classification and taxonomy." Journal of virology **79**(24): 15265-15276.

Matsuoka, S., et al. (2007). "ATM and ATR substrate analysis reveals extensive protein networks responsive to DNA damage." science **316**(5828): 1160-1166.

McCormick, F. (2001). "Cancer gene therapy: fringe or cutting edge?" Nature Reviews Cancer **1**(2): 130.

Metcalf, J. P., et al. (1994). "Adenovirus E1A 13S gene product up-regulates the cytomegalovirus major immediate early promoter." American journal of respiratory cell and molecular biology **10**(4): 448-452.

Meyer, N. and L. Z. Penn (2008). "Reflecting on 25 years with MYC." Nature Reviews Cancer **8**(12): 976.

Min, A., et al. (2017). "AZD6738, a novel oral inhibitor of ATR, induces synthetic lethality with ATM deficiency in gastric cancer cells." Molecular cancer therapeutics **16**(4): 566-577.

Muller, S. and T. Dobner (2008). "The adenovirus E1B-55K oncoprotein induces SUMO modification of p53." Cell Cycle **7**(6): 754-758.

Muthuswami, R., et al. (2000). "A eukaryotic SWI2/SNF2 domain, an exquisite detector of double-stranded to single-stranded DNA transition elements." Journal of Biological Chemistry **275**(11): 7648-7655.

Nawrocki, S. T., et al. (2012). "MLN4924: a novel first-in-class inhibitor of NEDD8-activating enzyme for cancer therapy." Expert opinion on investigational drugs **21**(10): 1563-1573.

Nebenzahl-Sharon, K., et al. (2019). "Biphasic functional interaction between the adenovirus E4orf4 protein and DNA-PK." Journal of virology **93**(10): e01365-01318.

Nevels, M., et al. (1997). "The adenovirus E4orf6 protein can promote E1A/E1B-induced focus formation by interfering with p53 tumor suppressor function." Proceedings of the National Academy of Sciences **94**(4): 1206-1211.

Nevels, M., et al. (1999). "Transforming potential of the adenovirus type 5 E4orf3 protein." Journal of virology **73**(2): 1591-1600.

Nevels, M., et al. (2001). "“Hit-and-run” transformation by adenovirus oncogenes." Journal of virology **75**(7): 3089-3094.

Nieminuszczy, J., et al. (2016). "The DNA fibre technique–tracking helicases at work." Methods **108**: 92-98.

Norrby, E., et al. (1976). "Adenoviridae." Intervirology **7**(3): 117-125.

O'Shea, C. C., et al. (2004). "Late viral RNA export, rather than p53 inactivation, determines ONYX-015 tumor selectivity." Cancer cell **6**(6): 611-623.

O’Cathail, S. M., et al. (2017). "Combining oncolytic adenovirus with radiation—a paradigm for the future of radiosensitization." Frontiers in oncology **7**: 153.

Orazio, N. I., et al. (2011). "The adenovirus E1b55K/E4orf6 complex induces degradation of the Bloom helicase during infection." Journal of virology **85**(4): 1887-1892.

Orlando, J. S. and D. A. Ornelles (1999). "An arginine-faced amphipathic alpha helix is required for adenovirus type 5 E4orf6 protein function." Journal of virology **73**(6): 4600-4610.

Ou, H. D., et al. (2012). "A structural basis for the assembly and functions of a viral polymer that inactivates multiple tumor suppressors." Cell **151**(2): 304-319.

Pantelidou, C., et al. (2016). "The E1B19K-deleted oncolytic adenovirus mutant AdΔ19K sensitizes pancreatic cancer cells to drug-induced DNA-damage by down-regulating Claspin and Mre11." Oncotarget **7**(13): 15703.

Pehere, A. D., et al. (2019). "Tripeptide analogues of MG132 as protease inhibitors." Bioorganic & medicinal chemistry **27**(2): 436-441.

Pelka, P., et al. (2009). "Transcriptional control by adenovirus E1A conserved region 3 via p300/CBP." Nucleic acids research: gkn1057.

Petermann, E., et al. (2006). "Chk1 requirement for high global rates of replication fork progression during normal vertebrate S phase." Molecular and cellular biology **26**(8): 3319-3326.

Petermann, E., et al. (2010). "Chk1 promotes replication fork progression by controlling replication initiation." Proceedings of the National Academy of Sciences **107**(37): 16090-16095.

Plummer, M., et al. (2016). "Global burden of cancers attributable to infections in 2012: a synthetic analysis." The Lancet Global Health **4**(9): e609-e616.

Poiesz, B. J., et al. (1980). "Detection and isolation of type C retrovirus particles from fresh and cultured lymphocytes of a patient with cutaneous T-cell lymphoma." Proceedings of the National Academy of Sciences **77**(12): 7415-7419.

Poole, L. A. and D. Cortez (2017). "Functions of SMARCAL1, ZRANB3, and HLTF in maintaining genome stability." Critical reviews in biochemistry and molecular biology **52**(6): 696-714.

Poole, L. A., et al. (2015). "SMARCAL1 maintains telomere integrity during DNA replication." Proceedings of the National Academy of Sciences **112**(48): 14864-14869.

Postow, L., et al. (2009). "Identification of SMARCAL1 as a component of the DNA damage response." Journal of Biological Chemistry **284**(51): 35951-35961.

Prince, A. M. (1968). "An antigen detected in the blood during the incubation period of serum hepatitis." Proceedings of the National Academy of Sciences of the United States of America **60**(3): 814.

Querido, E., et al. (2001). "Degradation of p53 by adenovirus E4orf6 and E1B55K proteins occurs via a novel mechanism involving a Cullin-containing complex." Genes & development **15**(23): 3104-3117.

Quinet, A. and A. Vindigni (2018). Superfast DNA replication causes damage in cancer cells, Nature Publishing Group.

Rasti, M., et al. (2006). "Roles for APIS and the 20S proteasome in adenovirus E1A-dependent transcription." The EMBO journal **25**(12): 2710-2722.

Raychaudhuri, P., et al. (1991). "Domains of the adenovirus E1A protein required for oncogenic activity are also required for dissociation of E2F transcription factor complexes." Genes & development **5**(7): 1200-1211.

Rein, D. T., et al. (2006). "Current developments in adenovirus-based cancer gene therapy."

Reyes, E. D., et al. (2017). "Identifying host factors associated with DNA replicated during virus infection." Molecular & Cellular Proteomics **16**(12): 2079-2097.

Robbins, C. B. (2012). Identifying and defining the genome maintenance functions of SMARCAL1, University of Nashville. **PhD**.

Rous, P. (1910). "A transmissible avian neoplasm.(sarcoma of the common fowl.)." Journal of Experimental Medicine **12**(5): 696-705.

Rous, P. (1911). "A sarcoma of the fowl transmissible by an agent separable from the tumor cells." The Journal of experimental medicine **13**(4): 397.

Rowe, W. P., et al. (1953). "Isolation of a cytopathogenic agent from human adenoids undergoing spontaneous degeneration in tissue culture." Experimental Biology and Medicine **84**(3): 570-573.

Russell, W. (2000). "Update on adenovirus and its vectors." Journal of General Virology **81**(11): 2573-2604.

Saban, S. D., et al. (2006). "Visualization of α-helices in a 6-Ångstrom resolution cryoelectron microscopy structure of adenovirus allows refinement of capsid protein assignments." Journal of virology **80**(24): 12049-12059.

Saha, B., et al. (2014). "The adenovirus genome contributes to the structural stability of the virion." Viruses **6**(9): 3563-3583.

Sancar, A., et al. (2004). "Molecular mechanisms of mammalian DNA repair and the DNA damage checkpoints." Annual review of biochemistry **73**(1): 39-85.

Sarkaria, J. N., et al. (1999). "Inhibition of ATM and ATR kinase activities by the radiosensitizing agent, caffeine." Cancer research **59**(17): 4375-4382.

Sarnow, P., et al. (1984). "Adenovirus early region 1B 58,000-dalton tumor antigen is physically associated with an early region 4 25,000-dalton protein in productively infected cells." Journal of virology **49**(3): 692-700.

Sarnow, P., et al. (1982). "A monoclonal antibody detecting the adenovirus type 5 E 1 b-58Kd tumor antigen: Characterization of the E 1 b-58Kd tumor antigen in adenovirus-infected and-transformed cells." Virology **120**(2): 510-517.

Schreiner, S., et al. (2012). "Adenovirus degradation of cellular proteins." Future microbiology **7**(2): 211-225.

Schreiner, S., et al. (2011). "Adenovirus type 5 early region 1B 55K oncoprotein-dependent degradation of cellular factor Daxx is required for efficient transformation of primary rodent cells." Journal of virology **85**(17): 8752-8765.

Schreiner, S., et al. (2010). "Proteasome-dependent degradation of Daxx by the viral E1B-55K protein in human adenovirus-infected cells." Journal of virology **84**(14): 7029-7038.

Shaw, A. R. and M. Suzuki (2016). "Recent advances in oncolytic adenovirus therapies for cancer." Current opinion in virology **21**: 9-15.

Shay, J. W. and W. E. Wright (2019). "Telomeres and telomerase: three decades of progress." Nat. Rev. Genet **20**: 299-309.

Shibata, A. and P. Jeggo (2018). ATM: Its Recruitment, Activation, Signalling and Contribution to Tumour Suppression. Targeting the DNA Damage Response for Anti-Cancer Therapy, Springer**:** 129-154.

Shope, R. E. and E. W. Hurst (1933). "Infectious papillomatosis of rabbits: with a note on the histopathology." Journal of Experimental Medicine **58**(5): 607-624.

Shtrichman, R., et al. (2000). "Adenovirus E4orf4 protein interacts with both Bα and B′ subunits of protein phosphatase 2A, but E4orf4-induced apoptosis is mediated only by the interaction with Bα." Oncogene **19**(33): 3757.

Sieber, T. and T. Dobner (2007). "Adenovirus type 5 early region 1B 156R protein promotes cell transformation independently of repression of p53-stimulated transcription." Journal of virology **81**(1): 95-105.

Simanshu, D. K., et al. (2017). "RAS proteins and their regulators in human disease." Cell **170**(1): 17-33.

Sohn, S.-Y. and P. Hearing (2016). "The adenovirus E4-ORF3 protein functions as a SUMO E3 ligase for TIF-1γ sumoylation and poly-SUMO chain elongation." Proceedings of the National Academy of Sciences **113**(24): 6725-6730.

Soria, C., et al. (2010). "Heterochromatin silencing of p53 target genes by a small viral protein." Nature **466**(7310): 1076.

Soucy, T. A., et al. (2009). "An inhibitor of NEDD8-activating enzyme as a new approach to treat cancer." Nature **458**(7239): 732.

Steegenga, W. T., et al. (1998). "The large E1B protein together with the E4orf6 protein target p53 for active degradation in adenovirus infected cells." Oncogene **16**(3): 349.

Stehelin, D., et al. (1976). "DNA related to the transforming gene (s) of avian sarcoma viruses is present in normal avian DNA." Nature **260**(5547): 170.

Stevens, J. L., et al. (2002). "Transcription control by E1A and MAP kinase pathway via Sur2 mediator subunit." Science **296**(5568): 755-758.

Stracker, T. H., et al. (2002). "Adenovirus oncoproteins inactivate the Mre11–Rad50–NBS1 DNA repair complex." Nature **418**(6895): 348.

Sundararajan, R., et al. (2001). "Tumor necrosis factor-α induces Bax-Bak interaction and apoptosis, which is inhibited by adenovirus E1B 19K." Journal of Biological Chemistry **276**(48): 45120-45127.

Surget, S., et al. (2014). "Uncovering the role of p53 splice variants in human malignancy: a clinical perspective." OncoTargets and therapy **7**: 57.

Täuber, B. and T. Dobner (2001). "Molecular regulation and biological function of adenovirus early genes: the E4 ORFs." Gene **278**(1-2): 1-23.

Thomas, D. L., et al. (2001). "Several E4 region functions influence mammary tumorigenesis by human adenovirus type 9." Journal of virology **75**(2): 557-568.

Trentin, J. J., et al. (1962). "The Quest for Human Cancer Viruses: A new approach to an old problem reveals cancer induction in hamsters by human adenovirus." science **137**(3533): 835-841.

Turnell, A. (2008). Adenoviruses: Malignant Transformation and Oncology, Encyclopedia of Virology (Third Edition).(Oxford: Academic Press).

Turnell, A. S. and R. J. Grand (2012). "DNA viruses and the cellular DNA-damage response." Journal of General Virology **93**(10): 2076-2097.

Turnell, A. S., et al. (1999). "The replicative capacities of large E1B-null group A and group C adenoviruses are independent of host cell p53 status." Journal of virology **73**(3): 2074-2083.

Uziel, T., et al. (2003). "Requirement of the MRN complex for ATM activation by DNA damage." The EMBO journal **22**(20): 5612-5621.

Valentine, R. and H. Pereira (1965). "Antigens and structure of the adenovirus." Journal of molecular biology **13**(1): 13-IN13.

Vassilev, L. T., et al. (2006). "Selective small-molecule inhibitor reveals critical mitotic functions of human CDK1." Proceedings of the National Academy of Sciences **103**(28): 10660-10665.

Vendetti, F. P., et al. (2015). "The orally active and bioavailable ATR kinase inhibitor AZD6738 potentiates the anti-tumor effects of cisplatin to resolve ATM-deficient non-small cell lung cancer in vivo." Oncotarget **6**(42): 44289.

Vennstrom, B., et al. (1982). "Isolation and characterization of c-myc, a cellular homolog of the oncogene (v-myc) of avian myelocytomatosis virus strain 29." Journal of virology **42**(3): 773-779.

Viarisio, D., et al. (2017). "Human papillomaviruses and carcinogenesis: well-established and novel models." Current opinion in virology **26**: 56-62.

Vogelstein, B., et al. (2000). "Surfing the p53 network." Nature **408**(6810): 307.

Weiden, M. D. and H. S. Ginsberg (1994). "Deletion of the E4 region of the genome produces adenovirus DNA concatemers." Proceedings of the National Academy of Sciences **91**(1): 153-157.

Weitzman, M. D., et al. (2004). "Interactions of viruses with the cellular DNA repair machinery." DNA repair **3**(8-9): 1165-1173.

Weitzman, M. D. and A. Fradet-Turcotte (2018). "Virus DNA replication and the host DNA damage response." Annual review of virology **5**: 141-164.

Weitzman, M. D. and D. A. Ornelles (2005). "Inactivating intracellular antiviral responses during adenovirus infection." Oncogene **24**(52): 7686-7696.

White, E. (2001). "Regulation of the cell cycle and apoptosis by the oncogenes of adenovirus." Oncogene **20**(54): 7836.

Wold, M. S., et al. (1987). "Initiation of simian virus 40 DNA replication in vitro: large-tumor-antigen-and origin-dependent unwinding of the template." Proceedings of the National Academy of Sciences **84**(11): 3643-3647.

Wold, W., et al. (1995). E3 transcription unit of adenovirus. The Molecular Repertoire of Adenoviruses I, Springer**:** 237-274.

Woo, J. L. and A. J. Berk (2007). "Adenovirus ubiquitin-protein ligase stimulates viral late mRNA nuclear export." Journal of virology **81**(2): 575-587.

Wu, E. and G. R. Nemerow (2004). "Virus yoga: the role of flexibility in virus host cell recognition." Trends in microbiology **12**(4): 162-169.

Yew, P. R. and A. J. Berk (1992). "Inhibition of p53 transactivation required for transformation by adenovirus early 1B protein." Nature **357**(6373): 82.

Yew, P. R., et al. (1994). "Adenovirus E1B oncoprotein tethers a transcriptional repression domain to p53." Genes & development **8**(2): 190-202.

Ying, B., et al. (2014). "Ganciclovir inhibits human adenovirus replication and pathogenicity in permissive immunosuppressed Syrian hamsters." Antimicrobial agents and chemotherapy **58**(12): 7171-7181.

Yousef, A. F., et al. (2009). "Requirements for E1A dependent transcription in the yeast Saccharomyces cerevisiae." BMC molecular biology **10**(1): 32.

Yusufzai, T., et al. (2009). "The annealing helicase HARP is recruited to DNA repair sites via an interaction with RPA." Genes & development **23**(20): 2400-2404.

Zantema, A., et al. (1985). "Adenovirus serotype determines association and localization of the large E1B tumor antigen with cellular tumor antigen p53 in transformed cells." Molecular and cellular biology **5**(11): 3084-3091.

Zhang, L., et al. (2012). "Targeting SMARCAL1 as a novel strategy for cancer therapy." Biochemical and biophysical research communications **427**(2): 232-235.

Zhang, Q., et al. (2000). "Acetylation of adenovirus E1A regulates binding of the transcriptional corepressor CtBP." Proceedings of the National Academy of Sciences **97**(26): 14323-14328.

Zhao, H., et al. (2014). "A new look at adenovirus splicing." Virology **456**: 329-341.

Zheng, Z.-M. (2010). "Viral oncogenes, noncoding RNAs, and RNA splicing in human tumor viruses." International journal of biological sciences **6**(7): 730.

Zur Hausen, H. (1976). "Condylomata acuminata and human genital cancer." Cancer Res **36**(2 pt 2): 794.

Zur Hausen, H. (2009). "The search for infectious causes of human cancers: where and why." Virology **392**(1): 1-10.